THE THEORETICAL DETERMINATION OF THE FLUID POTENTIAL DISTRIBUTION IN JOINTED ROCKS

BY

J.A. CALDWELL

A THESIS SUBMITTED TO THE UNIVERSITY OF THE WITWATERSRAND IN PARTIAL FULFILMENT OF THE REQUIREMENTS FOR THE DEGREE OF MASTER OF SCIENCE IN ENGINEERING

AUGUST, 1971.

SYNOPSIS

Based on Piteau's geological propositions the theory of the determination of the fluid potential distribution in a jointed rock mass is built up. The jointed rock mass is modelled both as a continuum and as a discontinuum. The mathematics which arises from these models is formulated and those rock joint catagories which the models best represent are indicated. Vector and Tensor coefficients of permeability for an anisotropic medium are defined and their mathematical properties are investigated. It is shown that a regularly jointed rock mass can be best characterised by a permeability tensor. The influence of jointing irregularities on the accuracy of the permeability tensor is discussed. It is shown that provided there are sufficient joints in a region considered, the solutions for the fluid potential distribution from the various analytical methods converge.

DECLARATION

I, THE UNDERSIGNED, DECLARE THAT
THIS THESIS

1. IS ENTIRELY MY OWN WORK.
2. HAS NOT BEEN SUBMITTED TO ANOTHER UNIVERSITY FOR THE DEGREE M.Sc.(Eng.)

J.A. CALDWELL.

ACKNOWLEDGEMENTS

To Professor J.E. Jennings and Mr. K.A. Lyell under whose supervision this thesis was carried out, the author would like tc express his thanks for friendly guidance, direction and encouragement.

Financial assistance, through generous scholarships was given by Mr. J.A. Thompson and the C.S.I.R., for which the author is very grateful.

TABLE OF CONTENTS

CHAPTER I

STATEMENT OF THE PROBLEM

Water in a jointed rock mass causes pressures which are usually detrimental to the stability of the rock mass. The determination of such water pressures is a complex task as rock is inherently anisotropic and heterogeneous.

It is therefore necessary to measure, as far as possible, the existing water pressure in a rock mass and to extend these results by performing theoretical analyses, adjusting the parameters used in such analyses until calculated results correspond to measured states of pressure.

In order, however, to carry out analyses of the water pressure distribution, simplified models of the rock mass have to be postulated, and these should be such that they are readily amenable to mathematical manipulation and analysis.

Furthermore it is necessary that all the factors which influence both the flow of water in rock joints and the distribution of pressures in a rock mass be clearly understood. Only if a thorough background to the theoretical analysis is available can the method of determining field potential distributions by means of the measurement of field pressures and the fitting of analytical results be most efficiently utilised.

THE ATTEMPTED SOLUTION AS PRESENTED IN THIS THESIS

1. The Proposed Proceedure for determining practical pressure distributions

The ultimate objective of any hydraulic analysis of a jointed rock mass is a quantitative description of the water pressures in the joints and interstices of the rock mass. All analyses attempt to determine the water pressure situation in a practical jointed rock mass under certain conditions.

By means of piezometers it is however possible to measure the actual water pressures which exist in a jointed rock mass at any given time. In fact if sufficient piezometers could be installed, there would be no need for any analytical solution of the as is water pressure situation in the rock mass, for contours of equal potential could be drawn and thus the exact flow net determined.

However, it is practically impossible to ever obtain sufficient piezometer readings to be able to draw complete flow nets. Moreover it is usually necessary to be able to predict what future water pressure situations will be under different boundary conditions, and not those which are extant at the time of taking the piezometer readings.

Thus a complete investigation of the hydraulic regime, both present and projected, of a jointed rock mass requires the use of both piezometers installed in the field and theoretical analyses of the pressure distributions. Taken alone, a set of piezometer readings are valuable and instructive but they do not enable predictions to be made of future situations. Likewise, any calculation not associated with practical states is instructive in that it can pinpoint areas where problems could be expected. However, taken in conjunction, that is the use of analytical proceedures tied closely and adjusted to actual measured states in the field, a very powerful and versatile method of investigation results.

This combination gives rise to the method called in this thesis - the method of *adjusting hydraulic parameters to obtain correspondence between measured and calculated pressure distributions.*

In essence this method entails the following proceedure - (See Lyell (1970))

1. Install piezometers in selected positions in the field and obtain the pore pressure at those points.
2. Estimate the value of the rock mass hydraulic parameters, such as the permeabilities of the rock mass, the inflow at the phreatic line or the value of the coefficients which appear in the flow laws describing the flow in individual joints.
3. Using these estimated parameters, carry out an analysis of the potential distribution in the rock mass. This analysis may be any one of the proceedures discussed in this thesis.

4. Check the analytical results of pore pressures against the actual values measured by the piezometers in the field.

5. If the two sets of pressures do not correspond, successively adjust the values of the parameters used in the analysis until the best possible fit is obtained between measured and calculated pressures.

6. Those parameters which produce the best fit are accepted as the true rock joint hydraulic parameters and are used in further analysis of the rock region under changed boundary conditions.

At present there are still theoretical difficulties attached to this method but they are being investigated. Nevertheless, even at the present time this is a powerful, workable approach.

In order to perform the theoretical analysis of the jointed rock mass, it is necessary to have a thorough understanding of

(a) All the physical factors which influence the flow of water in rock joints.

(b) All the configurations of rock joints which affect the parameters describing the hydraulic response of the jointed rock mass.

(c) All the available methods of analysing potential distributions in jointed rock masses.

The primary purpose of this thesis is to establish the basis for such theoretical analyses as are required in order to apply the method as described above of fitting analytical results to field pressure readings.

2. The Theoretical Solution of Pressure Distributions

In order to perform the theoretical analysis which is required in the method called above the "adjusting of hydraulic parameters to obtain correspondence between measured and calculated pressure distributions", it is necessary to make a mathematical model of the jointed rock mass.

Hence the problem of determining the fluid pressure distribution in a jointed rock mass is one of deciding on suitable models to represent the rock and of deciding what factors both theoretical and practical affect the accuracy of any postulated models.

In order to do this the following proceedure has been adopted in this thesis.

Three of Piteau's (1970) four geological propositions are accepted as a basis for this thesis. The concepts involved in the propositions are extended to include their relevance to the problem of analysing the hydraulic regime in a jointed rock mass.

According to Piteau's third geological proposition a model of the jointing of a rock mass can be contructed. For purposes of an hydraulic analysis there are three ways of modelling a jointed rock mass. One model views the rock mass as a continuum. The second views the rock as a discontinuum while the third combines the first two methods to enable complex geological discontinuities to be modelled. Each of these approaches to the hydraulic modelling of jointed rock masses gives rise to distinct methematical theories.

The continuum approach accepts that there are sufficient joints in the rock for it to be described as a porous medium. The permeability of this porous medium can be quantitised by vector or tensor permeability coefficients. These coefficients are substituted into Laplace type equations which are solved to yield the fluid potential distribution the rock.

The discontinuum approach assumes that the rock is composed of individual rock blocks and discrete flow paths which are formed by the joints which form a network. If the flow characteristics in each joint are known the total flow network can be solved to yield the fluid potential distribution within the rock mass.

The third model is essentially a combination of certain aspects of the first two approaches. It models the rock mass as a porous continuum traversed by major geological discontinuities which constitute flow channels or planar conductors and which are analysed as such.

Two types of permeability coefficients are defined, namely the vector and tensor permeability coefficients.

The tensor method of describing permeability is the more versatile. Hence the permeability tensor for a regularly jointed rock mass has been derived and those factors which influence its value and accuracy have been investigated particularly for the case where the jointing is irregular.

To determine the accuracy of the tensor method of modelling the jointed rocks and to investigate the effect of irregularities in the jointing system, tests on electrical analogue models were performed. The analogue models also showed that, if a sufficient* number of joints exist in the rock mass then the solutions from the continuum and the discontinuum methods converge.

A practical example of the drawdown of the phreatic line in a slope composed of homogeneous rock is given to illustrate the use of the methods detailed in this thesis.

SOME RELATED BACKGROUND REMARKS

1. *The importance of water in a rock slope*

Numerous authors have pointed out the importance of water pressures on the stability of rock masses. The pressures that arise in the rock joints and the material interstices as a result of a static or dynamic state of the water in the rock mass have a controlling effect on the stability of such masses. Many failures of slopes, dam foundations and abutments can be attributed to the effects of water pressure. As a result of pressures caused by water flowing in the slope, its critical angle of stability can be reduced by as much as 50% (Jennings 1970)

* Criteria for the number of joints which are sufficient are discussed in Chapter 6.

Water flowing in a rock mass has the following main effects.

(a) It creates an uplift force on the potential failure plane which reduces the frictional resistance both in the intact rock and on the joints which form a part of the potential failure plane. In most instances the pressure acts in such a direction that it cuases a disturbing force on the potential failure wedge.

(b) It contributes to the weathering of the intact materials thus reducing their strength and increasing the possibilities of failure. The strength of the intact rock is also reduced by the presence of water.

Jennings (1970) presents the results of calculations to determine the safety factor of various slopes both in the presence and the absence of water pressures. His results demonstrate the large influence of water pressures in lowering the safety factor of a slope. Hence a thorough knowledge of the pressure distribution in the rock mass is vital to any analysis of the stability of rock masses.

A reduction of the water pressure is necessary if the stability of the rock mass is to be improved. Depending on the porosity and the permeability of the rock mass and the available supply of water it may be necessary to remove either a little or a lot of water to achieve a commensurate pressure reduction. All the analyses presented in this thesis are therefore oriented to the determination of water pressures in the rock mass rather than the flow rates.

2. <u>The geological propositions underlying the theory of the calculation of the stability of slopes and their application to the determination of the pressure distribution.</u>

Piteau presents four geological propositions each of which represents a particular concept or premise which is necessary "before the definition of the properties in a slope can be described in a numerical form". (Piteau - 1970). The mathematical theory which is used in calculating the stability of a slope is founded on these propositions. Only three of Piteau's propositions are relevant when calculating the potential distribution in a rock mass. These propositions are as follows:

1. <u>The proposition that structural discontinuities are detectable features of a rock mass and can be described quantitatively.</u>

It is taken as a basic hypothesis that structural discontinuities in a rock mass are detectable and that the physical properties which control or influence the flow of water in such discontinuities can be described quantitatively.

The data describing the structural discontinuities and their physical properties which are required for the hydraulic analysis of a rock mass, fall into the following groups.

(a) Factors describing the spatial position and orientation of the joints such as the co-ordinates and the dip and strike of each joint.

(b) Factors describing the nature of the joints i.e. their length, continuity, apertures, gouge filling and surface properties.

A full, detailed knowledge of the above listed rock joint properties would enable the values of parameters which are to be used in a theoretical analysis of the hydraulic state in a rock mass to be determined or predicted.

However, it is very seldom that sufficiently detailed information is available to state with confidence correct values of the rock mass hydraulic parameters derived from rock joint properties.

Accordingly a more powerful technique is being developed. This is the technique of measuring the effects of artificial or naturally occuring flow situations and from the measured results predicting the values of the rock joint parameters which give rise to such results.

This technique is discussed in detail later in this thesis.

However, it should always be remembered that regardless of which of the two approaches is adopted as basic; that is the use of rock joint properties to predict hydraulic parameters or the measurement and fitting to existing flow states, it is always necessary to have a thorough and detailed knowledge and understanding of the principles which underlie and control the phenomenon being studied. That is the purpose of this thesis, namely to establish the theoretical background to the understanding of the flow of water in jointed rock masses in order that practical situations may be studied with increased understanding.

2. <u>The proposition that structural regions exist in a rock mass.</u>

In an extensively jointed rock mass the jointing will be heterogeneous. However, regions will exist within the rock mass which will have similar jointing patterns. These regions are defined as structural regions. For purposes of hydraulic analysis of a rock slope it is more convenient to consider hydraulic regions which can be defined as areas of an extensive rock mass within which the jointing is sufficiently homogeneous for it to be analysed either as an homogeneous porous medium or as a region characterised by regularly spaced joints. (See proposition No. 3)

To facilitate the determination of hydraulic regions in a rock mass sufficient information is required to estimate the following factors.

a. The degree of homogeneity of the rock mass.
b. The degree of isotropy of the rock mass.
c. The position and nature of major geological discontinuities.
d. The position and magnitude of the boundary conditions.

Knowledge of the nature of the rock joint pattern of the joint assemblages* will aid in judging the degree of homogeneity and

* See definitions in Appendix 1.

isotropy of the jointed rock mass. Moreover the rock joint pattern will influence the choice of the type of model which is to be used to simulate the rock mass. Accordingly the following four rock joint catagories are proposed. A discussion of the models which best represent each rock joint catagory is postponed until Chapter 3.

(a) Intact Rock Masses - characterised by an absence of fissures or joints. Such a mass can be homogeneous or heterogeneous and also isotropic or anisotropic.

(b) Regular Jointing - indicates that the joints in the rock are, on the average, uniformly orientated and evenly spaced.

(c) Irregular Jointing - indicates that the cracks and joints are non-uniformly orientated and that their spacing is decidedly uneven. However, on the average the joints display a certain tendency to lie in preferred directions. Such rock masses are usually distinctly anisotropic and heterogeneous.

(d) Major Geological Discontinuities - are those structural discontinuities which are sufficiently well-developed* for them to have a major influence on the hydraulic response of the surrounding rock region.

3. The Proposition that a reliable model representing jointing of a rock mass can be constructed.

Before any systematic attempt to analyse the hydraulic regime in a rock mass can be made, it is necessary to construct a model or a picture of the rock mass on hand. Such a model should be a good representation of the jointing patterns of the rock mass and be such that on the average the pressures determined from analysis of the

* i.e. they are highly or very slightly permeable with respect to the surrounding rock masses, or are of large extent relative to neighbouring structural discontinuities.

model correspond to the pressures that apply in the rock mass as a whole.

The joint assemblages that occur in nature in a rock mass (see previous section) vary greatly from one another. Accordingly it is necessary to postulate at least two basic models which can be used to best represent various types of rock joint assemblages.

Muskat (1949) first proposed the idea of the two basic models when he stated with regard to fractured media

"When such fractures are of limited extent and uniformly distributed through the pay, they will give a resultant effect equivalent to that of a porous medium. However, when they are of extended length and limited in number, they may be considered separately as linear channels."

Snow (1965) states that "fractured media can be modelled adequately for two extreme cases seldom realised in nature: 1) when individual planar conductors, such as joints in rock, are so independent and infrequent that each may be analysed as a separate channel or 2) when aggregates of fractures as in fault breccia so resemble sedimentary pores that the medium is assumed to be a continuum."

In this thesis these two basic models have been extended and their mathematical formulation and manipulation has been explored. In addition a third model, a combination of the two basic models, has been proposed and is described.

These three models are called in this thesis -

(a) The Equivalent Continuous Medium Model.

(b) The Discrete Flow Channel Model.

(c) The Composite Medium Model.

Chapter 2 details the mathematical formulation of the above three models.

(Piteau's Fourth Geological Proposition is not applicable to this thesis and is hence ommitted here)

CONCLUSION

The pressures to which water gives rise in a slope are an important factor in the stability of the slope. The determination of these pressures is thus an important task. The most rational and practical approach to the determination of such water pressure is to measure them in the field by means of piezometers. To yield further, fuller information it is also necessary to calculate such water pressures. Such calculations require a theoretical background and understanding of the phenomonon of water flow in jointed rock masses. Accepting Piteau's geological propositions, this thesis aims to build up the necessary theoretical background but leaves the detailed exposition of the method of fitting calculated and measured fluid pressures to later publications.

CHAPTER 2

THE ANALYTICAL DETERMINATION OF THE POTENTIAL DISTRIBUTION IN A JOINTED ROCK MASS

Piteau's third geological proposition stated that a reliable model representing jointing of a rock mass can be constructed. It has already been stated that for purposes of determining the water pressure distribution a jointed rock mass can be modelled in one of three ways, depending on the rock joint catagory into which the joint assemblage falls. The models were called

(1) The Equivalent Continuum Model.
(2) The Discrete Flow Channel Model.
(3) The Composite Medium Model.

The essence of the first model is that the joints are sufficiently numerous for the jointed mass to be represented as an equivalent isotropic or anisotropic, *homogeneous or non-homogeneous medium* within which the potential distribution can be described by means of an equation of the Laplace form, which can then be solved by any of a number of methods, all of which are detailed in the relevant section below.

The Discrete Flow Channel Model takes each rock joint or certain selected combinations of rock joints to form individual paths which define a pipe or electrical type network. Accepting this as the model of the physical reality the equivalent network may be solved by standard network theories.

The third model considers the joints to form discrete flow paths that are bounded by permeable media of sufficient permeability to influence the joint *flows and hence the regional flow pattern*. The joints are usually major geological discontinuities. A sub division of class 3 occurs where two dimensional continuum theories are used to solve for the potential distribution on three dimensional joints which then form a class 2 type system.

CLASS 1 THE EQUIVALENT CONTINUUM MODEL

The assumptions regarding the field conditions that must be made in the Equivalent Continuum Approach are -

(a) The intensity, continuity and pattern of the jointing is such that the rock region can be adequately modelled by an equivalent continuous homogeneous or non-homogeneous, isotropic or anisotropic medium.

(b) The rock region to be analysed is not traversed by any major geological discontinuities of such a nature that they will interfere with a continuous smooth variation of the regional potential distribution.

(c) The Boundary Conditions do not have a discrete and different influence on each joint traversing the boundary.

The assumptions are only valid in so far as they are representative of actual field conditions.

As corollaries to the above assumptions the following statements can be made -

(1) The potential gradient is not necessarily parallel to any particular joint or joint set within the rock mass. The real joint gradient is the projection of the field* gradient onto the joint per se, from which the joint flow can be computed.

(2) The rock mass permeability coefficients account for individual joint variations in size, location and direction, and hydraulic losses at intersections.

* field - The word is here used in a strictly mathematical sense. See Appendix 1 for definition of all terms used.

Background Theory

Accepting that the jointed rock mass can be modelled by a continuous medium, the field potential distribution can be found by solving the following form of the Laplace equation (derived in Chapter 4) which holds for slow steady, incompressible fluid flow.

$$\sum_{i=x}^{z} \sum_{j=x}^{z} k_{ij} \cdot \frac{\partial^2 \phi}{\partial x \partial y} = 0 \qquad (2.1)$$

where ϕ is the hydraulic potential.

k_{ij} are the coefficients of a permeability tensor describing the medium.

x,y,z are the designations of the orthogonal axes defining the system for which the equation is written.

This equation reduces for isotropic media to the familiar form of Laplace's equation

$$\frac{\partial^2 \phi}{\partial x^2} + \frac{\partial^2 \phi}{\partial y^2} + \frac{\partial^2 \phi}{\partial z^2} = 0 \qquad (2.2)$$

Note that only cases of incompressible fluid and media will be considered in this thesis as rock by its incompressible nature seldom gives rise to compressible flow situations.

The water pressure at any point is then obtained from the equation

$$u = (\phi - H) \gamma_w \qquad (2.3)$$

where u is the water pressure

γ_w unit weight of water

H height of point above datum

ϕ is the potential function

The following methods for solving equations (2.1) and (2.2) exist

(a) *Direct intergration of the equations.*

(b) Complex variable Techniques.

(c) The Finite Difference Method.

(d) The Finite Element Method.

(e) Graphical Methods.

(f) Analogue Methods.

Application of these methods.

(a) Direct integration of the equations.

For simple cases of rectilinear flow in confined and unconfined aquifers or for simple two dimensional radial flow situations, direct analytical solutions to equation (2.2) may be obtained. However, such methods are impractical for anisotropic or isotropic situations of even mildly complex geometry. As practical rock masses are seldom if ever, isotropic and the practical field situations encountered are never simple, these methods will not be pursued further here. Verruijt (1969) deals most adequately with the problems that can be solved by this method.

(b) Complex Variable Techniques.

This is another rigorous approach to the solution of equation (2.2). The method is merely mentioned here. Since the subject is long and involved, and the range of problems which it can solve are limited, fairly specialised and not likely to be of any great importance in practical problems involving rock masses.

(c) The Finite Difference Method.

This method is used in the numerical solutions presented in this thesis.

It should be noted that the Finite Difference Method is no more than a particular case of the more general body of Relaxation Methods developed by Southwell (1946).

Appendix 4 presents the Finite Difference forms of all the equations used in this thesis as well as the extended finite difference equations for anisotropic media for a number of specialised cases. For the present only the finite difference form of equation (2.2) will be considered.

In the Finite Difference Method the continuous potential distribution is replaced by a finite number of discrete values of the potential. These discrete values are normally assumed to occur at the node points of a rectangular grid. The variation of the potential from one grid to another is taken to be linear. For transient conditions it is assumed that the rate of change of potential at each node of the grid is linear over small time intervals.

Consider the form of the relevant Finite Difference equations for a two dimensional isotropic field. The values of ϕ at the points 1,2, 3 and 4 in the grid shown in fig. 2.1 can be related to the value of ϕ_0 at the central point by means of a Taylor series expansion.

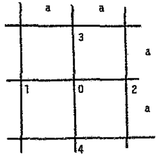

FIG. 2.1 THE GRID USED IN THE FINITE DIFFERENCE FORM OF THE LAPLACE EQUATION

$$\phi_1 = \phi_0 + a\frac{\partial\phi}{\partial x}\bigg|_0 + \frac{1}{2}a^2\frac{\partial^2\phi}{\partial x^2}\bigg|_0 + \frac{1}{6}a^3\frac{\partial^3\phi}{\partial x^3}\bigg|_0 \cdots\cdots$$

$$\phi_2 = \phi_0 + a\frac{\partial\phi}{\partial y}\bigg|_0 + \frac{1}{2}a^2\frac{\partial^2\phi}{\partial y^2}\bigg|_0 + \frac{1}{6}a^3\frac{\partial^3\phi}{\partial y^3}\bigg|_0 \cdots\cdots$$

$$\phi_3 = \phi_0 - a\frac{\partial\phi}{\partial x}\bigg|_0 + \frac{1}{2}a^2\frac{\partial^2\phi}{\partial x^2}\bigg|_0 - \frac{1}{6}a^3\frac{\partial^3\phi}{\partial x^3}\bigg|_0 \cdots\cdots \qquad (2.3)$$

$$\phi_4 = \phi_0 - a\frac{\partial\phi}{\partial y}\bigg|_0 + \frac{1}{2}a^2\frac{\partial^2\phi}{\partial y^2}\bigg|_0 - \frac{1}{6}a^3\frac{\partial^3\phi}{\partial y^3}\bigg|_0 \cdots\cdots$$

Where 'a' is the grid size, and ϕ 1,2,3 or 4 are the values of the potential at the nodes indicated. Rearranging eqn. (2.3) and combining yields.

$$a^2\left(\frac{\partial^2\phi}{\partial x^2} + \frac{\partial^2\phi}{\partial y^2}\right) = (\phi_1 + \phi_2 + \phi_3 + \phi_4 - 4\,\phi_0) + \frac{a^4}{12}\left(\frac{\partial^4\phi}{\partial x^4} + \frac{\partial^4\phi}{\partial y^4}\right) \qquad (2.4)$$

From equation (2.2) the left hand side of (2.4) is zero and provided 'a' is sufficiently small, such that the last term of (2.4) vanishes compared to the first, the following equation results.

$$\phi_0 = \frac{1}{4}(\phi_1 + \phi_2 + \phi_3 + \phi_4) \qquad (2.5)$$

For anisotropic media extended equations of the form (2.5) result. Thus, regardless of the nature of the field to be analysed, equations describing each nodal potential in terms of the surrounding nodal potentials can be derived. Lyell (1970) has demonstrated how for the five classes of points that arise in practical problems, a number of equations equal to the number of unknown nodal potentials can be derived, i.e. for the water table, interior points, flowline boundaries, seepage faces and equipotential boundaries.

Any of the numerous available numerical methods can be used to solve the resulting set of simultaneous linear equations. Some of these methods are as follows.

(i) Relaxation.

(ii) Iteration.

(iii) Matrix Inversion.

The problems solved in this thesis involved the solution of the resulting equations by relaxation using an I.B.M. 360/50 computer. Average time of solution per field was 50 secs. Numerous convergence techniques can be used to speed up these iterative proceedures, some of which are described by Sharp (1970).

No general computer programs exist to handle general flow fields by means of Finite Differences. The power and versatility of this method is demonstrated by the program presented by Lyell (1970). His program has been somewhat extended and used in this thesis to study the effects of anisotropy on a typical practical situation.

(d) The Finite Element Method.

As with the Finite Difference Method the Finite Element Method requires that the continuous potential distribution be replaced by discrete values of the potential at arbitrary node points. Unlike the Finite Difference Methods these nodes may be quite arbitrarily place with respect to each other in the field of flow.

Originally developed as a method for computing stresses and strains in elastic continua (see references 27 and 28) the Finite Element Method has been extended by many workers in recent years i.e. Zienkiewicz, Clough, Argyris and Chung. With the recognition of the fact that the resulting stress equations occuring in the Finite Element formulation were only special cases of the general mathematical theory of functional minimisation or variational calculus (i.e. the field potential energy should be a minimum) it became possible to extend the Finite Element Method to flow fields.

Many fine, concise derivations of the finite element equations have been presented, e.g. Zienkiewicz (1960) and Verruijt (1970) use the principles of minimisation of the field potential energy or general vairational principles. These methods are rigorous but tend to obscure the inherent simplicity of the finite element method. Accordingly the following simplified exposition of the finite element method is presented. It is in the nature of a practical intuitive proof rather than a strict mathematical derivation.

The derivation is presented for a two dimensional triangular element, but three dimensional a ' arbitrarily shaped elements can be handled by the same method.

The flow field is divided up into a series of triangles. For purposes of this argument one triangle ijm as shown in fig. (2.2) is considered.

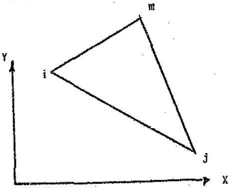

FIG. 2.2 THE ELEMENT USED IN THE FINITE ELEMENT DERIVATION

The nodal potentials are $\{\ \phi_i \quad \phi_j \quad \phi_m\ \}$

The potential of a point within the element is assumed to vary as a linear function of the coordinates of the point

$$\text{i.e.} \quad \phi = A + Bx + Cy \tag{2.6}$$

Note that A,B and C will necessarily be different for each element.

The triangle vertices, nodal potentials are determined by substituting their coordinates directly into equation (2.6)

$$\text{i.e.} \quad \begin{aligned} \phi_i &= A + Bx_i + Cy_i \\ \phi_j &= A + Bx_j + Cy_j \\ \phi_m &= A + Bx_m + Cy_m \end{aligned} \tag{2.7}$$

In matrix form equation (2.7) can be written as

$$\begin{Bmatrix} \phi_i \\ \phi_j \\ \phi_m \end{Bmatrix} = \begin{vmatrix} 1 & x_i & y_i \\ 1 & x_j & y_j \\ 1 & x_m & y_m \end{vmatrix} \begin{Bmatrix} A \\ B \\ C \end{Bmatrix} \tag{2.8}$$

$$\text{i.e.} \quad \phi^e = X\,A \tag{2.9}$$

It can be shown that DET X or $|X| = 2\Delta$ (2.10)

where Δ = the area of triangle ijm.

Using equation (2.8) to solve for A,B, and C in terms of nodal potentials and coordinates the following equations result, by application of simple matrix algebra.

$$A = \frac{1}{2\Delta}\begin{vmatrix} \phi_i & x_i & y_i \\ \phi_j & x_j & y_j \\ \phi_m & x_m & y_m \end{vmatrix} \qquad B = \frac{1}{2\Delta}\begin{vmatrix} 1 & \phi_i & y_i \\ 1 & \phi_j & y_j \\ 1 & \phi_m & y_m \end{vmatrix}$$

$$C = \frac{1}{2\Delta}\begin{vmatrix} 1 & x_i & \phi_i \\ 1 & x_j & \phi_j \\ 1 & x_m & \phi_m \end{vmatrix} \tag{2.11}$$

If the following substitutions are made

$$\begin{aligned} a_i &= -(x_j y_m - x_m y_j) / 2\Delta \\ b_i &= -(y_j - y_m) / 2\Delta \\ c_i &= -(x_m - x_j) / 2\Delta \end{aligned} \tag{2.12}$$

And similarly for a_j , a_m -----c_m by cyclic permutation. A,B,C can be written as

$$\begin{aligned} A &= - a_i\phi_i - a_j\phi_j - a_m\phi_m \\ B &= - b_i\phi_i - b_j\phi_j - b_m\phi_m \\ C &= - c_i\phi_i - c_j\phi_j - c_m\phi_m \end{aligned} \tag{2.13}$$

Substituting these values back into equation (2.6) yields

$$\begin{aligned} \phi &= A + Bx + Cy \\ &= -(a_i + b_i x + c_i y) \phi_i \\ &\quad - (a_j + b_j x + c_j y) \phi_j \\ &\quad - (a_m + b_m x + c_m y) \phi_m \end{aligned} \tag{2.14}$$

The following law holds for the flow velocity in the field.*

$$\begin{Bmatrix} V_x \\ V_y \end{Bmatrix} = - \begin{vmatrix} k_{xx} & k_{xy} \\ k_{yx} & k_{yy} \end{vmatrix} \begin{Bmatrix} \frac{\partial \phi}{\partial x} \\ \frac{\partial \phi}{\partial y} \end{Bmatrix} \qquad (2.15)$$

OR

$$\underset{\sim}{V} = -\underset{\sim}{K} \;\text{grad}\; \phi \qquad (2.16)$$

where $\underset{\sim}{V}$ is the flow velocity vector

$\underset{\sim}{K}$ is the permeability tensor

grad ϕ the potential gradient vector

It should be noted that K should be in the global co-ordinate axis system of the field as distinct from the local element co-ordinate axes system. Should it be necessary to transform a known K in local axes to the global axis this can be done by the methods given in Chapter 5.

Differentiating (2.4) with respect to x and y gives

$$\frac{\partial \phi}{\partial x} = - b_i\phi_i - b_j\phi_j - b_m\phi_m$$

$$\frac{\partial \phi}{\partial y} = - c_i\phi_i - c_j\phi_j - c_m\phi_m$$

or in matrix notation

$$\begin{Bmatrix} \frac{\partial \phi}{\partial x} \\ \frac{\partial \phi}{\partial y} \end{Bmatrix} = - \begin{vmatrix} b_i & b_j & b_m \\ c_i & c_j & c_m \end{vmatrix} \begin{Bmatrix} \phi_i \\ \phi_j \\ \phi_m \end{Bmatrix} \qquad (2.17)$$

* As derived in Chapter 4.

or concisely, $\quad \text{grad}\phi = - b\ \phi^e \qquad (2.18)$

This is the general form that would hold true irrespective of the shape of the element or whether a two or three dimensional field was being considered.

Substituting (2.18) into (2.15)

$$\begin{Bmatrix} V_x \\ V_y \end{Bmatrix} = \begin{vmatrix} k_{xx} & k_{xy} \\ k_{yx} & k_{yy} \end{vmatrix} \ast \begin{vmatrix} b_i & b_j & b_m \\ c_i & c_j & c_m \end{vmatrix} \begin{Bmatrix} \phi_i \\ \phi_j \\ \phi_m \end{Bmatrix} \qquad (2.19)$$

or in the general form

$$\underset{\sim}{V} = \underset{\sim}{K}\ b\ \phi^e \qquad (2.20)$$

It is necessary now to compute the total flow rate into and out of the element. Flow will occur across the sides of the element, but for computational purposes the flow through half of each side of the triangle adjacent to each node is assigned to that node.

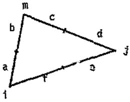

Fig 2.3

With reference to fig. 2.3 the flow through segments a and f are assigned to node i, through b and c to node m and through d and e to node j.

Note that strictly it is the flow rate at each node that is being considered.

Now the flow rate through a per unit time is

$$V_x(y_m - y_i)/2 - V_y(x_m - x_i)/2$$

and through f is

$$V_x(y_i - y_j)/2 - V_y(x_j - x_i)/2$$

Thus the total flow at node i is

$$Q_i = V_x(y_m - y_j)/2 - V_y(x_m - x_j)/2 \tag{2.21}$$

but note that from equation (2.12), (2.21) can be written as

$$Q_i = - \Delta b_i V_x - \Delta c_i V_y \tag{2.22}$$

Similarly for nodes j and m to give

$$\begin{Bmatrix} Q_i \\ Q_j \\ Q_m \end{Bmatrix} = - \Delta \begin{vmatrix} b_i & c_i \\ b_j & c_j \\ b_m & c_m \end{vmatrix} \begin{Bmatrix} V_x \\ V_y \end{Bmatrix} \tag{2.23}$$

In the general form

$$\text{i.e.} \quad \underset{\sim}{Q}^e = - \Delta b^t \underset{\sim}{V} \tag{2.24}$$

Substituting equation (2.20) into (2.24) gives

$$\underset{\sim}{Q}^e = -\Delta\, b^t \underset{\sim}{K}\, b\, \phi^e \tag{2.25}$$

This is the vector of element flows. However, it is necessary to write a vector of nodal flows i.e. sum the contributions to the flow at each node from the surrounding elements.

For fig. (2.4) the relevant form of equation (2.25) for triangle 1 may be written

$$\begin{Bmatrix} Q_{i1} \\ Q_{j1} \\ Q_{m1} \end{Bmatrix} = -\Delta \begin{vmatrix} b_i & c_i \\ b_j & c_j \\ b_m & c_m \end{vmatrix} \begin{vmatrix} k_{xx} & k_{xy} \\ k_{yx} & k_{yy} \end{vmatrix} \begin{vmatrix} b_i & b_j & b_m \\ c_i & c_j & c_m \end{vmatrix} \begin{Bmatrix} \phi_i \\ \phi_j \\ \phi_m \end{Bmatrix} \quad (2.26)$$

Multiplying out the first three matrices on the right hand side yields an equation of the form

$$\begin{Bmatrix} Q_{i1} \\ Q_{j1} \\ Q_{m1} \end{Bmatrix} = \begin{vmatrix} A_1 & B_1 & C_1 \\ D_1 & E_1 & F_1 \\ G_1 & H_1 & I_1 \end{vmatrix} \begin{Bmatrix} \phi_i \\ \phi_j \\ \phi_m \end{Bmatrix} \quad (2.27)$$

A similar equation is valid for triangles 2 and 3

i.e.

$$\begin{Bmatrix} Q_{i2} \\ Q_{m2} \\ Q_{12} \end{Bmatrix} = \begin{vmatrix} A_2 & B_2 & C_2 \\ D_2 & E_2 & F_2 \\ G_2 & H_2 & I_2 \end{vmatrix} \begin{Bmatrix} \phi_i \\ \phi_m \\ \phi_1 \end{Bmatrix} \quad (2.28)$$

and

$$\begin{Bmatrix} Q_{i3} \\ Q_{j3} \\ Q_{13} \end{Bmatrix} = \begin{vmatrix} A_3 & B_3 & C_3 \\ D_3 & E_3 & F_3 \\ G_3 & H_3 & I_3 \end{vmatrix} \begin{Bmatrix} \phi_i \\ \phi_j \\ \phi_1 \end{Bmatrix} \quad (2.29)$$

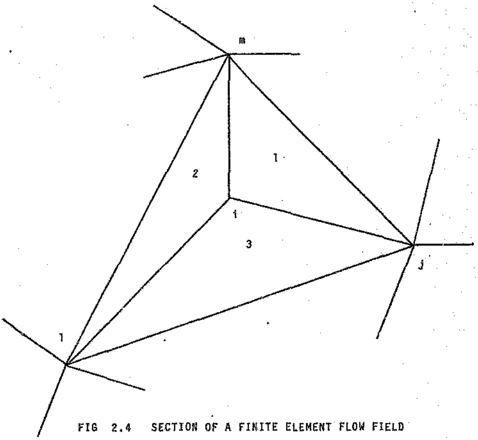

FIG 2.4 SECTION OF A FINITE ELEMENT FLOW FIELD AS USED TO ILLUSTRATE THE ASSEMBLY OF THE ASSEMBLED PERMEABILITY TENSOR

and similarly for each triangle in the field.

The vector of element flows then may be written as follows

$$\begin{Bmatrix} Q_{i1} + Q_{i2} + Q_{i3} \\ Q_{m1} + Q_{m2} \cdots\cdots \\ Q_{i2} + Q_{i3} \cdots\cdots \\ Q_{j1} + Q_{j3} \cdots\cdots \\ \cdot \\ \cdot \\ \cdot \\ \cdot \end{Bmatrix} = \begin{vmatrix} A_1+A_2 \\ +A_3 & B_1+B_3 & C_1+B_2 & C_2+C_3 \\ G_1+D_2 & H_1 & I_1+E_2 & F_2 \\ \cdots & \cdot\cdot & \cdot\cdot & \cdot\cdot \\ \vdots \\ \cdot & \cdots & \cdots & \cdots \end{vmatrix} \begin{Bmatrix} \phi_i \\ \phi_j \\ \phi_m \\ \phi_1 \\ \cdot \\ \cdot \\ \cdot \\ \cdot \end{Bmatrix}$$

(2.30)

In matrix notation this can be written

$$\Sigma Q_n = - \Sigma \Delta b^t \underset{\sim}{K} b \phi_n \qquad (2.31)$$

where ΣQ_n is the nodal flow vector

and $\Sigma \Delta b^t \underset{\sim}{K} b \phi_v$ is the assembled nodal permeability matrix Ka.

Writing this more simply as

$$\hat{} Q_n = - K_a \phi_n \qquad (2.32)$$

Note that eqn. (2.32) contains the equations describing the nodal potential - flow rate relationships for all nodes in the flow field. As boundary conditions are known it follows that at certain nodes either the potential or the flow quantity or both are known.

Thus if

Q_{n1} = known nodal outflows
Q_{n2} = unknown nodal outflows
ϕ_{n1} = unknown nodal potentials
ϕ_{n2} = known nodal potentials

it is possible to appropriately partition the matrices of eqn. (2.27) as

$$\begin{Bmatrix} Q_{n1} \\ Q_{n2} \end{Bmatrix} = - \begin{vmatrix} K_{n11} & K_{n12} \\ K_{n21} & K_{n22} \end{vmatrix} \begin{Bmatrix} \phi_{n1} \\ \phi_{n2} \end{Bmatrix} \tag{2.32}$$

or written in full

$$\begin{aligned} Q_{n1} &= - K_{n11}\, \phi_{n1} - K_{n12}\, \phi_{n2} \\ Q_{n2} &= - K_{n12}\, \phi_{n1} - K_{n22}\, \phi_{n2} \end{aligned} \tag{2.33}$$

Note that set (a) of eqn. (2.33) has one set of unknowns hence this equation can be solved for ϕ_{n1} which when substituted into (b) will yield Q_{n2}. From eqn. (2.19) nodal flow velocities may be solved if so required. The problem is thus solved.

The Finite Element Method is most suited to computer solution, in that general programs to handle arbitrary field geometries and random anisotropics may be written. The method can be extended to moving phreatic lines. The extension to three dimensions is a necessary task at present being undertaken by Dr. Wittke et al (1970).

It is important to note the use of a permeability tensor in this method, a method which is likely to be more extensively used in the future.

(The following two methods can only handle isotropic cases. All anisotropic flow situations must first be reduced to isotropic fields by means of standard techniques.)

(e) Graphical Methods.

This is an approximate method of determining the potential distribution in an homogeneous, isotropic situation. A net of orthogonal lines is sketched by trial and error onto the flow field such that it fits the boundary conditions and the condition that the intersection of any two lines must be orthogonal i.e. as far as possible all 'blocks' should be square.

One set of the lines forming the network are known as equipotential lines, for at all points on one of these lines the potential is unchanged. The orthogonal set of lines are called flow lines, and at any point on a flow line the vector of flow of the fluid in the field is tangential to the flow line.

Mathematically flow lines can be described by a function ψ defined as the stream function. It can be shown, Verruijt (1970), that the stream function obeys a Laplace equation of the form

$$\frac{\partial^2\psi}{\partial x^2} + \frac{\partial^2\psi}{\partial y^2} = 0 \qquad (2.34)$$

where the potential function ϕ and the stream function are related to each other by the equation

$$\frac{\partial\phi}{\partial s} = \frac{\partial\psi}{\partial n} \qquad (2.35)$$

where s and n are orthogonal directions.

(f) Analogue Methods.

The Laplace equation describing the potential distribution in a jointed rock mass which can be considered both isotropic and homogeneous (or can be transformed to the equivalent isotropic, homogeneous situation) is the same equation which describes the potential in an electrical field, the flow of heat in a body and many other phenomena in hydrostatics, thermodynamics and electrostatics.

Making use of the analogy between the fluid potential and the potential in an electrical field or network it is possible to solve complex field situations in a relatively quick and inexpensive manner. The two most commonly used methods are

(i) Use of electrical conductive paper.

The use of electrical conductive paper is a simulation of the continuous field. A thin, uniform conducting sheet (marketed under the name Teledeltos paper) is used. The field to be analysed is cut from the paper to some suitable scale. (As the paper is uniform any practical anisotropic field must first be converted to an equivalent isotropic field). Equipotentials, sources or sinks are created by applying a suitable voltage along or at the relevant positions.

Using a special conductive probe attached to a Wheatstone bridge the value of the potential at any point can be measured. For the experiments conducted in this thesis a Servomex Field Plotter (28) was used.

Hence the potential distribution is immediately measured for an isotropic medium or is obtained after transforming back to original scales for an anisotropic field.

(ii) Electrical networks.

The Laplace equation is solved by firstly replacing the continuous field by a grid such as is used in the finite difference method. The grid is next simulated by an electrical network with resistance between the node points to represent the resistance to flow from one node point to another. The nodal voltages are then analogous to the field nodal potentials.

Anisotropy can be introduced by varying the values of the resistances used. Arbitrary flow field geometry is handled easily. A disadvantage of the method is that the lines of the resistances must be orientated along the principal axes of the medium being analysed.

This method has been used extensively to solve problems of three dimensional unconfined ground water flow by Herbert and Rushton and Sharp

CLASS 2 . <u>THE DISCRETE FLOW CHANNEL APPROACH</u>

The following assumptions which should be representative of the actual field conditions must be made in the discrete flow channel approach.

(a) The intensity, continuity and interconnection of the jointing is such that the rock region can be adequately modelled by a network of individual flow channels, which may be represented as interconnected pipes.

(b) The flow characteristic of each joint is accurately known.

(c) The boundary conditions are such that the potential in each joint traversing the boundaries can be described.

(d) Major discontinuities in the field such as tabular zones of crushed rock or dykes can be adequately represented by an equivalent pipe or channel.

As corollaries to the above assumptions the following statements can be made.

(i) The aperture, wall roughness, gouge filling and waveness of each individual joint in the field is known so that the flow characteristics of the joint can be determined.

(ii) The location and direction of each joint in the field is known.

Accepting that values are available for all the above mentioned parameters the flow characteristics in each joint may be defined and the total flow regime calculated.

Louis (1969) and Sharp (1970) have studied the flow laws governing the flow in between flat parallel plates considered to represent a joint. Generally they find that there exist three domains of flow: a zone of linear laminar, a zone of transition and a zone of turbulent flow. They find that the linear laminar flow in joints is restricted to flow under small head gradients through joints of relatively small aperture. There is a transition zone from laminar to fully turbulent flow.

The equations in table 2.1 are abstracted from Louis (1970) and Sharp (1970) and give the relationship between

q – the quantity of flow per unit width of a joint

and J – the potential gradient in the joint.

B – a coefficient which is different for each joint and is a function of the joint aperture, the velocity of the flowing water, the joint wall roughness, the joint gouge filling and the type of flow occuring in the joint. i.e. parallel laminar or turbulent or non-parallel laminar or turbulent.

Louis presents a complete list of formulae for values of B for various cases. In addition he presents a table of equations giving the

TABLE 2.1 FLOW LAWS FOR DIFFERENT TYPES OF FLOW

TYPE OF FLOW			EQUATION FOR FLOW RATE q	
			LOUIS	SHARP
PARALLEL FLOW	LAMINAR		$q = B\ J$	
PARALLEL FLOW		TRANSITIONAL		$q = B\ J^{0.75}$
PARALLEL FLOW	TURBULENT	HYDRAULICALLY *SMOOTH*	$q = B\ J^{4/7}$	
PARALLEL FLOW	TURBULENT	COMPLETELY ROUGH	$q = B\ J^{0.5}$	$q = B\ J^{0.5}$
NON-PARALLEL FLOW *	LAMINAR		$q = B\ J$	
NON-PARALLEL FLOW *	TURBULENT		$q = B\ J^{0.5}$	

* For an explaination of non-parallel flow see Louis' thesis (1969)

coefficient which occurs in the joint flow equation (2.36) for different types of flow and joints:

$$\frac{\partial\phi}{\partial n} = \lambda \frac{1}{D_h} \frac{V^2}{2g} \qquad (2.36)$$

where V is the joint flow velocity.

D_h is the joint hydraulic radius.

Louis moreover presents the results of investigations into the effects of variable joint openings and macroscopic joint waviness on the flow in the joint. Hence a sound quantitisation of the flow characteristics for different joint characteristics exists and can if necessary be consulted when considering practical cases of flow in fissured rock masses.

The difficulties of determining the practical field characteristics of actual joints means that in most cases the equations discussed above will be used more as a guide to the understanding than as an appreciation of what is actually occuring in practice. Nevertheless they constitute a valuable tool to assist the engineer in judging the practical field problem.

The solution of the total flow regime requires a q-V and a J-V relationship for each joint and the equations presented by Louis provide the rigorous forms of these relationships for all joint characteristic combinations. If the joint characteristics are not accurately known estimates of the values of the parameters in the relationships should be made, based upon Louis' equations.

Solution of the Total Flow Regime.

A two dimensional jointed rock mass is to be analysed and composed of i joint segments so arranged that there exist n joint intersection points or nodes, m closed paths through rock joints, and p open flow paths along the boundaries. Consideration of any simple network will show that for such a system there exists $n + m + p + 1$ distinct joint sections i.e. $i = n + m + p + 1$

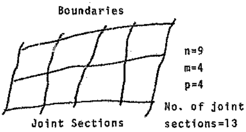

Fig 2.5 Showing calculation of number of equations required to solve network eqns.

Thus $n + m + p + 1$ equations are required to solve for the unknown potential gradients J in each joint.

These equations arise from consideration of the following facts.

1. From considerations of continuity at each intersection of two or more joint segments the algebraic sum of the incoming and outgoing flows from the joints entering the node must be zero. i.e. The sign of the incoming and outgoing flows in any one equation must be opposite. As there are n such intersection points a set of n equations of the form of equation (2.37) can be written

$$\sum_{j=1}^{N_r} q_j = 0 \qquad r = 1 \ldots\ldots\ldots n \tag{2.37}$$

where q_j is the flow rate in the j joint coming into the r intersection point.

N_r is the number of joint sections coming into the r^{th} intersection

2. From considerations of conservation of energy it follows that the sum of the flow losses in any arbitrary closed flow path through joint segments in the system is zero. If the traverse direction around the closed flow path is in the same direction as the flow in the joint the losses are taken as positive, if the traverse direction is in the opposite direction of the joint flow the flow losses are considered negative.

This fact leads to a set of m equations of the form

$$\sum_{j_r=1}^{N_r} l_j \left(\frac{\partial\phi}{\partial n}\right)_j = 0 \qquad r=1\ldots\ldots m \tag{2.38}$$

where l_j is the length of the j^{th} joint segment in the r^{th} closed path in the system

N_r is the number of joint sections in the closed path in the system

$\left(\frac{\partial\phi}{\partial n}\right)_j$ is the potential gradient in the j^{th} joint of the closed path.

3. Paths along a boundary are no longer closed but are open. Hence the sum of the flow losses along a path from one point on the boundary to another on the same boundary is equal to the difference in potential at the beginning and end points on the boundary of the open path. Thus a set of p equations of the form of equation (2.39) can be written

$$\sum_{j_r=1}^{N_r} l_j \left(\frac{\partial\phi}{\partial n}\right)_j = \phi_s - \phi_e \tag{2.39}$$

where ϕ_s and ϕ_e are the potentials at the start and end of the open path.

4. One additional equation to give j equations can be gained by relating two boundary conditions for different boundaries. That is along any path going from one boundary to a second independent boundary the sum of the flow losses is equal to the difference in potential between the two points on the boundaries.

$$\sum_{b_1}^{b_2} l_j \left(\frac{\partial\phi}{\partial n} \right)_j = \phi_s - \phi_e \qquad (2.40)$$

where b_1 and b_2 denote the first and second boundaries.

Thus $i = m + n + p + 1$ equations can be written and can be solved for to yield $\frac{\partial\phi}{\partial n}$ in each joint segment.

Any of the numerous solution techniques for solving large numbers of simultaneous equations may be used.

The above method is also applicable if the flow in any of the joints becomes turbulent. If this occurs an iterative approach must be used to determine the correct flow law, and the equations involving $\frac{\partial\phi}{\partial n}$ must be linearised using techniques explained by Louis (1969) and Sharp (1970).

In some cases where many joints must be considered it is possible to replace a number of them by an equivalent substitute joint. If all the joints to be replaced belong to the same joint set, and each joint has an aperture a_i then if n joints are combined into one equivalent joint the equivalent joint aperture a_e is given by

$$(a_e)^3 = \sum^{n} (a_i)^3 \qquad (2.41)$$

Direct extension of above method to three dimensions is not possible. However, recently Wittke (1970) has presented a method, based on the idea of considering the flow in each three dimensional joint seperately to solve the field flow regime. This method more properly belongs in the Composite Medium Approach considered in the next section.

CLASS 3 THE COMPOSITE MEDIUM APPROACH

This section deals with the approach to those practical field problems where neither of the above two approaches, i.e. the equivalent continuous medium approach or the discrete flow channel approach can be used in its pure form to adequately describe and model the practical field situation. Two such practical field situations occur. They are

(a) Three dimensional joints of limited extent which it is desired to consider as individual planar conductors.

(b) Regions of jointed rock traversed by hydraulically active major geological discontinuities of such a nature that their presence discernably affects the regional flow pattern.

Consider in detail the methods employed for each of the above cases.

(a) Three dimensional planar conductors.

The development of this method is due to Wittke (1970). It is a powerful method for handling certain cases of three dimensional sparsely jointed rock masses, for which the joint characteristics are known. The assumptions which are required for this method are

(i) The intensity, continuity and interconnection of the jointing are such that the rock region can be adequately modelled by a system of intersecting planar conductors.

(ii) Each planar conductor can be represented by a two dimensional porous medium, for which the flow characteristics are known.

The corollaries to the above assumptions are the same as for the discrete flow channel approach.

The potential distribution is solved for by imposing on each joint section a finite element grid, the nodes at the joint intersections being taken to be common to the two or more joint sections meeting at the intersection. Then, using the methods described in the subsection on finite elements, the total system of element nodal potentials is found. Hence the potential gradients and the joint flow characteristics can be solved. Wittke (1970) shows how this method can be used to study transient field conditions.

(b) Major Geological Discontinuities.

The method presented in this section has been evolved to deal with those particular cases where a jointed rock mass is traversed by hydraulically active major geological discontinuities and it is desired to analyse the rock mass as an Equivalent Continuous Medium. The method presented will handle cases of highly impermeable dykes, highly permeable major faults or joints and, as a special case, tension cracks with static water in them.

The following assumptions are made.

(i) The major geological discontinuity can be adequately modelled as a planar conductor through the sides of which water is percolating.

(ii) The jointed rock surrounding the major discontinuity can be adequately modelled as an Equivalent Continuous Medium.

The corrolaries to the above assumptions are,

(i) Some representative hydraulic parameters can be estimated to describe the conductivity of the major geological discontinuity.

(ii) All the assumptions and corollaries given for the Equivalent Continuous Medium Approach apply to the jointed rock mass surrounding the major geological discontinuity.

Fig. (2.6) illustrates the type of region assumed in the following analysis and a possible practical field occurence.

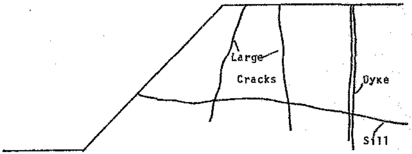

FIG. 2.6 <u>THE PRACTICAL OCCURENCE OF MAJOR GEOLOGICAL DISCONTINUITIES</u>

Consider first an infinite joint in which water is flowing and through the sides of which water is percolating as illustrated in Fig. (2.7). The percolation per unit area of joint side is L.

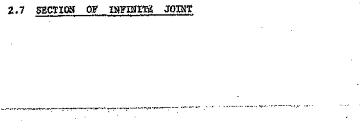

FIG. 2.7 <u>SECTION OF INFINITE JOINT</u>

Assume that the "non-percolation" joint hydraulic characteristics are known and that the flow rate can be described by an equation of the form given in table 2.1.

$$q_n = B_n \, J^{\alpha}$$

where α is a coefficient dependent [illegible] ing in the joint in the n direction.

Fig. 2.8 represents an elemen ut from the parallel joint.

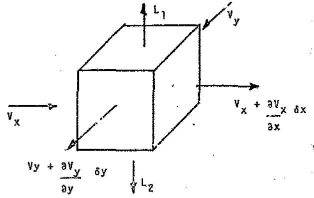

FIG. 2.8 <u>ELEMENT FROM BETWEEN TWO PARALLEL PLATES</u>

Assume that the rock mass on one side of the joint is characterised by a permeability tensor of the form

$$K^1 = \begin{vmatrix} k^1_{xx} & k^1_{xy} & k^1_{xz} \\ k^1_{yx} & k^1_{yy} & k^1_{yz} \\ k^1_{zx} & k^1_{zy} & k^1_{zz} \end{vmatrix} \qquad (2.42)$$

and that the rock mass on the other side is characterised by a permeability tensor K^2 where the superscripts denote indexes and not exponentation.

Total inflow into the element shown in fig. (2.7) is

$$(q_x - \frac{\partial q_x}{\partial x} \frac{\delta x}{2}) \ \delta y \ + (q_y - \frac{\partial q_y}{\partial y} \ \frac{\delta y}{2}) \ \delta x$$

Total outflow is

$$-(q_x + \frac{\partial q_x}{\partial} \ \frac{\delta x}{2}) \delta y - (q_y - \frac{\partial q}{\partial} \ \frac{\delta y}{2}) \delta x - L_1 \delta x \delta y \ - L_2 \delta x \delta y$$

but

$$L_1 = k^1_{zx} \frac{\partial \phi}{\partial x} + k^1_{zy} \frac{\partial \phi}{\partial y} + k^1_{zz} \frac{\partial \phi}{\partial z} \qquad (2.43)$$

and

$$L_2 = k^2_{zx} \frac{\partial \phi}{\partial x} + k^2_{zy} \frac{\partial \phi}{\partial y} + k^2_{zz} \frac{\partial \phi}{\partial z} \qquad (2.44)$$

Hence from continuity, considering that no storage occurs within the element and by combining equations

$$- \frac{\partial q_x}{\partial x} \delta x \delta y \ - \frac{\partial q_y}{\partial y} \delta x \delta y - L_1 \ \delta x \delta y - L_2 \ \delta x \delta y = 0 \qquad (2.45)$$

i.e.

$$\frac{\partial q_x}{\partial x} + \frac{\partial q_y}{\partial y} + L_1 + L_2 = 0 \qquad (2.46)$$

From the equation

$$q_n = B_n \ (\frac{\partial \phi}{\partial n})^{\alpha} \qquad (2.47)$$

This in its most general form equation (2.46) can be written thus

$$\frac{\partial}{\partial x}\{ B_x(J_x)^{\alpha}\} + \frac{\partial}{\partial y}\{ B_y(J_y)^{\alpha}\} + (k^1_{zx} + k^2_{zx})\, J_x$$

$$+ (k^1_{zy} + k^2_{zy})\, J_y + (k^1_{zz} + k^2_{zz})\, J_z = 0 \qquad (2.48)$$

For the two dimensional case of laminar flow in a joint (2.48) reduces to

$$B_x \frac{\partial^2 \phi}{\partial x^2} + (k^1_{zx} + k^2_{zx})\, J_x + (k^1_{zz} + k^2_{zz})\, J_z = 0 \qquad (2.49)$$

For static water in the joint the equation along the joint (2.48) reduces to

$$(k^1_{zz} + k^2_{zz})\, J_z = 0 \qquad (2.50)$$

since

$$J_x = 0 \qquad (2.51)$$

For cases where the field potential is to be found using finite difference methods, the grid can be taken to run parallel to the discontinuity and the finite difference form of equation (2.48) can be written. The extended forms of the equations linking neighbouring points can then be incorporated in the solution routine.

If the discontinuity does not lie parallel to the grid directions then the grid spacing in the vicinity of the joints should be so altered as to ensure that all nodal points fall on the discontinuity. The relationship between nodes on and adjacent to the discontinuity resulting fro⁣m equation (2.48) can then be incorporated in the solution routine.

For tension cracks and joints containing static water, the nodal points of the finite difference grid have specified potentials, the potentials being the static potential in the joint which is usually known from boundary conditions. At all stages of the solution proceedure this specified nodal potential is stipulated at the node and the surrounding nodes are solved in terms of the specified nodal potential.

CONCLUSION

There are many different solution techniques which may be utilised to determine the potential distribution and the flow regime in a jointed rock mass. Each technique involves a different way of modelling the rock mass and hence will lead to different answers.

The accuracy of the answer obtained will depend upon the correctness of the model which is used to represent the jointed rock and of the accuracy and extent of the geological data available to use in the analysis.

It will however be shown in this thesis that the answers obtained from an Equivalent Continuum Approach and a Discrete Flow Channel Approach are for most practical field cases i[illegible]tical and that the choice of one method or the other will be influenced by the nature of the physical problem being investigated.

CHAPTER 3

THE APPLICABILITY OF THE ROCK JOINT MODELS TO THE VARIOUS JOINT CATEGORIES.

It has been stated that an essential part of the method of adjusting flow parameters until correspondence is obtained between measured and calculated fluid pressures is the actual calculation of values of the fluid pressures. In order to perform this step it is necessary to model the jointed rock mass by means of one of the models discussed in the previous Chapter.

Each of these models views the rock mass in a fundamentally different way. As it is important that the model chosen be as good a representation of the rock mass as possible, it follows that the model chosen to represent the rock mass will depend on the actual physical nature and configuration of the joints in the rock mass. Four rock joint categories have been defined. The model which best represents each category and the computational difficulties involved in each method are discussed in this chapter.

Generally the choice of model to represent the rock mass will depend on which model is the most accurate and realistic representation of the jointing of the joint assemblage, the different hydraulic regions, their spatial relationships and the boundary conditions which apply to the region and the whole rock mass. The extent to which the rock is heterogeneous or anisotropic, plus the presence or absence of major geological discontinuities also affects the choice of model.

1. INTACT ROCK, can be homogeneous or heterogeneous and also isotropic or anisotropic. When such a rock mass is both homogeneous and isotropic the Equivalent Medium Approach should be used. Laboratory tests will yield the primary permeability of the material and this can be used in any of the Equivalent Continuous Medium Approaches.

If a numerical computation is desired the finite difference method is suitable provided the boundaries are simple and regular. If the rock material is anisotropic the application of numerical proceedures requires that the equations account for the anisotropy. For the Finite Difference Method this would mean a changed relationship between any particular node and its surrounding nodes. The relevant Finite Difference Equation for any degree of anisotropy is tabulated in Appendix 4. For the Finite Element Method the permeability tensor would then be a diagonal matrix only for the principal axes of the system and the diagonal tensor coefficients would not have the same values.

If the potential distribution for an anisotropic homogeneous rock material is to be determined by graphical or analogue methods the field must first be transformed to the equivalent isotropic field.

The most practical method to adopt when the region is non-homogeneous is to divide the region up into homogeneous subregions. A matrix of permeabilities giving the permeability characteristics at each set of nodes or even each node can then be set up for use in both the Finite Difference and the Finite Element Method. The elements of this matrix would in themselves be matrices.

Where the heterogeneity is completely random a mean value of the statistical distribution can be used. *

2. <u>REGULAR JOINTS</u>. Tests described in this thesis show that both, the Equivalent Continuum Approach and the Discrete Flow Channel Approach can be utilised to model a rock mass composed of regular interconnected joints. These tests as described in Chapter 8 also indicate that the potential distributions determined by these two methods converge to a common answer as the number of joints in the region is increased.

The convergence of the answers is due to the fact that it is possible to derive a rigorous formula and hence a correct value for the permeability tensor for regular interconnected joints. This correct permeability tensor (as derived in Chapter 5) is used in the Equivalent Continuum Approach.

* This is discussed further in Chapter 9.

The Discrete Flow Channel Approach is a rigorously correct model of the practical field situation and provided that the joint characteristics are accurately known, any solution obtained will be correct. Thus the convergence of the answers obtained by the two approaches.

The decision as to which model to use will be based upon

(a) The number of joints in the practical field situation to be analysed.

(b) The availability and ease of utilisation of computer programs to solve the flow regime.

(c) The degree of accuracy required in the solution.

Another method for handling continuous regular joints is presented by Sharp (1970). His method is to assume that the joints form regular squares. From a knowledge of the hydraulic characteristics of the joints he writes equations linking the potentials at each joint intersection node. The final form of the resulting set of equations is exactly the same as the form of the finite difference equations derived for a square grid. In place of a principle axes permeability coefficient occuring in the equations a coefficient describing the hydraulic characteristics of the joints appears. This method is only a special case of the general method of the Discrete Flow Channel Approach. *It could also be considered a variation of the* finite difference method of analysis.

3. <u>IRREGULAR JOINTS</u>. Such rock joint systems are probably the most commonly occuring of all practical field situations. The joints while being irregularly spaced and orientated and incompletely interconnected, usually display a certain tendency to lie in certain preferred directions.* Such rock masses are usually distinctly anisotropic and heterogeneous.

* This preferred direction is referred to in this thesis as the "joint set central tendency".

It would thus appear desirable to always use the Discrete Flow Channel Approach as this could rigorously account for all the effects of random joint spacings, orientations and hydraulic characteristics. However, this implies a complete knowledge of the practical field geometry, which it is practically impossible to obtain. Certain simplifications and assumptions must therefore be made to render the problem amenable to solution by the Discrete Flow Channel Approach. This usually involves assuming that all joint apertures are the same and that the joints are uniformly orientated and spaced.

Should it however be desired to model the rock as a Continuous Medium the value of the permeability tensor to be used has to be estimated. If the irregularity of jointing is such that there exist certain central tendencies for the data describing orientation, spacing and length of joints in each joint set, it is possible to use a corrected value of the permeability tensor for an equivalent regular continuously jointed medium. Correction factors would have to be applied to the contribution from each joint set to the joint assemblage permeability tensor. Such corrections would account for the deviation from the mean of the joint set characteristics. Chapter 6 discusses the theoretical background to this problem. Tests described in Chapters 7 and 8 were performed to study the effects of irregular jointing on the potential distribution in such a mass.

In deciding which of the two main Approaches to use, consideration will have to be taken of the following factors.

(a) Are the joint spacings and lengths large or small in relation to the size of the region or subregions into which for purposes of computation the region is to be divided.

(b) What is the degree of interconnection of the joints.

(c) What is the degree of regularity, i.e. the variance from the central tendency of the joint spacings, orientations and continuity.

(d) What is the extent and reliability of the available data describing the joint patterns and the joint characteristics.

(e) What degree of accuracy of solution is required.

For cases where the joint spacing and lengths are small relative to the region and the subregions considered and where there is a high degree of interconnection the Equivalent Continuum Approach is the more suitable. For relatively few joints in the practical field situation where the joints are long relative to the region, the Discrete Flow Channel Approach will provide the more accurate answer.

4. MAJOR GEOLOGICAL DISCONTINUITIES. This is the particular case for which an analytical method was given in Chapter 2 as a subclass of the Combined Medium Approach.

The equations presented there can be used to describe the flow in individual joints surrounded by highly pervious rock blocks, as well as in major geological discontinuities surrounded by jointed rock.

A serious attempt should always be made in any practical field investigation to locate such geological discontinuities, which may sometimes be no more than an individual highly conductive joint. Failure to locate such discontinuities may well invalidate any calculations that neglect this discontinuity. Rigerous maintainance and checks on practical field piezometers will considerably reduce the likelihood of such discontinuities remaining undetected.

CONCLUSION

The inherent difficulties involved in accurately modelling a jointed rock mass in order to analyse its hydraulic regime, clearly underline the power of the method of adjusting hydraulic parameters.

The field piezometer readings give the correct values of the water pressures at the particular points in the field at which the piezometers are situated. Provided that all precautions are taken to ensure the correct functioning of the piezometers, the results from such piezometers provide the value of the water pressure which is a result of all the irregularities of jointing and known and unknown geological discontinuities.

Therefore, provided care is taken in choosing the most suitable method of modelling the jointed rock mass, and correspondence can be attained between measured and calculated fluid pressures, the parameters which give the best correspondence can be used with confidence in predicting changes in fluid pressures which would occur due to altered boundary conditions.

However, at the heart of the whole process lies the fact that ultimately to apply the method a mathematical model must be made of the jointed rock mass, in order that a series of calculated fluid pressures may be obtained. The discussion contained in the present Chapter should guide the choice of the model which is to be used for any particular joint assemblage.

CHAPTER 4.

VECTOR AND TENSOR METHODS OF DESCRIBING THE PERMEABILITY OF AN ANISOTROPIC ROCK MASS WHICH IS MODELLED AS AN EQUIVALENT CONTINUUM.

An anisotropic, but homogeneous, medium can be characterised by a set of vector or a set of tensor permeability coefficients. It has been stated that if a jointed rock mass is modelled according to the Equivalent Continuous Medium Approach, both the finite difference and the finite element methods involve the use of a permeability tensor. Certain graphical and analogue techniques and in certain circumstances the finite difference method involve the use of vectors of permeability. It is thus instructive to compare the methods and to evolve the relationships between the two types of permeability coefficients.

Strictly the use of the terms Vector and Tensor are anomalous, for what in this thesis is usually called a tensor is actually a tensor of rank two and a vector is a tensor of rank one. (see appendix 2) However, the terms Vector and Tensor method appear to be accepted and are standard terminology amongst writers on the subject. Accordingly, they will be used in this thesis.

A REVIEW OF THE HISTORICAL DEVELOPMENT OF THE IDEAS OF TENSOR AND VECTOR PERMEABILITIES.

Darcy (1856) as a result of experiments performed in investigating the public water supply for the French city of Dijon, noted the proportionality between the velocity of flow in a porous medium and the hydraulic gradient applied to the medium. Thus Darcy's law which defines the proportionality between a velocity vector and a parallel potential gradient in an isotropic medium arose.

$$V_n = -k \frac{\partial \phi}{\partial n} = -k J_n \qquad (4.1)$$

when V_n is the velocity vector of flow

k is the permeability coefficient of the medium

J_n the potential gradient parallel to n

The first recorded experiments to study anisotropy are those by Duhammel who in 1832 studied anisotropic conductivity by measuring the elliptic shape of the melting front around a small heat source embedded in crystals coated with paraffin.

Versluys in 1915 was the first to explain anisotropic permeability by modelling the conductors as arbitrarily-oriented bundles of tubes. He showed that any four arbitrary sets of conductors may be replaced by three mutually orthogonal sets with conductivities Kx, Ky and Kz respectively. Thus these K coefficients are the principal axes permeabilities.

In 1948 Ferrandon derived the tensor form of the permeability coefficients from a model consisting of a bundle of tubes. In the same year Johnson and Hughes (1948) studied experimentally the significance of directional permeabilities in oil bearing sandstones by cutting small horizontal plugs at varying directions and determining their permeability.

Scheidegger (1954) analysed the data of Johnson and Hughes according to Ferrandon's theory, and also plotted their original results as ellipses of permeability. The test results, published without physical explanation, substantiated Ferrandon's theory originally published without any test results. Scheidegger published two further definitions of vector permeability in the same year.(given on Page 63)

Snow (1965) presented a thorough investigation of the form of the permeability tensor for jointed rock masses and the effect of joint orientation dispersion and aperture size distribution on the value of the tensor permeability coefficients.

The presentations in this chapter are similar to the original presentation by Ferrandon and Scheidegger. The expression for the permeability tensor for jointed rocks was derived independently of Snow and hence is different to that given by him.

ISOTROPIC FLOW

Starting with Darcy's original observation that there exists a proportionality between the flow velocity and the head lost per unit distance of flow in a porous medium the following can be written.

$$V \quad \alpha \frac{\Delta\phi}{\Delta s} \qquad (4.2)$$

where V is the fluid flow velocity

$\Delta\phi$ is the change in head or potential through a distance Δs measured in the direction of flow.

k is defined as the isotropic permeability coefficient ccording to the following equation

$$V = -k \frac{\Delta\phi}{\Delta s} \qquad (4.3)$$

k is a function of the geometric properties of the medium and of the properties of the fluid.

By definitio.. as Δs tends to zero.

$$\frac{\partial\phi}{\partial s} = \lim_{\Delta s \to 0} \frac{\Delta\phi}{\Delta s} \qquad (4.4)$$

Where $\frac{\partial\phi}{\partial s} = J_s$ are defined as the potential gradient in the direction s

Hence $$V_s = -k \frac{\partial\phi}{\partial s} = -k\ J_s \qquad (4.5)$$

This equation implies that the velocity is parallel to the potential gradient.

The components of the velocity relative to a co-ordinate axis system (x,y,z) can then be written

$$V_x = -k\ J_x \qquad V_y = -k\ J_y \qquad V_z = -k\ J_z \qquad (4.6)$$

where Jx, Jy, and Jz are the components of the potential gradient along the (x,y,z) axes.

The form of the Laplace equation describing the potential distribution in an isotropic medium is thus

$$\frac{\partial^2\phi}{\partial x^2} + \frac{\partial^2\phi}{\partial y^2} + \frac{\partial^2\phi}{\partial z^2} = 0 \qquad (4.7)$$

ANISOTROPIC FLOW

The isotropic form of Darcy's Law implies that the velocity vector is always parallel to the potential gradient. For anisotropic media in general this is not true. It will be shown that the velocity is parallel to the gradient only along three mutually orthogonal axes defined as the principal axes of the medium.

1. TENSOR PERMEABILITY.

Two derivations of the tensor form of the permeability matrix are given below; one an intuitive type derivation and the other Ferrandon's rigerous mathematical derivation.

(a) The "intuitive" derivation of the Permeability Tensor.

For purposes of this derivation it is necessary to consider the anisotropic medium to be such that if a potential gradient is imposed on it, flow takes place in such a manner that the velocity vector has three components, one parallel to the imposed gradient, the other two at right angles to it. *The proportionality coefficient between the imposed potential gradient and the velocity of flow orthogonal to it is known as the cross permeability coefficient usually written k_{ij} where j is the gradient direction and i is orthogonal to the j direction. It is necessary to assume that the principle of superposition is valid, i.e. the velocity vector due to one potential gradient can be added directly to the velocity vectors due to second and third potential gradients. This is true in particular if the flow velocities, both individually and combined, are within the range of laminar flow.

If a potential gradient J_x is imposed on an anisotropic medium, flow results with a macroscopic velocity vector not necessarily parallel to J_x. The components of the velocity vector along the x,y,z axes are then from the above definition of the cross permeability coefficient

* see footnote over.

* This can be most easily illustrated by the following example. If a jointed mass as shown in fig. (4.1) is confined in between two impermeable boundaries and a different potential is applied at opposite sides, (AB and CD) then the applied gradient is as shown. Flow will occur from face AB to face CD if AB is at the higher potential. However, because of the nature of the joints at no point will flow be solely parallel to the imposed gradient. The flow will always be such that at any point there is one component of flow parallel to the applied gradient and one orthogonal to it.

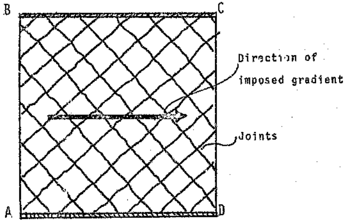

FIG 4.1 A JOINTED ROCK MASS INBETWEEN IMPERMEABLE PLATES

$$v_x^1 = -k_{xx}\, J_x \qquad v_y^1 = -k_{yx}\, J_x \qquad v_z^1 = -k_{zx}\, J_x \tag{4.8}$$

where the superscrips are indices. Remove the potential gradient Jx and apply a potential gradient Jy. Hence again the components of the velocity vector are

$$v_x^2 = -k_{xy}\, J_y \qquad v_y^2 = -k_{yy}\, J_y \qquad v_z^2 = -k_{zy}\, J_y \tag{4.9}$$

Remove Jy and apply Jz. Then the velocity components are

$$v_x^3 = -k_{xz}\, J_z \qquad v_y^3 = -k_{yz}\, J_z \qquad v_z^3 = -k_{zz}\, J_z \tag{4.10}$$

Now simultaneously apply Jx, Jy and Jz.
From the assumption that the principle of superposition is valid the velocity components are the sum of the velocity components due to the separate applications of the gradients Jx, Jy, Jz i.e.

$$\begin{aligned} v_x &= -k_{xx}\, J_x - k_{xy}\, J_y - k_{xz}\, J_z \\ v_y &= -k_{yx}\, J_x - k_{yy}\, J_y - k_{yz}\, J_z \\ v_z &= -k_{zx}\, J_x - k_{yz}\, J_y - k_{zz}\, J_z \end{aligned} \tag{4.11}$$

In matrix notation

$$\begin{Bmatrix} v_x \\ v_y \\ v_z \end{Bmatrix} = \begin{vmatrix} k_{xx} & k_{xy} & k_{xz} \\ k_{yx} & k_{yy} & k_{yz} \\ k_{zx} & k_{zy} & k_{zz} \end{vmatrix} \begin{Bmatrix} J_x \\ J_y \\ J_z \end{Bmatrix} \; * \tag{4.12}$$

It can be shown from energy considerations, that K is a symmetric tensor. Ferrandon's derivation demonstrates the symmetry of K by rigorous mathematics.

* Or in vector notation $V = -K \text{ grad } \Phi$ (4.13)

(b) Ferrandon's Derivation of the Permeability Tensor.

Ferrandon (1948) produced the following derivation of the permeability tensor. At a point M (fig 4.2) in an anisotropic porous body a surface is taken such that this surface S' has a unit normal vector $\bar{n}'$ (α' β' γ') and that there exists another surface S bounded by the solid angled $d\Sigma$ which has unit normal vector $\bar{n}$ (α β γ)

. If the potential gradient J is in the direction $\bar{n}'$, $\mu_n d\Sigma$ is the effective conducting area corresponding to the unit area s , where μ_n is the factor that accounts for the occurrence of the solids forming the filtering medium, and is function of $\bar{n}$. The scalar product of the two unit vectors $\bar{n}.\bar{n}'$ is the cosine of the angle between the vectors $\bar{n}$ and $\bar{n}'$ and hence $\mu_n\ \bar{n}.\bar{n}'\ d\Sigma$

is the effective conducting area in the direction n . From this it follows that the elementary quantity of flow across the unit area S is

$$dq_n = k_n \mu_n \bar{n}.\bar{n}' J d\Sigma \qquad (4.14)$$

where k_n is the medium permeability in the direction n .

The total outflow through the unit area s' through the filter medium is obtained by direct intergration of dq through the portion of solid space (solid angle 2π) situated on the same side of the area S' as the +ve normal n' .

However

$$J = -\frac{d\phi}{dn} = -\left(\alpha\frac{\partial\phi}{\partial x} + \beta\frac{\partial\phi}{\partial y} + \gamma\frac{\partial\phi}{\partial z} \right) \qquad (4.15)$$

However, k and μ are functions of n (α β γ) thus the result of the integration must remain a definite function of n (α β γ) which leads us to put

$$A = \int_0^{2\pi} k\ \mu\alpha^2 d\Sigma \qquad B = \int_0^{2\pi} k\ \mu\beta^2 d\Sigma \qquad C = \int_0^{2\pi} k\ \mu\gamma^2 d\Sigma$$

$$(4.16)$$

$$D = \int_0^{2\pi} k\mu\alpha\beta d\Sigma \qquad E = \int_0^{2\pi} k\mu\alpha\gamma d\Sigma \qquad F = \int_0^{2\pi} k\mu\beta\gamma d\Sigma$$

and to introduce the right symmetric matrix

$$K = \begin{vmatrix} A & F & E \\ F & B & D \\ E & D & C \end{vmatrix} \qquad (4.17)$$

Thus (4.14) can be integrated and written in the form

$$q_n = - \bar{n}' \; (\bar{K} \; \text{grad}\Phi) \qquad (4.18)$$

a unit area is being considered, so $\quad q_n = v_n$

$$\text{thus} \quad v_n = - \bar{n}' \; (\bar{K} \; \text{grad}\Phi) \qquad (4.19)$$

If v_n is written as $\begin{Bmatrix} v_x \\ v_y \\ v_z \end{Bmatrix}$ then (4.19)

becomes

$$\begin{Bmatrix} v_x \\ v_y \\ v_z \end{Bmatrix} = - \bar{K} \; \text{grad}\Phi \qquad (4.20)$$

which is the same as (4.13)

Fig. 4.2 THE SURFACES AND VECTORS CONSIDERED IN FERRANDON'S DERIVATION OF THE PERMEABILITY TENSOR.

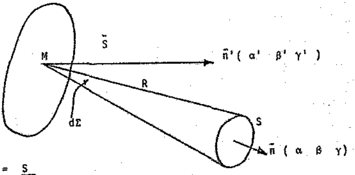

$$d\Sigma = \frac{S}{R^2}$$

Some Consequences of the Fact that Permeability can be written as a Tensor.

The fact that the permeability of an anisotropic porous medium can be written as a symmetric second order tensor, leads immediately to the following conclusions.

(a) In general the velocity vector $\underset{\sim}{V}$ and the potential gradient $\underset{\sim}{J}$ do not have the same direction.

(b) There exist three mutually orthogonal axes in space along which the directions of the velocity vector and the potential gradient are parallel. These axes are the principal axes of the medium. Their direction is that of the eigenvectors of the permeability tensor.

(c) For any three-dimensional porous medium there are six independent permeability coefficients. For a two dimensional medium there are three permeability coefficients.

(d) The fact that the velocity vector can be written $\underset{\sim}{V} = -K \, \mathrm{grad}\Phi$ leads to the fact that when values for $\{v_x \;\; v_y \;\; v_z\}$ are substituted into the continuity equation

$$\frac{\partial v_x}{\partial x} + \frac{\partial v_y}{\partial y} + \frac{\partial v_z}{\partial z} = 0 \qquad (4.21)$$

The following equation describing the potential distribution in an anisotropic medium results.

$$\sum_{i=x}^{z} \sum_{j=x}^{z} k_{ij} \frac{\partial^2 \phi}{\partial i \partial j} = 0 \qquad (4.22)$$

For two dimensions this can be written

$$k_{xx} \frac{\partial^2 \phi}{\partial x^2} + 2k_{xy} \frac{\partial^2 \phi}{\partial x \partial y} + k_{yy} \frac{\partial^2 \phi}{\partial y^2} = 0 \qquad (4.23)$$

(e) If the value of the permeability tensor is known for one set of axes it can readily be obtained frr any other set of axes.

The Manipulation of the Permeability Tensor.

Assume that the permeability tensor is known for one axis system $(x\ y\ z)$

$$\text{i.e.} \qquad K = \begin{vmatrix} k_{xx} & k_{xy} & k_{xz} \\ k_{yx} & k_{yy} & k_{yz} \\ k_{zx} & k_{zy} & k_{zz} \end{vmatrix} \tag{4.24}$$

If the equivalent permeability tensor $\bar{K}$ with respect to the axes $(\bar{x}\ \bar{y}\ \bar{z})$ is required, the following procedure is to be adopted.

Let L be the axes transformation matrix i.e.

$$\begin{Bmatrix} \bar{x} \\ \bar{y} \\ \bar{z} \end{Bmatrix} = \begin{vmatrix} \lambda_1 & \mu_1 & \eta_1 \\ \lambda_2 & \mu_2 & \eta_2 \\ \lambda_3 & \mu_3 & \eta_3 \end{vmatrix} \begin{Bmatrix} x \\ y \\ z \end{Bmatrix} \tag{4.25}$$

$$\text{i.e.} \quad \bar{x} = L\, x \tag{4.26}$$

Either by means of tensor transforms (see Appendix 2) or by reasoning from first principles it can be shown that

$$\bar{K} = L\, K\, L^t \tag{4.27}$$

where L^t is the transpose of L

If V_1 is the velocity vector in the $(x\ y\ z)$ axes system,
V_2 is the velocity vector in the $(\bar{x}\ \bar{y}\ \bar{z})$ axes system,
$grad\phi_1$ is the gradient vector in the $(x\ y\ z)$ axis system,
$grad\phi_2$ is the gradient vector in the $(\bar{x}\ \bar{y}\ \bar{z})$ axis system,

it is true that
$$V_1 = -K\ grad\phi_1 \tag{4.28}$$

and
$$V_2 = -K\ grad\phi_2 \tag{4.29}$$

but
$$V_2 = L\ V_1 \tag{4.30}$$
$$= -L\ K\ grad\phi_1 \tag{4.31}$$

Also
$$grad\phi_2 = L\ grad\phi_1 \tag{4.32}$$

therefore
$$grad\phi_1 = L^{-1}\ grad\phi_2 \tag{4.33}$$

but L is an orthogonal matrix i.e. $L^{-1} = L^t$
where L^{-1} is the inverse of L
Thus (4.33) becomes
$$grad\phi_1 = L^t\ grad\phi_2$$

Substituting into (4.31) gives
$$V_2 = -L\ K\ L^t\ grad\phi_2 \tag{4.34}$$

Thus from
$$\bar{K} = L\ K\ L^t \tag{4.35}$$

Equation (4.35) is true in two and three dimensions. This is an important result and is used particularly in the finite element method to transform a permeability tensor in a local co-ordinate axis system to the equivalent tensor in the global co-ordinate axis system.

If the two dimensional form of equation (4.35) is expanded the following relationships amongst the permeability coefficients *in the two axes systems (x y z) and ($\bar{x}$ $\bar{y}$ $\bar{z}$) whose X axes are at* an angle θ to each other result.

$$\bar{k}_{xx} = k_{xx}\cos^2\theta + 2k_{xy}\cos\theta\sin\theta + k_{yy}\sin^2\theta \qquad a$$

$$\bar{k}_{xy} = (k_{yy} - k_{xx})\cos\theta\sin\theta + k_{xy}(\cos^2\theta - \sin^2\theta) \qquad b \quad (4.36)$$

$$\bar{k}_{yy} = k_{yy}\cos^2\theta - 2k_{xy}\cos\theta\sin\theta + k_{xx}\sin^2\theta \qquad c$$

From these relationships the direction of the Principal Axes of Permeability can be derived. The axes ($\bar{x}$ $\bar{y}$ $\bar{z}$) will be the principal axes for the special case $\bar{k}_{xy} = 0$. Hence equating the right hand side of equation (4.36b) to zero and re-arranging gives

$$\tan 2\bar{\theta} = \frac{2k_{xy}}{(k_{xx} - k_{yy})} \qquad (4.37)$$

Where $\bar{\theta}$ is the angle between the X axes and the $\bar{x}$ axis of the principal axes system. See fig. 4.3

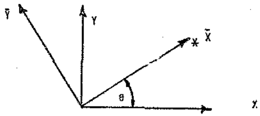

FIG. 4.3 THE RELATIVE ORIENTATION OF THE TWO SETS OF AXES USED IN EQN.4.36

The practical situation which often arises is that estimates have to be made of the values of *the permeability tensor coefficients* for a jointed rock. Certain estimates which at first might appear reasonable often are inadmissable as they might lead to values of the diagonal tensor terms for other axes which are negative, and this denotes a physically impossible situation. However, it is possible for negative values for the off-diagonal terms of the permeability tensor to exist. This only implies that a potential gradient in the positive direction of one of the axes causes flow such that there is a component of velocity of the flow in the negative direction of the orthogonal axis.

The following inequality can thus be used as a criterion for the validity of the tensor coefficients. This inequality can be derived from the fact that k_{xx} and k_{yy} must always be greater than zero.

$$k_{xy}^2 < \frac{\sqrt{4k_{xy}^2 + (k_{xx} - k_{yy})^2} * (k_{xx} + k_{yy})}{4} - \frac{(k_{yy}-k_{xx})^2}{2} \tag{4.38}$$

Similar equations could be derived for three dimensional systems. The tensor form of writing the permeability of an anisotropic medium is particularly useful in that manipulation of the tensor is simple and the equations to which it gives rise in both the finite difference and the finite element methods are convenient to use.

2. VECTOR PERMEABILITY.

In general in an anisotropic, homogeneous body the direction of the velocity vector and the potential gradient are not parallel. Thus there exist two ways in which a vector coefficient of permeability can be defined. (Scheidegger 1954)

i The Vector Permeability Coefficient k' is defined as the ratio of the flow velocity to the component of the potential gradient in the direction of the flow.

ii The Vector Permeability Coefficient k'' is defined as the ratio of the component of the velocity vector in the direction of the potential gradient to the potential gradient.

k' and k'' are scalars.

These definitions result in the different values of k' and k''. The difference between the two is a function of the anisotropy of the material and of the directions of flow and the potential gradient relative to the principal axes of the system.

The following physical representation of these two types of permeability coefficients is usually given.

Cut from the anistropic medium, a long thin pencil shaped specimen, the specimen being encased along the sides. In such a case the seepage velocity must obviously be along the pencil's axis, whereas the direction of the equipotentials is unknown, for generally the equipotentials will be oblique to the axis of the pencil i.e. non-orthogonal to the flow velocity. This situation is a representation of the sort of test that would yield a value for k'.

Cut a pancake like slice from the porous medium, and impose constant potentials on the broad surfaces. Thus the gradient is fixed and known while the velocity is generally oblique to the equipotentials and inclined to the principal axes of permeability. This represents the situation from which k'' can be derived.

It follows that for each direction in the medium there exists a different value of k' and k''. The variation of k' and k'' with direction in the medium is as detailed in the following section.

The Variation of k' and k'' with Direction.

The anisotropy of a porous medium is described by the two principal permeabilities k_x and k_y where k_x is larger than k_y. These quantities should not be confused with the double subscripted variables used in the previous section, although if the axes x and y are the principal axes it follows that $k_x = k_{xx}$ and $k_y = k_{yy}$.

The flow conditions at each point are defined by the magnitude and direction of the velocity V and the magnitude and direction of the potential gradient $J_n = \frac{\partial\phi}{\partial n}$ (see fig. 4.4)

From fig. (4.3) the components of the velocity in the direction of the axes are

$$v_x = -k_x J_n \cos\alpha \qquad v_y = -k_y J_n \sin\alpha \qquad (4.39)$$

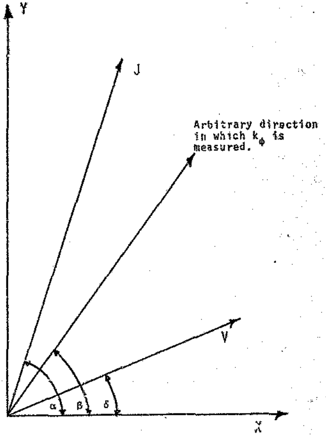

FIG. 4.4 GENERAL FLOW CONDITIONS IN AN ANISOTROPIC MEDIUM

The potential gradient at any arbitrary angle β can be expressed as

$$J_\beta = J \cos(\alpha - \beta) \qquad (4.40)$$

If k_β is defined as the ratio V_β / J_β by resolving V_x and V_y to the direction β it follows

$$k_\beta = \frac{k_x \cos\alpha \cos\beta + k_y \sin\alpha \sin\beta}{\cos\alpha \cos\beta + \sin\alpha \sin\beta} \qquad (4.41)$$

Beginning with the components of the potential gradient in the direction of the axes k_β can be derived in a similar fashion to give

$$k_\beta = \frac{\cos\delta \cos\beta + \sin\delta \sin\beta}{\dfrac{\cos\delta \cos\beta}{k_x} + \dfrac{\sin\delta \sin\beta}{k_y}} \qquad (4.42)$$

If the arbitrary angle β coincides with the angle α equation (4.41) reduces to

$$k_\alpha = k_x \cos^2\alpha + k_y \sin^2\alpha \qquad (4.43)$$

k_α is thus the permeability coefficient in the direction of the potential gradient as a ratio of the component of the velocity in that direction.

From the definition of k'' it follows

$$k_\alpha = k'' \qquad (4.44)$$

i.e.

$$k'' = k_x \cos^2\alpha + k_y \sin^2\alpha \qquad (4.45)$$

Similarly if β coincides with the angle δ

$$\frac{1}{k_\delta} = \frac{\cos^2\delta}{k_x} + \frac{\sin^2\delta}{k_y} \tag{4.46}$$

Thus k_δ in equation (4.46) is the permeability coefficient in the direction of the velocity as a ratio of the component of the potential gradient in that direction. From the definition of k' therefore

$$k_\delta = k' \tag{4.47}$$

i.e.

$$\frac{1}{k'} = \frac{\cos^2\delta}{k_x} + \frac{\sin^2\delta}{k_y} \tag{4.48}$$

To study the relationship between k' and k'' consider what occurs where $\alpha=\delta$. Take the ratio k_α/k_δ

$$\frac{k_\alpha}{k_\delta} = 1 + \frac{k_x}{k_y}\left(1 - \frac{k_y}{k_x}\right)^2 \sin^2\alpha \cos^2\alpha \tag{4.49}$$

Since $\alpha=\delta$ the ratio k_α/k_δ should equal 1

Therefore the term

$$\frac{k_x}{k_y}\left(1 - \frac{k_y}{k_x}\right)^2 \sin^2\alpha \cos^2\alpha$$

is the difference between k_α and k_δ .

Marcus (1962) has presented graphs plotting the percentage difference between k_α and k_δ as a function of the ratio k_x/k_y. For $k_x/k_y = 0.5$ the percentage difference between k_α and k_δ is 10% and this difference increases rapidly to 80% for $k_x/k_y = 0.2$ and to greater than 400% for $k_x/k_y = 0.1$. Thus the use of a vector approach for the analysis of practical field problems should be avoided, or at worst used with extreme care. As the analytical methods are tailored to the tensor permeability approach the shortcomings of the vector approach are of little practical importance.

The vector approach and the anomalies it induces are likely to be of significance only in the small scale laboratory testing of anisotropic soils.

As k_x was assumed the maximum and k_y the minimum permeability an ellipse of permeability can be drawn giving values of k' and k'' for any angle from the principal axes. The ellipse has major and minor axes of $k_x^{1/2}$ and $k_y^{1/2}$ in the case of equation (4.46) and $k_x^{-1/2}$ and $k_y^{-1/2}$ in the case of equation (4.48) the radius of the two ellipses being $k_\alpha^{1/2}$ or $k_\delta^{-1/2}$ respectively.

THE RELATIONSHIP BETWEEN TENSOR AND VECTOR PERMEABILITY COEFFICIENTS

The permeability of a medium is an intrinsic property of the material, hence the values of permeability coefficients as derived by different mathematical approaches are related.

Consider briefly the salient differences between the vector and tensor methods before exploring their mathematical inter-relationships.

The tensor approach is based on the fact that the velocity components along the system axes are expressed as functions of the mutually orthogonal potential gradients also along the system axes. The vector approach however, expresses the velocity vector as a function of the component of the potential gradient in the direction of the velocity or the velocity component in the direction of the potential gradient as a function of the potential gradient.

Define n as the unit vector in the direction of k' and k''.

From Ferrandon's derivation of the permeability tensor, the following equation resulted.

$$V_n = - n \ (K \ \mathrm{grad}\phi \ ). \qquad (4.50)$$

For a two dimensional system where $n = (\cos\theta \quad \sin\theta)$

$$K = \begin{vmatrix} k_{xx} & k_{xy} \\ k_{yx} & k_{yy} \end{vmatrix} \qquad \mathrm{grad}\phi = \begin{Bmatrix} J_x \\ J_y \end{Bmatrix}$$

when multiplied out equation (4.50) yields

$$V_n = (k_{xx} \cos\theta + k_{xy} \sin\theta) J_x + (k_{xy} \cos\theta + k_{yy} \sin\theta) J_y \qquad (4.51)$$

From equation (4.50)

$$\mathrm{grad}\phi = - V_n K^{-1} n'$$

where K^{-1} is the inverse of K

n' is the transpose of n

If a tube is cut from an aniso-ropic medium, the filter velocity V is parallel to the axis of the tube i.e. $V = V_n$. If the ratio of the length of the sample to the cross-section is large ϕ the potential drop across the ends of the tube is also parallel to n i.e. $\phi = \phi n$. V_n and ϕ are therefore parallel. From the definition of k' herefore

$$k' = - \frac{V_n}{\phi n} \qquad (4.52)$$

However, it has been shown that in general the equipotentials in such a tube are oblique to the axes of the tube and the following fact must be utilised.

$$\Phi_n = n \text{ grad}\phi \qquad (4.53)$$

Thus from equation (4.52)

$$\Phi_n = - n K^{-1} n' V_n \qquad (4.54)$$

Substituting into (4.52) gives

$$k' = \frac{1}{n K^{-1} n'} \qquad (4.55)$$

which expresses the relationship between the value of k' in the direction with unit direction vector n and the permeability tensor.

For a two dimensional system, if the principal axes of the system are chosen as the reference frame with corresponding principal permeability coefficients k_{xx} and $_{yy}$ equation (4.55) reduces to

$$\frac{1}{k'} = \frac{\cos^2\theta}{k_{xx}} + \frac{\sin^2\theta}{k_{yy}} \qquad (4.56)$$

which checks with equation (4.48)

If a flat pancake is cut from the porous anisotropic medium instead then Φ is again parallel to n .

From equation (4.53)

$$\text{grad} = n' \phi_n \qquad (4.57)$$

By definition

$$k'' = \frac{V_n}{\phi n} \qquad (4.56)$$

In this instance $v_n = n\ K\ \text{grad}\phi$ (4.59)

Substituting (4.59) and (4.57) into (4.53) yields

$$k'' = n\ K\ n' \qquad (4.60)$$

For a two dimensional system, n at an angle θ to the axes (x y)

$$k'' = k_{xx} \cos^2\theta + 2k_{xy} \cos \sin\theta + k_{yy} \sin^2\theta \qquad (4.61)$$

For $k_{xy} = 0$ i.e. (x,y) the principal axes (4.61) reduces to (4.45) . k'' is equal to the $\bar{k}_{xx}$ tensor coefficient in the ($\bar{x}\ \bar{y}$) axes system situated at θ to the (x y) axes, equation (4.36c). This illustrates well the power and advantages of the tensor method over the vector method.

Consider the velocity component v_x .

From the vector method and for the definition of k'' .

$$\bar{v}_x = - k''\ J \qquad (4.62)$$

For this equation to be valid J must lie along the $\bar{x}$ axes, otherwise the definition of k'' is not satisfied.

From the tensor method

$$v_{\bar{x}} = k_{\bar{x}\bar{x}}\ J_{\bar{x}} + k_{\bar{y}\bar{y}}\ J_{\bar{y}} \qquad (4.63)$$

In this case $J_{\bar{x}} = J$ and $J_{\bar{y}} = 0$

If J is displaced such that it does not lie along the $\bar{x}$ axis then equation (4.62) is no longer valid. The new value of k''_z say in the new direction of J must be found to apply equation (4.63). However, for equation (4.63) the components of J in its new position i.e. $J_{\bar{x}}$ and $J_{\bar{y}}$ are merely found the substituted into (4.63), the values of $k_{\bar{x}\bar{x}}$ and $k_{\bar{y}\bar{y}}$ remaining unchanged.

For the practical field problems encountered in Civil Engineering and in Rock Mechanics in particular, the tensor approach to permeability appears to be the more versatile and powerful. It is easier to manipulate, easy to use in analytical methods and values of the tensor coefficients can be calculated rigorously from joint characteristics and orientation data. Hence the tensor approach will be used in this thesis and methods will be presented in the next Chapter for determining the value of the tensor permeability coefficients.

CHAPTER 5

THE DETERMINATION OF THE PERMEABILITY TENSOR FOR A REGULARLY JOINTED ROCK MASS.

If a jointed rock mass is to be modelled according to the Equivalent Continuum Approach it is necessary to have values of the tensor permeability coefficients for use in a theoretical analysis, which may be carried out by the finite difference or the finite element method. The present chapter considers the value of these coefficients for a jointed rock mass traversed by continuous joints, uniformly spaced, all the joints in any one particular joint set having the same orientation.

The Flow of Water in an Individual Joint

Assume that water is flowing inbetween two parallel plates a distance e apart, fig.5.1, which in practice would be the sides of rock blocks. It is necessary that the rock material be assumed impervious, so that the flow from the rock material into the joint may be neglected.

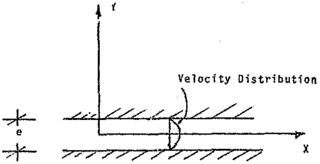

Fig 5.1 FLUID FLOW INBETWEEN TWO PARALLEL IMPERVIOUS PLATES

A standard equation from classical fluid mechanics giving the velocity distribution inbetween two plates is

$$v_x = \frac{1}{2\mu} \left(y^2 - \frac{e^2}{4} \right) \frac{\partial\phi}{\partial x} \qquad (5.1)$$

where v_x is the fluid flow velocity at a distance
y from the origin (see fig. 5.1)
μ is the viscosity of the water
e is the joint aperture
$\frac{\partial\phi}{\partial x}$ is the potential gradient in the x direction

From this equation the average velocity in the joint may be calculated to give

$$v_{ave} = - \frac{e^2}{12\mu} \frac{\partial\phi}{\partial x} \qquad (5.2)$$

The Permeability of Jointed Masses

Consider fig. 5.2 which shows a system of parallel joints in a jointed rock.

Let d = the joint spacing
e = the joint apertures
V = the average joint flow velocity from equation (5.1)
q = the total outflow from a fissure as shown in fig. (5.2)

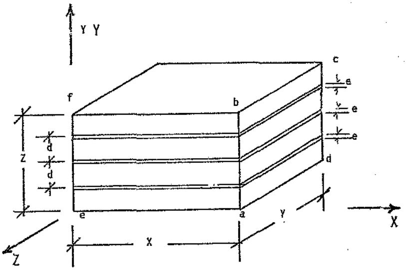

Fig 5.2 ELEMENT CUT FROM A ROCK MASS WITH ONE PARALLEL JOINT SYSTEM

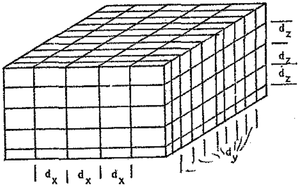

Fig 5.3 UNIT ELEMENT FROM ROCK MASS WITH THREE ROCK JOINT SYSTEMS

Then

$$q_x = v_x \; e \; Y \tag{5.3}$$

The total outflow in the X direction from the system of fissures shown is

$$\sum_{i=1}^{N} q_i = v \; e \; Y \; N \tag{5.4}$$

where N is the number of joints in the height Z

If $\bar{V}$ is taken as the apparent velocity of outflow from the face a b c d equation (5.5) can be written

$$\bar{V} = - K \frac{\partial \phi}{\partial x} \tag{5.5}$$

This equation implies that there is no variation of ϕ in the Z direction or that the average value of $\frac{\partial \phi}{\partial x}$ is used.

$$\text{Thus } \bar{v}_x = \frac{\Sigma q_i}{Y \; Z} = \frac{v_x \; e \; Y \; N}{Y \; Z} = \frac{v_x \; e \; N}{Z} \tag{5.6}$$

However $(N - 1) \; d = Z$

but if N is large then $Nd \approx Z$ and $Nd = Z$ can be used without significant error.

Substituting equation (5.1) into (5.6) yields

$$\bar{v}_x = - \frac{e^3}{12 \; \mu \; d} \frac{\partial \phi}{\partial x} \tag{5.7}$$

By comparison with (5.5)

$$K = \frac{e^3}{12\,\mu\, d} \tag{5.8}$$

Thus it can be seen that for the rock joint pattern illustrated in fig. (5.3) the following equation describes the macroscopic velocity vector

$$\begin{Bmatrix} v_x \\ v_y \\ v_z \end{Bmatrix} = \left|\begin{array}{c|c|c} \frac{e_y^3}{d_y} + \frac{e_z^3}{d_z} & & \\ \hline & \frac{e_z^3}{d_z} + \frac{e_x^3}{d_x} & \\ \hline & & \frac{e_x^3}{d_x} + \frac{e_y^3}{d_y} \end{array}\right| \begin{Bmatrix} \frac{\partial\phi}{\partial x} \\ \frac{\partial\phi}{\partial y} \\ \frac{\partial\phi}{\partial z} \end{Bmatrix} \tag{5.9}$$

Such joint systems do not usually occur and since it is necessary to be able to handle various joints at arbitrary angles to the axes, the following general derivation for a three dimensional case is given.

<u>The Permeability Tensor for a Three Dimensional Jointed Rock System</u>

Assume a jointed rock mass, characterised by one regular continuous set, with the following properties.

e the joint apertures

d the joint spacing

n the unit vector in the direction of the true dip of the joint set

$\bar{e} = \frac{e^3}{12\mu d}$ the form factor for the joint set.

The definition of a joint set dip as used in this paper is not the same definition as commonly employed by geologist. Dip as defined in this thesis is the direction of the joint orientation measured with respect to a right handed co-ordinate axes system, the Z axis pointing vertically upward.

Impose a potential gradient J on the jointed rock mass, such that the potential gradient vector is $\underset{\sim}{J}$

Thus the potential gradient in the n direction is

$$J_n = n \underset{\sim}{J} \tag{5.10}$$

From equation (5.7)

$$v_n = - \bar{e} J_n \tag{5.11}$$

From equation (5.10)

$$v_n = - \bar{e} n \underset{\sim}{J} \tag{5.12}$$

The velocity vector V of the velocity of flow v_n is

$$\underset{\sim}{V} = n' v_n \tag{5.13}$$

hence

$$\underset{\sim}{V} = - n' \bar{e} n \underset{\sim}{J} \tag{5.14}$$

where n' is the transpose of n

However by definition of the permeability tensor

$$\underset{\sim}{V} = - K \underset{\sim}{J} \tag{5.15}$$

therefore

$$K = n' \bar{e} n \tag{5.16}$$

If there are N joint sets in the rock mass each with form factor $\bar{e}_r$ and unit dip vectors n_r the total permeability matrix is

$$K = \sum_{r=1}^{N} (n_r' \bar{e}_r n) \tag{5.17}$$

The Permeability Tensor for a Two Dimensional Jointed Rock System

Assume a two dimensional jointed rock system as shown in fig.(5.4)

Fig 5.4 TWO DIMENSIONAL ROCK JOINT SYSTEM.

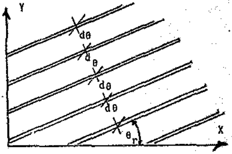

For this system $\quad n = (\cos\theta \quad \sin\theta \ )$

$$\bar{e} = \frac{e_\theta^3}{12\ d} \qquad \underset{\sim}{V} = \begin{Bmatrix} V_x \\ V_y \end{Bmatrix}$$

Thus from (5.10)

$$J_\theta = (\cos\theta \quad \sin\theta) \begin{Bmatrix} J_x \\ J_y \end{Bmatrix} = J_x \cos\theta + J_y \sin\theta \qquad (5.18)$$

From equation (5.12)

$$V_\theta = - \bar{e}_\theta (J_x \cos\theta + J_y \sin\theta)$$

but

$$\underset{\sim}{V} = \begin{Bmatrix} V_x \\ V_y \end{Bmatrix} = \begin{pmatrix} \cos\theta \\ \sin\theta \end{pmatrix} V_\theta = - \begin{pmatrix} \cos\theta \\ \sin\theta \end{pmatrix} \bar{e} \ (\cos\theta \ \sin\theta \ ) \begin{Bmatrix} J_x \\ J_y \end{Bmatrix} \qquad (5.19)$$

Multiplying the vectors out yield

$$\underset{\sim}{V} = - \bar{e}_\theta \begin{vmatrix} \cos^2\theta & \cos\theta \sin\theta \\ \cos\theta \sin\theta & \sin^2\theta \end{vmatrix} \begin{Bmatrix} J_x \\ J_y \end{Bmatrix} \qquad (5.20)$$

i.e.

$$K = \bar{e} \begin{vmatrix} \cos^2\theta & \cos\theta \sin\theta \\ \cos\theta \sin\theta & \sin^2\theta \end{vmatrix} \qquad (5.21)$$

This is K for one set of joints. For two or more sets the value of K would be the sum of the individual contributions for each joint set, each of which would have the same form as equation (5.17)

Snow (1965) has proved that for two or more joint sets the value of the permeability tensor is not altered by the interference to flow by one joint set upon the other.

<u>Some Rules for Estimating the Direction of Principal Axes of Permeability for a Jointed Rock Mass</u>

For any jointed rock mass with any number of joint sets, the value of K can be calculated or estimated by means of equation (5.17). It has been shown that the eigenvector of the permeability tensor gives the direction of the principal axes of the jointed rock mass. Equation (4.37) gives the direction of the principal axes for a two dimensional system, and similarly by finding the axes for which the three dimensional form of the permeability tensor is diagonalised the principal axes of the system are determined.

Examination of equation (5.17) allows the following rules for estimating the direction of the principal axes to be postulated.

1. For a rock mass characterised by two equal orthogonal joint sets there exists one unique principal axis of permeability. This axis is parallel to the line of intersection of the two joint sets. The plane perpendicular to this unique principal axis is isotropic. The permeability normal to the plane of isotropy is twice the value of the isotropic permeability.
2. For two different orthogonal joint sets there is one axis of principal permeability parallel to

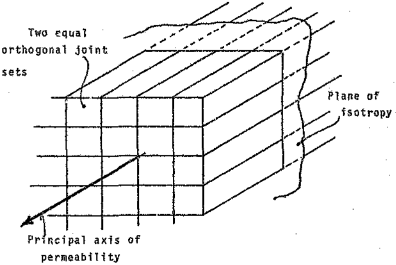

Fig 5.5 DIAG. TO EXPLAIN RULE 1 FOR ESTIMATING DIRECTIONS OF PRINCIPAL AXES OF PERMEABILITY

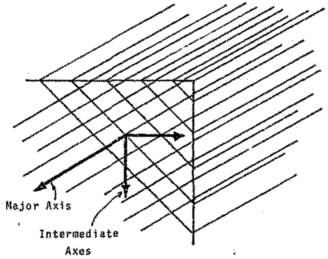

Fig 5.6 DIAG. TO EXPLAIN RULE 3 FOR ESTIMATING DIRECTIONS OF PRINCIPAL AXES

the central tendency of each joint set. The major axis of permeability is parallel to the line of intersection of the joint sets.

3. For two equal non-orthogonal joint sets the major axis of permeability is parallel to the line of intersection of the joints, the intermediate axis bisecting the acute angle and the minor axis bisecting the obtuse angle between joint central tendencies.
4. Two unequal orthogonal sets have the major axis parallel to the joint intersections, the intermediate parallel to the central tendency of the stronger* joint set and the minor parallel to the central tendency of the weaker* joint set.
5. Two unequal non-orthogonal joint sets, the same as for 3 above except the minor axis shifts closer to the weaker joint set central tendency.
6. Three equal orthogonal joint sets are isotropic.
7. Three orthogonal joint sets with two equal joint sets will have a plane of isotropy defined by the normals to the two equal joint sets. If the third set is weaker than the other two then the axis parallel

* Strength when used with reference to a joint set means the ability of that joint set to conduct water. Thus the strength of a joint set is proportional to the product of the cube of the joint apertures and the number of joints per unit length perpendicular to the direction of the joints. Two joint sets of equal strength therefore conduct equal amounts of water. Correspondingly one may speak of stronger and weaker joint sets.

to the line of intersection of the two equal joint sets is the major axis of permeability and if the third set is stronger then the axis parallel to the equal joint sets intersection line is the minor axis.

8. For three unequal orthogonal joint sets the principal axes are parallel to the normals to the joints, the major axis being parallel to the normal of the weakest joint set and the minor axis being parallel to the normal of the strongest joint set.
9. For three sets of joints with one set not orthogonal to the other two, equal sets, the major axis lies closest to the greatest number of intersections. The minor axis lies closest to the least number of intersections.
10. For three or more unequal, non-orthogonal joint sets use will have to be made of equation (5.17) and then it will have to be diagonalised to yield the directions of the principal axes.

Using these rules, it is possible to make an estimate if not calculate exactly the direction of the principal axes for a jointed rock mass. Values may be calculated for the coefficients of the permeability tensor for regularly jointed rock masses, by means of the equations derived in this chapter.

CHAPTER 6

THE NATURE AND EFFECT OF VARIOUS FACTORS WHICH INFLUENCE THE ACCURACY OF THE PERMEABILITY TENSOR FOR IRREGULARLY JOINTED ROCK MASSES

The main parameter used in the analysis be means of the Equivalent Continuous Medium Approach of the hydraulic regime in a jointed rock mass is the permeability tensor. (See Chapter 4 for definition) In the previous Chapter the expression for the permeability tensor for regularly jointed rocks was derived. Such rock masses are however very rare in nature and normally the rock mass is irregularly jointed. Thus methods are required for determining theoretically the value of the permeability tensor for irregularly jointed rock masses, and, if this is not possible, of at least detailing and discussing those factors which influence its value.

At present it is not possible to write exact expressions for the permeability tensor for irregularly jointed rock masses which account for all the irregularities of jointing. This is partially due to the fact that there is no way of quantitising the various factors that cause total joint assemblage patterns to be irregular, and partially due to the fact that the exact influence of the irregularities of jointing on the permeability tensor is unknown. Accordingly in this present Chapter an attempt is made to define those factors which contribute to the irregularities of a jointing pattern, to offer some expressions quantitising these factors and to relate them to the expression for the permeability tensor. In most cases it is only possible to state that there is some form of functional relationship between the permeability tensor and the parameters describing the jointing irregularity.

The Mathematical Form of the General Permeability Tensor for Irregularly Jointed Rock Masses

In order to study the form of the permeability tensor for irregularly jointed rock masses the following types of permeability tensors are defined.

K_e is the EQUIVALENT PERMEABILITY TENSOR for one joint set i.e. the permeability tensor for the joint set which is obtained when it is *assumed that* all the joints are continuous, have an aperture equal to the joint set mean aperture and are evenly spaced at d_m, the mean spacing between joints of the joint set.

K_a is the actual value of the permeability tensor for *a joint set* that results when all irregularities of jointing are considered.

K_f is the permeability tensor for two or more irregular joint sets.

In practice K_e is normally easy to determine, for information about the mean spacing is usually available and an estimate of the joint set mean aperture can be made, even if only relative apertures for the various joint sets in a joint group are used. The actual value of the permeability tensor, *for an irregular joint set*, is more difficult to determine. In fact it's determination is the central difficulty in all hydraulic analyses of irregularly jointed rock masses.

It is apparent that K_a is related to K_e and approaches it in value i.e. $K_a \to K_e$ as the jointing becomes more regular. Thus if a coefficient is defined such that

$$K_a = C \; K_a \tag{6.1}$$

it appears that C is a function of the irregularity of jointing. Moreover it is a function not only of the variation from complete regularity of the joint set to which it applies but is also a function of the total field geometry.

Thus if parameters S and I are defined as follows

S - the joint Set Statistical Spread. A precise definition of this parameter is not possible but it is taken to represent or to be a measure of the divergence from complete regularity of the joints in any one joint set. It will be a function of the joint aperture distribution, the variation in gouge filling and the other parameters which describe the nature of the joint surfaces.

I - the interconnection of the joints in the joint group. This is a measure of the extent to which each joint set interconnects with the other joint sets in the joint group and is hence hydraulically active.

This relationship or dependence can be formally stated as

$$C_i = f(S_i, I) \tag{6.2}$$

That is that C_i for the i^{th} joint set is a function of the spread of the joint parameters and the total interconnection of all the joint sets in the joint group. S_i and I in themselves are dependent on a number of different factors as discussed later.

If there is more than one joint set in a joint group K_f must be the sum of all the K_a's i.e. is the sum of the individual contributions from the individual joint sets.

Stated formally

$$K_f = \sum_{i=1}^{N} (Ka)_i \tag{6.3}$$

$$= \sum_{i=1}^{N} (C K_a)_i \tag{6.4}$$

K_f is the permeability tensor which ideally should be used in the analysis when the irregularly jointed rock mass is modelled as an Equivalent Continuum. Thus it appears that the basic problem resolves to one of determining the value of C for each joint set, as K_e is readily determined.

The Factors which Contribute to the Irregularity of Jointing

The jointing pattern of a rock mass is irregular because of the following factors which are not uniform from joint to joint.

(a) The joint aperture.
(b) The joint orientations.
(c) The joint length.
(d) The spacing between joints of a joint set.

The variation of aperture, orientation and length of the joints can normally be described by some statistical distribution function.

Factors (a), (b) and (c) influence the value of S_i and factors (c) and (d) together with other factors listed below influence the value of I.

The Influence of the Variation in the Joint Apertures and Orientations

To study the influence of the joint aperture distribution and the joint orientation distribution on the value of the permeability tensor, Snow (1965) assumed a number of joints with an orientation distribution described by a Fisher error distribution. He set up a continuous aperture size distribution. Next he paired a random aperture from his aperture distribution graph with a random orientation. This paired set of an aperture and an orientation was assigned to a joint. For this joint a permeability tensor was calculated. This process was repeated twenty five times and the resulting tensors were meaned, a correction factor applied to account for the joint spacings and then the final tensor was diagonalised. Fourty nine independent solutions of such permeability tensors were obtained and plotted on a stereographic projection. Also a frequency plot of the principal permeabilities was produced. He found that the geometric mean of the principal permeabilities approached the infinite sample size value after considering the mean of approximately two hundred conductors.

The Influence of the Joint Lengths and the Joint Spacings

For a joint to be hydraulically active it must be hydraulically connected to neighbouring joints. If all joints in the joint assemblage were continuous, all the joints would be completely interconnected i.e. they would all be hydraulically active. However, most joints are non-continuous. Moreover often the mean spacing between the joints of one joint set is of such a magnitude that it is not possible for all the joints of a second joint set to intersect at least two joints of the first joint set. Thus complete hydraulic interconnection of two joint sets does not always occur. Thus the manner in which two or more joint sets interconnect can materially affect the extent to which the joints of any one set contribute to the permeability of the rock mass. This is most easily visualised by imagining two joint sets. Both joint sets are such that the joints of that set do not connect to each other. (Each joint set has a finite value of K_e but a K_a that is effectively zero. i.e. C for each joint set is zero.) (See figs. 6.1 and 6.2)

If the two joint sets are superimposed with their central tendencies parallel, their combined permeability would be very small, if not zero. Again their C values would effectively be zero. However, if their central tendencies were perpendicular then their resultant permeability is likely to be very much greater than the sum of the individual permeabilities.

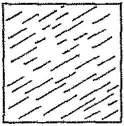

α Joint Set

$K_e > 0$

$K_a = 0$

$C = 0$

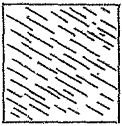

β Joint Set

$K_e > 0$

$K_a = 0$

$C = 0$

FIG. 6.1 TWO JOINT SETS FOR EACH OF WHICH K_a IS ZERO

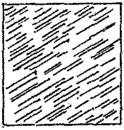

α and β joint set central tendencies parallel. C_α and C_β very nearly equal to zero.

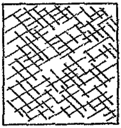

α and β joint set central tendencies orthogonal. C_α and $C_\beta > 0$

FIG. 6.2 THE TWO JOINT SETS SUPERIMPOSED

This is only possible if the values of C increase.

From this illustration it can be seen that the length and the mean joint set spacings influence the interconnection but that in addition the following factors have an influence on the joint set intersections.

(a) The mean joint spacings of each joint set relative to the mean lengths of the other joint sets.

(b) The relative orientation of the joint sets' central tendencies.

(c) The intensity of jointing.

The direct effect of each of these factors on the interconnection of the joint groups is not known but it is possible to partially quantitise their effects as follows.

1. <u>The relative mean spacings and lengths of joints</u>.

All other things being equal, and considering only two joint sets, it is apparent that the interconnection of the two sets will be influenced by the mean length of the joints of the α set, say, relative to the mean spacing of the β set of joints, and correspondingly the mean length of the β joints relative to the α joints set mean spacing. This can be quantitised by defining the dimensionless number.

$$\left(\frac{d_m}{l_m}\right)_r$$

for the r^{th} joint set

where d_m is the joint set mean spacing

l_m is the mean length of the joints.

FIG. 6.3 ILLUSTRATION OF STATISTICAL SCATTER OF d_α AND l_β

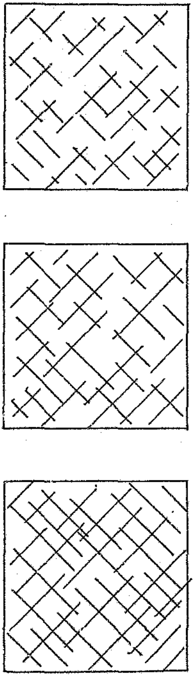

CASE a

$d_\alpha / l_\beta >> 1$

$I \rightarrow 0$

CASE b

$d_\alpha / l_\beta \approx 1$

$I \rightarrow 1$

CASE c

$d_\alpha / l_\beta < 1$

$I = 1$

For a joint group consisting of N joint sets a composite *dimensionless number* can be defined by the following equation

$$D = \frac{\prod_{r=1}^{N} \left(\frac{d_m}{l_m} \right)_r}{N} \qquad (6.5)$$

If two joint sets are considered the value of D is given by equation (6.6)

$$D_{\alpha\beta} = \frac{d_\alpha}{l_\beta} \cdot \frac{d_\beta}{l_\alpha} \qquad (6.6)$$

But d_α / l_β and d_β / l_α are measures of the effect of the mean *spacing* of one joint set relative to the mean joint length of the other set. This is then a measure of the joint group interconnection, for the smaller the mean spacing of any joint set relative to the mean lengths of the joints of another set the greater the interconnection of the two joint sets is likely to be.

Hence assuming that the statistical scatter on the values of d_α and d_β are small the following guidelines can be drawn. (see fig. 6.3)

(a) For $\frac{d_\alpha}{l_\beta} >> 1$ or $\frac{d_\beta}{l_\alpha} >> 1$ then $I \to 0$

(b) For $\frac{d_\alpha}{l_\beta} \simeq 1$ or $\frac{d_\beta}{l_\alpha} \simeq 1$ then $I \to 1$

(c) For $\frac{d_\alpha}{l_\beta} < 1$ or $\frac{d_\beta}{l_\alpha} < 1$ then $I > 1$

Thus it is possible to see that I is a function of D .

i.e. $$I = f(D) \tag{6.7}$$

2. <u>The relative orientations of the joint sets' central tendencies.</u> It has been stated that the relative orientation of the central tendencies of the joint sets influences the interconnection of the joint group. The angle between the central tendencies of any two neighbouring joint sets can be taken as the measure of their relative orientation.

If two joint sets α and β are at an angle θ to each other and the mean joint spacings are d_α and d_β respectively then for any joint of the α *joint set to connect two joints of the* joint set spaced d_α apart the β joint must have a length l_β such that $l_\beta/\sin\theta$ is at least greater than d_α .

Thus $l_\beta/\sin\theta$ can be considered the equivalent length of the joint orthogonal to the α joint set central tendency. Thus define the parameter (dimensionless)

$$\bar{D} = \left(\frac{d_\alpha}{l_\beta}\right)\sin\theta_{\alpha\beta}\ \left(\frac{d_\beta}{l_\alpha}\right)\left(\frac{d_\beta}{l_\gamma}\right)\sin\theta_{\beta\gamma}\ \left(\frac{d_\gamma}{l_\beta}\right)\ldots\ldots\sin\theta_{n\alpha}\left(\frac{d_n}{l_\alpha}\right) \tag{6.8}$$

where there are n joint sets in the joint group.

Thus $$I = f(\bar{D}) \tag{6.9}$$

Note that $\bar{D}$ is a composite factor in that it includes the parameter previously defined as D

3. <u>The intensity of jointing</u>, which may be defined as the number of joints per unit area. Thus if i is defined as the joint set intensity, then the joint group intensity factor for N joint sets can be defined as

$$\underline{i} = \left(\prod_{r=1}^{N} i_r \right) / N \tag{6.10}$$

The value of i_r for the r^{th} joint set will take into account the mean spacing as well as the mean separation of the joints, where spacing can be considered the distance between joints orthogonal to the joint set central tendency and the separation is the distance between joints parallel to the joint set central tendency.

Thus $\underline{i}$ accounts for the total effect of these factors for all the joint groups joint sets. The greater the value of $\underline{i}$ the higher will be the interconnection of the joints being considered. Moreover as will become apparent from consideration of the results of tests described in the next Chapter, the greater the value of $\underline{i}$ the greater the accuracy of the potential distribution obtained when an irregularly jointed rock mass is characterised by the equivalent permeability tensor.

From a consideration of the above arguments it is clear that I is a function of $\underline{i}$

i.e.

$$I = f(\underline{i}) \tag{6.11}$$

However I is also a function of $\bar{D}$

therefore

$$I = f(\bar{D}, \underline{i}) \tag{6.12}$$

but since

$$C_i = f(S_i, I) \tag{6.13}$$

it follows that

$$C_i = f(S_i, \bar{D}, \underline{i}) \tag{6.14}$$

and from equation (6.4) if follows that K_f is dependent on S_f , D and $\underline{i}$.

The inherent difficulty of completely quantitising all these parameters and hence of determining the correct value for K_f to use in any particular instance means that there will always be a degree or error involved in any potential distribution determined using an estimated or representative value of K_f .

The value of the permeability tensor reflects both the nature of the rock joints and their relative orientations and irregularities. It is in fact the only parameter substituted into continuous medium approach solutions which reflects directly the nature of the rock mass being modelled. Thus it follows that the better the permeability tensor represents such jointing patterns the more accurate the potential distribution determined using it will be.

However, the degree to which the permeability tensor is a good representation of the jointed rock mass is not the only factor which influences the accuracy of the calculated potential distribution. Other factors have as great an influence as the accuracy of the permeability tensor. They are

1. <u>The nature of the flow in the joints</u>

Louis (1969) and Sharp (1970) have demonstrated the occurence of turbulent flow in joints at low potential gradients.

However, in most practical cases laminar flow can be assumed and the corresponding potential distribution calculated. Louis has made a comparison of the equipotentials obtained assuming first laminar and then turbulent flow in the joints. From his results he concludes that

> "A consideration of turbulence does not cause a change worth mentioning in the potential distribution".

Sharp details methods of solving for the potential distribution in rock regions where laminar flow is occuring.

This method essentially involves a finite difference approach and the use of "linearising" coefficients to account for the non-laminar flow in the joints.

2. <u>The number of joints per element and the number of elements in the field being analysed</u>

If a jointed rock mass is to be modelled and analysed as a continuum both the finite element and the finite difference methods require that the mass to be analysed be divided into a number of elements. One of the main factors that will influence the size of such elements is the number of joints that will be contained in each element. It has already been shown that the jointing intensity influences the accuracy of the permeability tensor. Therefore if on the average each element contains a large number of joints the permeability tensor will represent both each element and the total rock mass well.

The more irregular the jointing the greater the number of joints that will be required per element. If the jointing is perfectly regular one or two joint segements* per element are quite sufficient for the medium to be accurately represented by a permeability tensor. The approach adopted by Sharp (1970) is an instance where only one joint segement per element is used and the equations he derives from a Discrete Flow Channel Approach are the same as result from a Continuous Medium Approach.

* A criterion stated by Lyell (1970) that there be at least four joints per element was tested as described in the following Chapter and found to be valid for certain practical cases. However, it would really be necessary to make a judgement decision in each case, concerning the number of joints in each element that will be required for sufficiency. This would be based on a knowledge of the complete field geometry.

If a sufficiently large number of elements are used to model the rock mass then it is possible to reduce the number of joints per element. This occurs because the local discontinuities and inaccuracies that will be introduced if certain elements in themselves have an inadequacy of joints will not materially affect the regional potential distribution obtained. The Laplace equation describing a field potential distribution is a square relationship thus the effect of any local error in any value of ϕ dies out as $1/r^2$ where r is the distance from the point at which the error occurs. The effect of local random variations of the value of the permeability tensor on the potential distribution in a rock mass is considered in further detail in Chapter 9.

CHAPTER 7

DESCRIPTION OF THE TESTS PERFORMED

A series of tests was performed to investigate a) the correctness of the extended Laplace equation describing the potential dissribution in an anisotropic mass, b) the validity of the expression giving the permeability tensor for a jointed rock mass and c) the effect of random joint sets on the accuracy of the permeability tensor and the resulting potential distribution in a mass characterised by *joint sets* of random joints.

In Chapter 4 the extended Laplace equation was derived as follows:

$$\sum_{j=x}^{N} \sum_{i=x}^{N} k_{ij} \frac{\partial^2 \phi}{\partial i \partial j} = 0 \qquad (7.1)$$

which in two dimensions reduces to

$$k_{xx} \frac{\partial^2 \phi}{\partial x^2} + 2\, k_{xy} \frac{\partial^2 \phi}{\partial x \partial y} + k_{yy} \frac{\partial^2 \phi}{\partial y^2} = 0 \qquad (7.2)$$

The permeability tensor K for a jointed rock mass was derived in Chapter 5 as

$$K = \sum_{r=1}^{N} (n_r' \; \bar{e}_r \; n_r) \qquad (7.3)$$

To prove the validity of both of these equations the following test proceedure was adopted.

1. A physical model was postulated.
2. Joint sets were cut from electrical conducting paper and the potential distribution which resulted in them was determined.
3. The permeability tensor for the assumed rock joint system was

substituted into equation (7.2)
which was solved by finite differences.

4. An equivalent homogeneous field was cut from electrical conducting paper and the potential distribution measured.
5. The various potential distributions were visually and statistically compared.

The results for all the tests performed will be found in Appendix 5. An extended discussion of the results obtained is given in Chapter 8.

THE MODEL

The following, simple situation was postulated, and used as the standard model on which all the theories presented in this thesis were tested.

A square of an anisotropic medium was assumed. The principal axes of permeability $\bar{x},\bar{y}$ were arbitrarily orientated with respect to the X and Y axes at an angle of θ (see fig. 7.1)

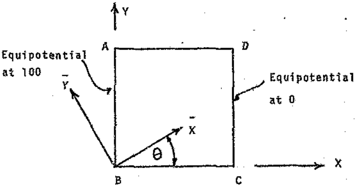

Fig 7.1 THE MODEL USED IN ALL TESTS PERFORMED

The size of the square is immaterial for it does not affect the final potential distribution. Thus different sized squares were used in different tests, the size used being that which was most convenient for the particular test being performed.

Further it was assumed that the opposite sides of the square AD and BC were impermeable and hence constituted flow lines. The other two sides were taken as equipotentials. In all tests the value of the left hand equipotential was taken as 100 and the right hand equipotential as zero.

THE TESTS PERFORMED

For each of the joint assemblages tested either all or at least two of the following tests were performed.

1. The finite difference form of equation (7.2) was written. This is

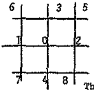

$$\phi_0 = \frac{k_{xx}}{2(k_{xx}+k_{yy})}\{\phi_1+\phi_2\} + \frac{k_{xy}}{4(k_{xx}+k_{yy})}\{\phi_6-\phi_5-\phi_7+\phi_8\} + \frac{k_{yy}}{2(k_{xx}+k_{yy})}\{\phi_2+\phi_4\} \qquad (7.4)$$

The square was divided into 100 square elements with 121 nodal points. Using an iteration proceedure the finite difference equation (7.4) was solved for the nodal potentials. Computer program ANEFF * was used to solve the equations. In all three hundred iterations were required to ensure complete convergence. ** Computer run time per

* See Appendix 3.

** Convergence of the solution was taken as being the stage at which the sum of skew symmetric potentials totalled one hundred. This arises from the skew symmetric nature of the model being tested, for if the potentials are reversed i.e. the equipotential with a value of one hundred is put to zero and the zero potential is put to a value of one hundred no change in the shape or position of the equipotentials solution was approximately 50 seconds. An attempt was made to use the over relaxation proceedures described by Sharp (1970) but no coefficient could be found which caused a speedier convergence.

2. The square anisotropic element was transformed to the equivalent isotropic element by contraction or expansion of all distances along the principal axes, in the proportion of the square root of the principal permeabilities. The transformed equivalent element was then cut from electrical conductive paper (marketed under the trade name TELEDELTOS PAPER). Silver paint was used to create the equipotentials along the left and right hand sides. Use was made of a SERVOMEX FIELD PLOTTER which is basically a Wheatstone bridge, to measure the potential at any point on the conducting paper. Normally the position of the equipotentials 90, 80, 70, ... 10 were determined and the potentials at the node points of a 100 element grid were measured.
The Servomex Field Plotter is rated 0.1% accurate. The Teledeltos paper however is not absolutely homogeneous, and in some tests, which had to be repeated,

---

** (cont.) will occur. The value of the equipotential will become one hundred minus its former value. This is equivalent to rotating the model through 180°. Hence the criteria for convergence of the numerical solution is that it should fulfill the condition that it can be rotated and have potentials which are one hundred minus their former value, i.e. that the values of the potential at skew symmetric nodes should equal one hundred.

distinct regions of greater and lesser conductivities than the average were noted. To eliminate as far as possible the errors resulting from such random heterogeneity, for each test the potentials were reversed, thus giving at each point two nodal potentials, which should, if the paper were completely homogeneous, total 100. (See footnote on previous page with regard to convergence) This seldom occured. However, by utilising the fact that the two nodal potentials should total 100, and also the test of skew symmetry of the field, it was possible to adjust the measured potentials to yield average results.

3. A representation or model of each postulated joint group was cut from the Teledeltos paper. The potentials at the node points of the 10 x 10 grid were measured wherever a joint crossed or occured at a node. This did not happen for each node so the position of the equipotentials 90, 80, 70, ... 10 were determined by seeking points on the joints at which these potentials occured.

The size of the models cut were 400mm x 400mm and the joints were cut approximately 5mm thick spaced at approximately 15mm.

THE JOINT GROUPS TESTED

Three series of tests were performed using different types of joint groups.

Series A tested groups of continuous, regularly spaced uniform joint sets.

Series B investigated the effects of non-continuity and non-regularity of the joints and the effects of changing the joint intensity of the joint groups.

Series C attempted to study the effects of changing the mean length of the joint sets on the permeability tensor and the final potential distribution.

Series A. Continuous, Regular Joint Sets.

The following three joint groups were tested.

I. Two joint sets at right angles to each other, the strength* of the α joint set being double the strength of the β joint set. (see fig.7.2) The α joint set was orientated at $+45^{\circ}$ to the X axis, and thus the β joint set was at -45° to the X axis.

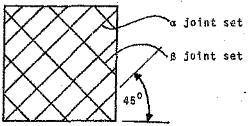

Fig 7.2 THE JOINT GROUP AS FOR TEST A.2

The apertures of the α and β joints were made equal. Thus the spacing of the α joints is half that of the β joints.

For this case K with respect to the X Y axes system is

$$K = \begin{vmatrix} 3 & 1 \\ 1 & 3 \end{vmatrix}$$

(Note that throughout only relative values of the coefficients of K are used, as the absolute values do not alter the potential distribution, although they would affect the flow rates and velocities)

* See Page 82

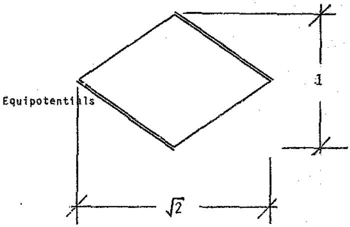

Fig 7.3 THE RELATIVE DIMENSIONS OF THE TRANSFORMED ANALOGUE

The principal axes are orientated at 45° to the X Y axes system. The value of the principal axes permeability tensor is

$$\overline{K} = \begin{vmatrix} 2 & 0 \\ 0 & 1 \end{vmatrix}$$

Using the values of K the transformed equivalent isotropic element with relative dimensions as shown in fig. (7.3) was obtained, cut from Teledeltos paper and tested.

2. Two orthogonal joint sets, the strength of the α joint set being four times that of the β joint set. The α joint set was orientated at 45° to the X axis. The α and β joints were taken to have ,ual apertures. Thus the α joint spacing is a quarter of the β joint spacing.

The value of K with respect to the X Y axis system is

$$K = \begin{vmatrix} 5 & 3 \\ 3 & 5 \end{vmatrix}$$

and the principal axes permeability tensor is

$$\overline{K} = \begin{vmatrix} 4 & 0 \\ 0 & 1 \end{vmatrix}$$

The jointing for this test was so sparse that it was not possible to measure nodal potentials on the joint analogue at sufficient points to perform any type of statistical analysis.

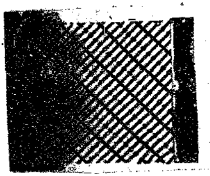

Fig 7.4 THE JOINT ANALOGUE FOR TEST A.2

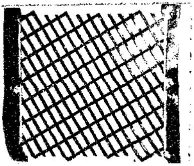

Fig 7.5 THE JOINT ANALOGUE AS FOR TEST A.3

3. Two orthogonal joint sets, with the α joints having twice the strength of the β joint set. The joint apertures of both sets were equal. The α joint set is orientated at 30° to the X axis.

The value of K with respect to the X Y axes system is

$$K = \begin{vmatrix} 75 & 26 \\ 26 & 105 \end{vmatrix}$$

The principal axes permeability tensor is

$$\overline{K} = \begin{vmatrix} 2 & 0 \\ 0 & 1 \end{vmatrix}$$

<u>Series B</u> Irregular, Non-continuous Joints.

Three groups of irregular, non-continuous joint sets were tested.

1. A superposition of three random joint sets. Fig. 7.6 shows a photograph of the joint analogue tested.

From the analogue the following relative spacings and orientations were estimated.

For the α joint set		$d_\alpha = 8$	$\theta_\alpha = 22^0$
β	" "	$d_\beta = 12$	$\theta_\beta = -12^0$
γ	" "	$d_\gamma = 8$	$\theta_\gamma = 90^0$

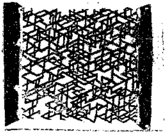

Fig 7.6 THE ANALOGUE AS FOR TEST 8.1

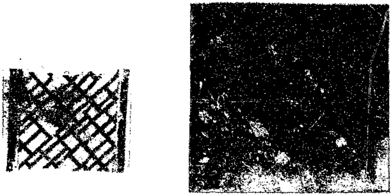

a. UNIT ELEMENT

b. UNIT ELEMENT REPEATED FOUR TIMES

Fig 7.7 THE JOINT ANALOGUE AS FOR TEST 8.2

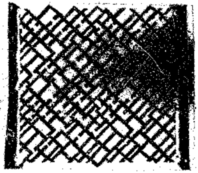

a. UNIT ELEMENT CUT   b. CUT REPEATED ELEMENT

Fig 7.8 JOINT ANALOGUES AS FOR TEST B.2

AS CUT

Assuming that the joints are continuous and uniformly spaced at the mean spacings given, the following values for the permeability tensor were calculated.

$$K = \begin{vmatrix} 140 & 8 \\ 8 & 126 \end{vmatrix}$$

and

$$\bar{K} = \begin{vmatrix} 143 & 0 \\ 0 & 123 \end{vmatrix}$$

at $24{,}5^0$ to the x axis

2. Two non-continuous irregular joint sets with the strength of the one joint set being twice that of the orthogonal joint set. This analogue was repeated four times as shown in fig7.7band tested.

Next certain of the joints were cut as shown in figs. 7.8a and 7.8b and again the joints were tested. The results were compared to the nodal potentials resulting from a permeability tensor with the following value

$$K = \begin{vmatrix} 3 & 1 \\ 1 & 3 \end{vmatrix}$$

$l_m = 20$ $i = 200$

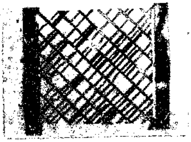

$l_m = 40$ $i = 200$

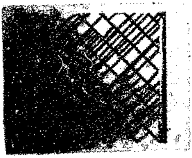

$l_m = 80$ $i = 100$

FIG 7.9 JOINT ANALOGUES FOR TEST SERIES C

Series C Varying mean Joint Lengths.

The aim of this series of tests was to study the effect of a variation in the mean length of the joints in a joint set on the value of the permeability tensor. It was hoped to quantise the effect by studying the relationship between l_m of one joint set and C_α as from equation (7.5)

$$K = C_\alpha K_{e\alpha} + C_\beta K_{e\beta} \tag{7.5}$$

Thus two orthogonal joint sets were chosen. The β joint set was assumed continuous, and regularly spaced with a spacing of 20 (again only relative spacings and lengths are given) Thus

$$C_\beta = 1$$

It was assumed that the α joint set had a mean spacing of 5, and that the joint length distribution was given by the equation presented by Robertson (1970)

$$y = e^{-\alpha x} \tag{7.6}$$

where y cumulative percentage frequency of joints with length greater than x

$\alpha = {}^1/l_m$ where l_m is the mean joint length.

Three mean lengths for the α joint set were chosen i.e. 20, 40, and 80, being one, two and four times the spacing of the orthogonal β joint set.

Use was made of computer program RNJSG to generate the random joint set.

For each of the three mean lengths a joint set was generated and then plotted on a piece of graph paper 20" x 20". For the case l_m = 80 one hundred joints were plotted. l_m = 40 two hundred joints were plotted and for $l_m = 20$ two hundred joints. Thus for purposes of comparison the following parameter is defined as

$$F = i\, d_m / l_m$$

where i is the joint intensity

then the relative values of F are

$$F_{80} = 1/8$$

$$F_{40} = 1/2$$

$$F_{20} = 1$$

The central 15" x 15" portion of the graph paper was taken and the random joints were superimposed on the β joint set.

The resulting joint assemblages were cut from Teledeltos paper, see fig.7.9,7.1

By visual inspection of the equipotentials which resulted when the joint analogue was tested it appeared that for $l_m = 80$ and 40 a potential distribution given by a permeability tensor $\begin{vmatrix} 5 & 3 \\ 3 & 5 \end{vmatrix}$ would give a reasonable fit with the measured equipotentials.

For the case $l_m = 20$ it seemed that a permeability tensor $\begin{vmatrix} 1 & 0 \\ 0 & 1 \end{vmatrix}$ would give a reasonable fit between calculated and measured equipotentials.

Accordingly the measured nodal potentials were compared with the calculated potentials for the cases suspected. Table A.5.17 in Appendix 5 gives the statistical distribution on the differences in the nodal potentials.

CHAPTER 8

A DISCUSSION OF THE TEST RESULTS

The results of the series of tests described in the previous Chapter are discussed here.

The General Accuracy of the Test Results.

1. The finite difference solution of the anisotropic field - In all cases convergence was assumed when skew symmetric points gave potentials totalling 100. This normally occured after three hundred iterations. One of the solutions was taken to five hundred iterations and the nodal potentials compared to those obtained for three hundred iterations. The mean difference was 0,002.

2. The Electrical Analogue. The Servomex Field Plotter was rated at 0,1% accurate. However, as has been noted, the Teledeltos paper was not homogeneous. A measure of the error introduced by this heterogeneity is provided by consideration of the value of the nodal potential at the mid-point of the field. From considerations of symmetry this should be 50. For the test A.1 this mid-point had a potential of 51,2. For test A.2 the value was 50,1 when using unadjusted nodal potentials and was 49,95 for adjusted nodal potentials. Test A.3 gave a value of 50,28.

3. The Cut Joint Sets. It was not possible to measure the nodal potential at each node. It was not considered meaningful to interpolate results from joints near but not on the nodes, therefore, only at certain nodes are potentials available.

The Accuracy of the Joint Set Permeability Tensor

Test series A was a test of the accuracy of the extended Laplace equation and the expression for the permeability tensor for jointed rocks.

*This test series provided moreover the opportunity of studying the representation of the jointed rock mass by means of the Discrete Flow Channel Approach. The joint analogues cut were a model of the

* As explained in the introduction to Chapter 7.

network formed by a joint assemblage and the determination of the potential distribution in the joints was an analogue solution of the equations resulting from the Discrete Flow Channel Approach.

Considerations of the plots of the equipotentials obtained and the statistical comparison of the differences in nodal potentials for the various cases shows that in all tests the correlation between calculated and measured results was good. The smallest mean difference of nodal potentials was 0,19. This was obtained for test A.3 for the calculated and the continuous transformed analogue results. The greatest difference was 1,36, also obtained for test A.3. This occured when comparing the joint analogue and the calculated potentials. Test A.2 for the same case gave a value of 1,13.

Tables A5.3 and A5.7 show that the distribution of the values of the nodal differences of potential was random. (Note in all cases only the absolute value of the difference is given) Table A5.7 shows only a slight tendency for the values closer to the edge of the model to have a greater difference. This is due probably to edge effects.

Fig. A5.2 (test A2) indicates that closer to the edges the position of the equipotentials is indeterminate. This is because it was impossible to measure the potential as one approached the edge. Fig. 7.4 showing a photograph of the analogue reveals that there were insufficient joints near the edges for meaningful readings to be taken. No nodal potentials were measured in test A.2 again because of the paucity of joints.

The correspondence among the equipotentials as they were determined by the different methods indicate the correctness of both the extended Laplace equation and the expression for the permeability tensor for jointed rocks.

The Influence of the Joint Set Intensity, and Non-Regular Joint Sets on the Potential Distribution

The joint set tested in test B.1 was intensely jointed, although the joints were neither regular nor continuous. The statistical distribution of the differences in the nodal potentials should be considered in the light of the results presented in Chapter 9. A mean difference of 1,67 was recorded, the standard deviation being 1,26. Results tabulated in Chapter 9 indicate that for a random distribution of the values of the principal axes permeability coefficients the major permeability varing uniformly by 25% on either side of its median value, the mean difference in nodal potentials was 2,55. Fig. 7.6 showing the analogue tested in test B.1 indicates that such a random variation in the principal axes permeability coefficient is quite conceivable. Thus the results obtained are good. They indicate moreover that a random joint set can be well represented by permeability tensors for equivalent joint sets.

Test B.2 attempted to study the influence of joint intensity on the accuracy of the equivalent permeability tensor and the final potential distribution. The joint group tested (as shown in fig. 7.7a) was arbitrarily drawn. It was repeated four times to yield the analogue of fig. 7.7b, which gave a mean difference of nodal potentials of 2,3 with standard deviation of 2,3 whereas the corresponding figures for the joint analogue of 7.7a were 3,13 and 3.40. Immediately it is apparent that greater accuracy has been achieved by using more joints. As has been shown for a random joint set a mean difference of 2,3 is not excessive. Consideration of result f of table 9.1 will show that even a mean difference of 3,13 denotes a fairly good representation of the field. Simultaneous random variation of 25% on k_{xx} and of 50% on k_{yy} is well what is occuring in fig. 7.7a.

In cutting the joints of the above two analogues a joint was cut in such a way that as far as possible the joints lengths were halved and the intensity doubled. If this were done exactly the joint assemblage should result in one of two equal, orthogonal joint sets. For this situation the medium is isotropic. Accordingly the results from the analogues as in figs. 7.8a and 7.8b were compared to the isotropic solution of the potential distribution. Fig. 7.8a yielded a mean difference of 6,0 with a standard deviation of 3,8. Fig. 7.8b gave a mean difference of 2,26 and a standard deviation of 2,3. It was considered that a mean difference of 6,0 was excessively high so the measured nodal potentials for each case was compared to an anisotropic medium characterised by a principal axes permeability tensor of $\begin{vmatrix} 2 & 0 \\ 0 & 1 \end{vmatrix}$ at 45^o to the element sides. Fig. 7.8a gave a mean and a standard deviation of 4,88 and 4,07 respectively and fig. 7.8b gave values of 4,04 and 3,18 for the same parameters. These results indicate no improvement in the accuracy of the analogue of fig. 7.8a and a deterioration of the accuracy of the analogue of fig. 7.8b.

The error distribution for fig. 7.8a is completely random for both cases where comparisons were made. Hence it is considered that the jointing is too sparse and irregular for the potential distribution to be determined by a continuous medium approach. The analogue of fig. 7.8a appears to contain sufficient joints for it to be analysed as a continuous medium, although a discrete flow channel analysis would yield more accurate results.

The analogues tested in test B.2 can be viewed in two ways. Firstly the analogues tested can be considered to each constitute one element of the flow field, or they can be considered to be composed of a number of elements. For purposes of this discussion it is convenient to regard the fig. 7.7a analogue as a basic element and the fig. 7.7b analogue as being composed of four such elements.

The analogue of fig. 7.7a obeys Lyell's criterion that at least four joints must be included in any element for it to be a valid element in a continuous medium approach. It has been seen that this is valid for both fig. 7.7a and 7.7b analogues.

When the joints become smaller however, the criterion breaks down as in the instance of fig. 7.8a. However, when four such elements are included in the flow field, the criterion appears to be adequate.

It should be recalled that for certain cases one joint per element is sufficient to represent the medium.*

Thus to state a blanket criterion for the sufficiency of joints per element is futile. The sufficiency is a function of the number of joints per element included in the field, the regularity of the jointing pattern and the continuity of the joints. Each case should be judged on its particular merits.

The Effect of Varing a Joint Set mean Length

Test series C provided an opportunity for studying the effect on the permeability tensor of a variation in the mean length of one of the joint sets of the assemblage. This was done by keeping all other factors constant and varying only the α joint set mean length and intensity.

From the correspondence obtained between the measured nodal potentials and the calculated potentials (see table A5.16) and the value of the permeability tensor used to determine the calculated potentials the value of C_α can be calculated to yield values as follows ...

TABLE 8.1 VALUES OF C_α FOR DIFFERENT l_α VALUES

l_α	K	K_e	K_α	C_α	F
20	$\begin{vmatrix} 1 & 0 \\ 0 & 1 \end{vmatrix}$	$\begin{vmatrix} 0 & 0 \\ 0 & 1 \end{vmatrix}$	$\begin{vmatrix} 1 & 0 \\ 0 & 0 \end{vmatrix}$	1/4	1
40	$\begin{vmatrix} 4 & 1 \\ 0 & 1 \end{vmatrix}$	$\begin{vmatrix} 0 & 0 \\ 0 & 1 \end{vmatrix}$	$\begin{vmatrix} 4 & 0 \\ 0 & 0 \end{vmatrix}$	1	1/2
80	$\begin{vmatrix} 4 & 0 \\ 0 & 1 \end{vmatrix}$	$\begin{vmatrix} 0 & 0 \\ 0 & 1 \end{vmatrix}$	$\begin{vmatrix} 4 & 0 \\ 0 & 0 \end{vmatrix}$	1	1/4

* See Sharp (1970) and discussion on page

Thus plotting F vs. C fig. 8.1 is obtained.

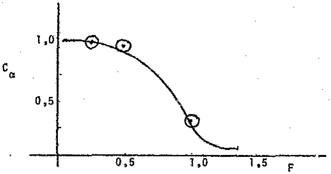

Fig 8.1 GRAPH OF C_α Vs. F FOR TEST SERIES C

As $l_m \to \infty$ for any joint set $C \to 1$ and as l_m gets smaller and smaller $C_\alpha \to 0$. This is reflected in fig. 8.1. The first two points for which l_m was 80 and 40 respectively give values of C that for all practical purposes are equal to 1. The mean spacing of the β joint set was 20, thus joints sets having mean lengths of 40 and 80 which were respectively 2 and 4 times the orthogonal joint set's mean spacing found most of their joints crossing orthogonal joints and being hydraulically active.

Equation (7.6) is of such a form that there is a wide scatter of joint lengths. Hence in those cases where the mean length is greater than the other joint set mean spacing the increased length of the joints longer than the mean length compensated for the joints which are shorter than the mean length. However, the joints are long enough for almost all the joints to be hydraulically active. Where the mean joint length was equal to the joint spacing then less than half of the joints were hydraulically active.

As can be seen from the test results about a quarter were hydraulically active. For a joint to be hydraulically active it has to cut at least two of the orthogonal joint set joints. If the joint length is only just equal to or slightly greater than the orthogonal joint set mean spacing then it can only occupy a very limited number of positions to be hydraulically active. This line of reasoning accounts for the rapid change of value of C in the region where l_α is approaching, equal to and just less than $d\ \beta$. Thus fig. 8.1 can be taken to give the general shape of the curve relating $C\ \alpha$ and F_α . The position of rapid decrease of C will depend on the ratio of $l\alpha\ /\ d\beta$. Fig. 8.1 is to be taken as more of a qualitisation than a quantitisation of the functional relationship between C, i, l, and d. From the results the following mathematical relationship appears to hold

$$C_\alpha = -A\ i\ \frac{d_\alpha}{l\alpha} + f(i)$$

where A is some empirical constant.

CONCLUSION

The tests conducted have proved the validity of the extended Laplace equation and the expression for the permeability tensor for jointed rock masses. The results have indicated that the use of the equivalent permeability tensor for irregularly jointed rock is a good approximation provided the number of joints per element and the number of elements used is large. The difficulty of obtaining the correct functional relationship between the parameters affecting and the actual value of the permeability tensor has been demonstrated although test series C provided a partial solution to the problem.

The single most important conclusion which can be drawn from the series of tests is that it is both logical and for all practical purposes sufficiently accurate to model a jointed rock mass as an Equivalent Continuous Medium.

CHAPTER 9

THE EFFECTS OF RANDOM VARIATIONS OF THE VALUE OF THE PERMEABILITY TENSOR ON CALCULATED AND ACTUAL POTENTIAL DISTRIBUTIONS

According to Piteau's second geological proposition structural regions exist in a rock mass. In this thesis this proposition has been extended to include the fact that hydraulic regions exist within a jointed rock mass. A hydraulic region has been accepted to be an area of a jointed rock mass in which the jointing patterns are sufficiently similar for that region to be treated as a homogeneous region.

However, it is recognized that in practice any hydraulic region will not be entirely homogeneous. There is always a tendency for some areas to be characterised by a concentration of joints while other areas will be sparsely jointed. Thus there exists a random distribution from point to point of the value of the permeability tensor for a jointed rock mass. Consideration of the figures in Chapter 7 showing the random joint set analogues tested will immediately reveal that at any node of the grid placed on the element the permeability can vary between wide limits, for at certain nodes there is a concentration of joints, at others, no joint at all.

This is a situation that will occur in almost all practical field situations. Thus it is apparent that some understanding of the effect of such random distributions of the value of the permeability tensor on the final field potential distribution is necessary.

FACTORS WHICH CAUSE RANDOM VARIATIONS IN THE VALUE OF THE PERMEABILITY TENSOR

An estimate of the value of the permeability tensor is likely to be made by considering the joint set data collected from exploratory tunnels and bore holes. Such data is inherently variable and hence a range of values for the permeability tensor will results. Thus it will be possible to predict the nature and values of the random permeability variations but will be nearly impossible to predict or determine the spatial distribution of such variations. The geological data will present an indication of the magnitude of the following factors which will cause the permeability of the rock mass to vary from position to position.

(a) The tendency for joints to cluster in certain position.
(b) The variation of the joint apertures from position to position.
(c) The presence or absence of gouge from position to position.
(d) The scatter of the joint lengths about their mean length.
(e) The variation about a central tendency of the joint orientations.

All these factors acting together but varying independently will cause the permeability tensor to vary in value in a random fashion.

Previous Investigations of the Problem

Warren and Price (1961) presented a comprehensive paper studying the effect of random heterogeneity on the flow regime in a porous medium.* In their study they postulated two hypothetical models. The first was a three dimensional rectangular parallelopiped and the second a three dimensional block with a well centrally situated. A three dimensional rectangular grid was placed over the model, with the grid spacing being uniform in each direction. To each element so formed there was assigned a random set of permeability coefficients. The grid axes were taken to be parallel

* This is an important paper which appears in a journal not commonly available. Hence a brief summary of their paper is given here.

to the principal axes of the medium which for each element were taken to be the same. Thus in effect a finite difference grid was set up. The potential distribution was then solved for.

These two authors tested the effect on the potential distribution of various statistical distributions of the values of the permeability coefficients. The distribution functions describing the frequency of occurence of various values of the permeability coefficients which they studied were Log-Normal, Exponential, Skewed log normal and Linear. No significantly different effects were observed for these various statistical distributions.

The general conclusions to which these authors were able to come were.

1. The most probable behaviour of a heterogeneous system approaches that of a homogeneous system having a permeability equal to the geometric mean of the individual permeabilities.
2. The effects of flow geometry and anisotropy on the most probable value for the effective permeability of a heterogeneous medium are finite but not significant.
3. Qualitative measures of the degree and the scale of the heterogeneity and its spatial configuration are obtainable if core analysis and pressure build up data are available.

Tests Performed for this Thesis

The approach adopted by the present author differs somewhat from that of Warren and Price, in that the value of the nodal permeability tensor for each node in the hypothetical model is determined from the nodal principal axes permeability tensor. The nodal principal axis permeability tensor is made to take random values within specified limits. This is done by allowing either the angle at which the axes are orientated to the global axes to vary, or the values of the principal axes permeability to vary. In certain cases both the axes and the values of the principal permeabilities were varied simultaneously but independently.

Having thus established a random value of the principal axes permeability tensor, the corresponding permeability tensor for the global axes was calculated.

The hypothetical model used was the same as the model considered and used in all the tests described in Chapter 7, i.e. a square with two opposite sides being flow lines and the other two being equipotentials, the principal axes of permeability being arbitrarily orientated with respect to the sides of the square.

Having set up a matrix (whose elements in themselves are matrices) of random nodal permeabilities the potential distribution in the hypothetical model was calculated. Then the nodal potentials were compared to the nodal potentials obtained by solving for the potential distribution, assuming that the field was homogeneous with permeability coefficients equal to the mean values of the random values.

Computer program DIWANI was written to do the above calculations. Table 9.1 shows the statistical distribution of the differences in nodal potentials between the homogeneous and the heterogeneous model which result when various components of the principal axes permeability tensor were caused to vary. The homogeneous situation investigated was the case of

$$\bar{K} = \begin{vmatrix} 4 & 0 \\ 0 & 1 \end{vmatrix} \quad \text{at } 45^0 \text{ to the X,Y axis}$$

axes giving

$$K = \begin{vmatrix} 5 & 3 \\ 3 & 5 \end{vmatrix}$$

From Table 9.1 it becomes apparent that the final potential distribution is relatively insensitive to variations of the direction of the principal axes of permeability, whereas variations in the value of the principal axes permeability coefficients have a marked effect on the final potential distribution.

The case which produced the most marked effect was that where k_{yy} was allowed to vary 50% on either side of its mean value. Causing k_{xx} to vary to a lesser degree simultaneously* appears to have a compensating effect of the final potential distribution.

CONCLUSION

The results of the tests described in this chapter indicate that the effect of random heterogeneity is not of such a magnitude as to seriously change the potential distribution from that of a homogeneous medium. Even fairly large variations in the values of certain parameters describing permeability tensors at each point (i.e. orientation of principle axes, value of the principal permeability etc.) cause only small differences in the nodal potentials from nodal potentials for homogeneous regions.

The practical significance of this is that although most rock masses are heterogeneous they can be assumed to be homogeneous without introducing serious errors into results based on this assumption.

* as the angle of orientation of the principal axes.

TABLE 9.1

STATISTICAL COMPARISON OF HOMO- AND HETEROGENEOUS NODAL POTENTIALS

	RANGE Kxx	RANGE Kyy	RANGE Deg.	MEAN N.P. DIFF.	MEAN DEVIATION	VARIANCE	STANDARD DEVIATION
a	4	1	44°-46°	0.076	0.074	0.010	0.104
b	4	1	42°-48°	0.188	0.159	0.055	0.235
c	3 5	1	45°	2.55	1.99	5.8	2.4
d	3.5 4.5	1	45°	0.952	0.738	0.794	0.891
e	4	0.5 1.5	45°	4.12	3.66	22.8	4.78
f	3.5 4.5	0.5 1.5	45°	3.73	2.96	13.26	3.64
g	4	1	38°-52°	0.382	0.313	0.144	0.37
h	4	0.5 1.5	38°-52°	4.46	4.08	27.8	5.27

CHAPTER 10

CONCLUSIONS

The determination of the potential distribution in a jointed rock mass is a vital task in many practical engineering situations e.g. the analysis of the stability of a slope or the foundations and abutments of a dam.

Jointed rock masses are usually anisotropic and often heterogeneous, thus the method evolved to analyse their hydraulic regimes should be such that they can cope with such conditions. This thesis has presented three models which may be postulated to represent a jointed rock mass. The mathematics which describes these models has been developed and some of the complexities involved in modelling an irregularly jointed rock mass have been discussed.

Experiments were performed to test the correctness and accuracy of a formula for the permeability tensor for a regularly jointed rock mass and also an extended form of the Laplace equation describing the potential distribution in an anisotropic mass.

The conclusions which result from this thesis are:

(a) A jointed rock mass can be modelled for purposes of hydraulic analysis as an Equivalent Continuum or a Discrete Flow Channel Network.

(b) The permeability tensor is the more versatile of the two methods of describing an anisotropic medium.

(c) An exact expression for the permeability tensor for a regularly jointed rock mass can be written.

(d) An irregularly jointed rock mass can be adequately represented, for most practical purposes, by an Equivalent Permeability Tensor.

Some guidelines have been given for estimating the number of joints per element required to adequately model a jointed mass as a continuum. Random variations in the value of the permeability tensor about a mean have been shown to have a finite but not significant effect on a potential distribution.

Basically the whole purpose of this thesis has been directed to studying and elucidating the fundamentals underlying the theoretical determination of the potential distribution in a rock mass. However, in practice a purely theoretical answer for the potential distribution is of little value unless it is crossed checked with and corresponds to field measured fluid pressures. Hidden geological discontinuities or inadequate and inaccurate data describing the joint parameters can, and do, introduce large errors into calculated potential distributions. The field pressure readings, provided they come from reliable piezometers account for all the irregularities which occur in nature. Thus it is recommended that the second approach to the determination of potentials in a practical rock mass be adopted whenever possible. This is the approach of fitting calculated potentials to field water pressure readings.

This approach still involves the theoretical calculation of potential distributions using estimated rock joint hydraulic parameters, thus the analyst requires a sound knowledge of theoretical proceedures. It is this knowledge which this thesis has attempted to extend.

REFERENCES

1. BARENBLATT, G.I., ZHELTOV, I.P., KOCH"NA, I.N. (1960) Basic Concepts in the theory of Seepage of Homogeneous Liquids in Fissured Rocks. Journal of Applied Mathematics and Mechanics. Vol. 24, No. 5 pp 852-864.

2. DARCY, H. (1856) Les Fontains Publiques de la Ville Dijon.

3. FERRANDON, J. (1948) Les Lois de l'ecoulement de la filtration. Le Genie Civil. 125, No. 2 pp 24-28.

4. HARR. (1962) Groundwater and Seepage. McGraw Hill. New York.

5. HERBERT, R. and RUSHTON, K.R. (1966) Groundwater Flow Studies by Resistance Networks. Geotechnique. 17 pp 53-75.

6. JENNINGS, J.E. (1970) A Mathematical Theory for the Calculation of the Stability of Slopes in Open Cast Mines. Symposium on the Theoretical Background to the Planning of Open Pit Mines with special reference to Slope Stability. Johannesburg.

7. JOHNSON, W.E. and HUGHES, R.V. (1948) Directional Permeability Measurements and their significance. Producers Monthly 13. No. 1 pp 17-25.

8. LOUIS, C. (1969) A Study of Groundwater Flow in Jointed Rock and its influence on the Stability of Rock Masses. Imperial College Rock Mech. Res. Report. 10.

9. LYELL, K.A. (1968) Transient Pore Pressures in Soils and Rocks Resulting from the Lowering of the Ground Water Table by Pumping from Boreholes. M.Sc. Thesis. University of the Witwatersrand.

10. LYELL, K.A. (1970) The Interpretation of Water Pressure Factors for use in slope Theory. (as for reference 6)

11. MARCUS, H. (1962) The permeability of a sample of an Anisotropic Porous medium. Journal of Geophysical Research. December.

12. MULLER, L. (1968) New Considerations on the Vaiont Slide. Rock Mechanics and Eng. Geology Vol. 6.

13. MUSKAT. (1946) The flow of Homogeneous Fluid through Porous Media. J.W. Edwards. Inc. Ann Arbor. Michigan.

14. PITEAU, D.R. (1970) Geological Factors Significant to the Stability of Slopes Cut in Rock. (As for reference 6).

15. SCHEIDEGGER, A.E. (1954) On Directional Permeability. Geofisica pura e applicata. 33.

16. SCHEIDEGGER, A.E. (1954) Directional Permeability of Porous Media to Homogeneous Fluids. Geofisica pura e applicata. 28 pp 75-90.

17. SCHEIDEGGER, A.E. (1960) The physics of Flow through Porous Media. Univ. of Toronto Press.

18. SERAFIM, J.L. and DEL CAMPO, A. (1965) Interstitial Pressures on Rock Foundations of Dams. Journal ASCE. SM5. September.

19. SERAFIM, J.L. (1968) Influence of Interstitial Water on the Behaviour of Rock Masses. Chapter 3 in Rock Mechanics in Engineering Practice. Wiley.

20. SHARP, J.C. (1970) Fluid Flow through Fissured media. Ph.D. Thesis. Imperial College.

21. SNOW, D.T. (1965) A Parallel Plate Model of Fractured Permeable Media. Ph.D. Thesis. Univ. of Berkeley. Ann Arbor. Michigan.

22. SOUTHWELL, R.V. (1946) Relaxation Methods in Theoretical Physics. Oxford University Press.

23. VERRUIJT. (1970) Theory of Groundwater Flow. Macmillan.

24. WARREN, J. and PRICE, H.S. (1961) Flow in Heterogeneous Porous Media. Journal of the Society of Petroleum Engineers. September.

25. WITTKE, W. (1970) Three Dimensional Percolation of Fissured Rocks. (See reference 6)

26. ZIENKIEWICZ, O.C. and CHEUNG, Y.K. (1965) Finite Elements in the Solution of Field Problems. The Engineer. Sept. pp 507-510.

27. ZIENKIEWICZ, O.C., MAYER, P. and CHEUNG, Y.K. (1966) Solution of Anisotropic Seepage by Finite Elements. Engr. Mech. Div. ASCE Vol. 92 pp 111-120 EM1.

28. SERVOMEX FIELD PLOTTER MANUAL. Crowborough Sussex, England.

APPENDIX 1

THE DEFINITION OF CERTAIN TERMS AS USED IN THIS THESIS

The terms which appear below are used in this thesis and are defined as follows:

A Terms relating to the rock mass

ROCK MASS The rock mass is defined as an aggregrate of blocks of solid rock material totally or partially separated from each other by structural features which constitute the mechanical discontinuities. The rock mass refers to any in situ rock with all the inherent geo-mechanical anisotropies (Piteau 1970)

ROCK MATERIAL OR INTACT ROCK This is the consolidated aggregrate of mineral particles forming the solid material in between structural discontinuities. (Piteau 1970)

ROCK REGION That is the particular section of the practical field problem which is to be analyse as a whole or in parts.

B Terms relating to the joints

FISSURES These are any clefts or mechanical discontinuities between blocks of solid rock material.

JOINTS A fracture or a fissure that traverses a rock mass.

MAJOR GEOLOGICAL DISCONTINUITIES Dykes , sills , faults or major joints of such a magnitude or nature that they dominate the flow pattern in their enviroment either by virtue of their greater permeability or impermeability.

For ease of reference in this thesis , in most cases the collective name - joints - will be used to denote the aggregate of all types of fissures, joints faults and major geological discontinuities that occur in a rock mass.

JOINT SET This is a group of nearlly parallel joints with approximately equal hydraulic properties.

JOINT GROUPS OF ASSEMBLAGES Both terms are taken to denote a combination of two or more intersecting joint sets.

JOINT SYSTEM OR PATTERN . The specific nature of the intersection of two or more joint sets.

JOINT REGION A body of jointed rock with recognisable boundaries within which the nature of the flow of the fluid is nearly uniform due to the uniformity of the pattern of the joint groups within the extent of the rock region.

JOINT SET CENTRAL TENDENCY Irregularly spaced and orientated joints of a joint set usually display a certain tendency to lie in certain preferred directions. This preferred direction is referred to as the "joint set central tendency"

C <u>Terms relating to the actual flow situation being investigated</u>

HYDROGEOLOGY This is taken to mean the total state of the fluid in the rock mass including all static and dynamic, mechanical and chemical effects of the fluid.

HYDRAULIC is the term which describes that which pertains to the flow of fluid subject to a potential gradient in the fissured rock mass.

FLOW REGIME This is the term which refers to the nature of the flow in the joints, i.e. its velocity, type etc. , and to the potential distribution in the jointed rock mass.

FIELD When used alone the term "field" is used in the mathematical sense to denote the extent and the nature of the hypothetical mathematical model being analysed.

PRACTICAL FIELD When used in conjuction with the term practical , the word "field" is taken to mean the actual situation which is occuring in practice.

CONDUCTIVITY The proportionality factor between the flow velocity and the potential gradient in a specified joint.

i.e. $V_s = B_s \dfrac{\partial\phi}{\partial s}$ where B_s is the conductivity

V_s is the joint flow velocity

$\dfrac{\partial\phi}{\partial s}$ is the joint potential gradient

PERMEABILITY This is the same as conductivity except it refers to the total aggregate of the jointed rock region viewed as a continuum.

STORAGE CAPACITY is the ability of a rock mass to retain fluid in storage.

PORE	PERMEABILITY STORAGE CAPACITY	These are the properties which result from the flow and storage of fluid in the interstices or voids of the rock material.
JOINT	PERMEABILITY STORAGE CAPACITY	These are the properties which result from the flow and storage of fluid in secondary rock structures such as joints, faults etc.

D <u>Terms describing the joint pattern</u>

CONTINUITY OF JOINTS The continuity of joints , from the hydraulic point of view , is the extent of the hydraulically active part of the joint with respect to the dimensions of the rock region being studied.

APPENDIX 2

THE FORMAL DEFINITION AND MANIPULATION OF TENSORS

Suppose $(x^1, x^2 \ldots\ldots x^n)$ and $(\underline{x}^1, \underline{x}^2 \ldots \underline{x}^n)$ are coordinates of a point in an N dimensional space in two frames of reference. The superscripts are indices and do not denote exponentiation. This is standard tensor usage.

Suppose that there exist N independent relations between the coordinates of the two systems having the form

$$
\begin{aligned}
\underline{x}^1 &= \underline{x}^1 (x^1, x^2, x^3, \ldots\ldots\ldots x^N) \\
\underline{x}^2 &= \underline{x}^2 (x^1, x^2, x^3, \ldots\ldots\ldots x^N) \\
&\cdot \\
&\cdot \\
\underline{x}^N &= \underline{x}^N (x^1, x^2, x^3, \ldots\ldots\ldots x^N)
\end{aligned}
\qquad (A.2.1)
$$

which is usually written or indicated by

$$\underline{x}^k = \underline{x}^k (x^1, x^2, x^3, \ldots\ldots\ldots x^N)$$

$$k = 1, 2, 3 \ldots\ldots N \qquad (A.2.2)$$

Conversely for each set of coordinates

($\underline{x}^1$,$\underline{x}^2$,$\underline{x}^3$, ... $\underline{x}^N$) there exists a corresponding unique set of coordinates (x^1 ,x^2 ,x^3 , ... x^N) given by

$$x^k = x^k (\underline{x}^1 ,\underline{x}^2 ,\underline{x}^3 , ... \underline{x}^N)$$

It is usual to adopt the summation convention when working with tensors. This convention is that whenever an index is repeated in a given term it denotes that summation be performed over the index from 1 to N. Thus the expression

$$a_1x^1 + a_2x^2 + a_3x^3 + a_4x^4 .... a_nx^n$$

can be written as a_jx^j by the summation convention.

Likewise $\underline{A}^p = \sum_{q=1}^{N} \frac{\partial \underline{x}^p}{\partial x^q} A^q \qquad p = 1,2,3 \ldots N$

can be written by the summation convention as

$$\underline{A}^p = \frac{\partial \underline{x}^p}{\partial x^q} A^q$$

Thus if N quantities A_1 , A_2 , ... A_n in a coordinate system (x^1 ,x^2 ,x^3 , ... x^N) are related to N other quantities $\underline{A}_1$, $\underline{A}_2$ ..... $\underline{A}_n$ in another coordinate system ($\underline{x}^1$,$\underline{x}^2$,$\underline{x}^3$.... $\underline{x}^N$) by the transformation

$$\underline{A}^p = \frac{\partial \underline{x}^p}{\partial x^q} A^q$$

the components are called the components of a contravarient tensor.

Such tensors arise when the relationship between two quantities involves one being a function of the differential of the other.

If N quantities A_1 ,A_2 , ... A_n are related to N other quantities $\underline{A}_1$, $\underline{A}_2$, ... $\underline{A}_n$ by the transformation

$$\underline{A}_p = \frac{\partial x^q}{\partial \underline{x}^p} A_q$$

they are called components of a covarient tensor of the first rank.

Such tensors occur when no differentials are involved in the relationship between the quantities in the field considered.

This is the formal definition of a tensor. A tensor or a tensor field is all possible sets of components of its field under any transformation of coordinates where the components transform according to the relationships

$$\underline{A}^{prm...n}_{ij....k} = \frac{\partial \underline{x}^p}{\partial x^q}\cdot\frac{\partial \underline{x}^r}{\partial x^s}\cdot\frac{\partial \underline{x}^m}{\partial x^t}\cdots\cdots\frac{\partial \underline{x}^n}{\partial x^z}\cdot\frac{\partial x^a}{\partial \underline{x}^i}\cdot\frac{\partial x^b}{\partial \underline{x}^j}\cdots\frac{\partial x^f}{\partial \underline{x}^k} A^{qst..z}_{ab...f}$$

Thus $\underline{A}^{prm...n}_{ij....k}$ are components of a mixed tensor of rank (n + k) contravarient of order n and covarient of order k.

By elementary substitution it can be shown that a Vector is a covarient tensor of rank one. Likewise what in this thesis has been called a Tensor can be shown to be a covarient tensor of rank two.

All the rules relating tensor or vector permeability coefficients as derived previously by simple axes transformations methods can be derived by means of the relationships given in this Appendix.

APPENDIX 3

COMPUTER PROGRAMS USED IN THIS THESIS

1 *PROGRAM ANEFF* (ANisotropic Element Flow Field)

This short program solves by iteration the potential distribution in the anisotropic element used as the standard model in the tests described in chapters 8 and 9.

Read in conjunction with the list of terms used the program is self explainatory.

List of terms used in the program

KXX KXY KYY	The elements of the two dimensional permeability tensor.
RXX SXX RXY SXY RYY SYY	Dummy variables used to avoid repetitive calculations.
H(I,J)	The potential at the i,j th node point.
NUM	The number of iterations to be performed.

Use of the program

The values of the coefficients of the permeability tensor and the number of iterations that it is considered will be sufficient for convergence should be fed in according to the formats given in format statements number 2 and 3.

The program ANEFF

```
      DIMENSION H(30,30)
      REAL KXX,KXY,KYY,II
      READ(5,2)KXX,KXY,KYY
2     FORMAT(3F5.0)
      READ(5,3)NUM
3     FORMAT(I3)
      II=KXX+KYY
      RXX=KXX/(2.*II)
      RXY=KXY/(4.*II)
      RYY=KYY/(2.*II)
      SXX=RXX
      SYY=KYY/II
      SXY=KXY/(2.*II)
C     SPECIFY ALL BOUNDARY CONDITIONS
      DO 6 I=1,21
      H(I,1)=100.0
6     H(I,21)=0.0
C     INITIAL INTERNAL POINT ESTIMATES
      DO 7 J=2,20
      RJ=J-1
      DO 7 I=1,21
7     H(I,J)=5.0*(21-RJ)
C     START OF RELAXATION PROCESS
      DO 8 K=1,NUM
C     TOP LINE
      DO 9 J=2,20
9     H(I,J)=SXX*(H(1,J-1)+H(1,J+1))+SYY*H(2,J)+SXY*
             (H(2,J-1)-H(2,J+1))
C     INTERIOR POINTS
      DO 10 I=2,29
      DO 10 J=2,20
      H(I,J)=RXX*(H(I,J+1)+H(I,J-1))+RXY*(H(I-1,J+1)
```

```
      -H(I-1,J-1)-H(I+1,J+1)+H(I+1,J-1))
10    H(I,J)=H(I,J)+RYY*(H(I-1,J)+H(I+1,J))
C     BOTTOM LINE
      DO 11 J=2,20
11    H(21,J)=SXX*(H(21,J-1)+H(21,J+1))+SYY*H(20,J)
                -SXY*(H(20,J-1)-H(20,J+1))
8     CONTINUE
      WRITE(7,72)
72    FORMAT(' FINITE DIFFERENCE SOLUTION OF ANISOTROPIC
                 FLOW FIELDS.')
      WRITE(7,73)NUM
73    FORMAT(/,' NUMBER OF ITERATIONS PERFORMED    ',I3)
      WRITE(7,77)
77    FORMAT(/,'  VALUES OF TENSOR PERMEABILITY COEFFICIENTS.')
      WRITE(7,61)KXX,KXY,KYY
61    FORMAT(/,'  KXX=',F5.1,3X,'KXY=',F5.1,3X,'KYY=',F5.1)
      DO 12 I=1,21
12    WRITE(7,21)(H(I,J),J=1,21)
21    FORMAT(//,2X,21F5.1)
      END
```

2 PROGRAM RNJSG (RaNdom Joint Set Generator)

The following program calculates from mean joint spacing and the mean joint length the number of joints that would occure in a square 100x100 units. (These units will be the same as those in which the mean length and spacing are given)

An IBM standard subroutine to generate uniformly distributed numbers between 0 and 1 has been inserted into the program to provide the required random numbers. For each joint four random numbers are generated.The first two give the coordinates of the midpoint of the joint. The third is inserted into the equation

$$y = e^{-x\alpha}$$

to yield a random joint length, which is distributed according to a well established distribution, given by Robertson (1970). It should be noted that α is taken a 1/(mean joint length) .

The fourth random number is used to generate a random orientation for the joint such that the orientation lies betwee previously specified maximum and minimum orientations.

Finally the program calculates the contribution to the total permeability tensor of each joint set generated. This contribution is calculated assuming that all joints are continuous , spaced uniformly at the mean joint spacing, and that no correction is made to account for the joint assemblage interconnections. The contributions from each joint set are assumed to yield the total permeability tensor.

Use of the program

The data required by the program is initially the number of joint sets for which random joint distributions are required. Next for each joint set the joint mean length, mean spacing and the maximum and minimum angles of orientation of the joints must be specified. Finally a random interger number of up to nine digits must be specified to act as a starting value for the generation of random numbers.

The formats for the input of this data are given in statements numbered 1,2 and 12 of this program.

<u>List of terms used in the program</u>

LM(I)	The i^{th} joint set mean length.
MD(I)	The i^{th} joint set mean spacing.
$\left\{ \begin{array}{l} \text{AGMAX(I)} \\ \text{AGMIN(I)} \end{array} \right\}$	The $\left\{ \begin{array}{l} \text{maximum} \\ \text{minimum} \end{array} \right\}$ angle of the spread of the joints in the i^{th} set
NJS	The number of joint sets for which random joint distribution are required.
RX(J)	The x coordinate of the j^{th} joint midpoint
RY(J)	" y " " " " " "
RL(J)	" length " " " " .
RO(J)	" orientation " " "
ALPH(I)	The value of α for the i^{th} joint set.
IX	A random integer number fed in to provide a starting value for the generation of random numbers.
IY	A dummy variable in the generation of random numbers.
YFL	The generated random number uniformly distributed between 0 and 1.
RN(K)	The k^{th} randomly generated number between 0 and 100
POW APY	Dummy variables used in the program.
IPX IPC IPY	The coefficients of the total permeability tensor.

The program RNJSG

```
        integer rx(3),ry(3),ri(3),ro(3)
        dimension lm(4),md(4),alpha(4),agmin(4),agmax(4),
                 nj(4),rn(12)
        dimension kxx(4),kxy(4),kyy(4)
        read(5,1)njs
1       format(i2)
        do 3 i=1,njs
        read(5,2)lm(i),md(i),agmin(i),agmax(i)
        do 9991 i=1,njs
9991    alph(i)=1./lm(i)
2       format(2i3,2f5.0)
        read(5,12)ix
12      format(i9)
c       calculate the number of joints per joint set
        do 14 i=1,njs
        inj=10000/(md(i)*lm(i))
        inj=inj/3
        inj=inj*3
14      nj(i)=inj
        do 66 i=1,njs
c       print all headings for each joint set
        write(7,76)i
76      format(///,2x,'JOINT SET NUMBER  ',i1,'DATA')
        write(7,75)lm(i),md(i),alph(i),agmin(i),agmax(i),nj(i)
75      format(//,2x,'length',i3,'  mean spacing',i3,
             '  alpha',f7.3,'  min ang',i5,'  max ang',i5,
             '  no joints',i5)
        write(7,74)
74      format(//,'      X    Y   LEN  ORN      X    Y
                LEN  ORN    X    Y  LEN  ORN')
c       generate random numbers
        nn=nj(i)/3
        do 7 j=1,nn
        do 48 k=1,12
        iy=ix*65539
        if(iy)61,61,61
```

```
      do 67 kkk=1,njs
      ipx=ipx+kxx(i)
      ipc=ipc+kxy(i)
67    ipy=ipy+kyy(i)
      write(7,68)
68    format(//,2x,'TOTAL PERMEABILITY TENSOR.')
      write(7,69)ipx,ipc,ipy
69    format(//,2x,'SXX=',i3,4x,'SXY=',i3,4x,'SYY=',i3)
      end
```

3 PROGRAM PSTCOM (Potential STatistical COMparison)

The following reads previously computed and measured values of the nodal potentials for the standard element used in this thesis and computes the difference at each node between the values of the computed and the measured potentials. The statistical mean,mean deviation , standard deviation and variance of the differences in nodal potentials is computed.

Use of the program

The dimensions of the matrix of nodal potentials is fed in first. Next the matrix of calculated nodal potentials is fed in ,then the matrix of measured , adjusted potentials is fed in all according to the relevant formats as given in the program.

List of terms used in the program

dev — The difference between the values of difm and dif(i,j) for the i,jth point

devm — The mean deviation of the difference in nodal potentials

dif(i,j) — The absolute value of sub for the i,jth point

DIFM	The mean value of DIF(I,J)
F2	Dummy variable used in the program
H(I,J) P(I,J)	The measured calculated value of the nodal potential
M N	The dimensions of the matrices of nodal potentials
SDEV SF2	Dummy variables used in the program
STD	The standard deviation of DIF(I,J)
SUB	The difference between the measured and calculated nodal potentials
SUM	The sum of the values of DIF(I,J)
VAR	The variance of DIF(I,J)

The program PSTCOM

```
      dimension h(21,21),p(21,21),dif(21,21)
c     read in all data for computation
      read(5,1)m,n
1     format(2i3)
      do 2 i=1,n
2     read(5,3)(h(i,j),j=1,m)
3     format(20f6.2)
      do 4 i=1,n
4     read(5,3333)(p(i,j),j=1,m)
3333  format(21f6.2)
      sum=0.0
c     calculation of nodal potential differences
      do 15 i=1,n
      do 15 j=1,m
      sub=h(i,j)-p(i,j)
      dif(i,j)=abs(sub)
15    sum=sum+dif(i,j)
c     statistical analysis of nodal potential differences
```

```
51      iy=iy+214748367+1
61      yfl=iy
        yfl=yfl*.4656615e-9
        ix=iy
        if(yfl)99,98,98
99      yfl=-yfl
98      continue
48      rn(k)=yfl*100
c       calculate coordinates etc for each point
        do 77 kk=1,3
        rx(kk)=rn(kk*4-3)
        ry(kk)=rn(kk*4-2)
        pow=rn(kk)/100.
        apx=-alog(pow)
        rl(kk)=apx/a-ph(i)
        ro(kk)=agmin(i)+(agmax(i)-agmin(i))*rn(kk*4)/100.
77      continue
        write(7,9)rx(1),ry(1),rl(1),ro(1),rx(2),ry(2),rl(2),
             ro(2),rx(3),ry(3),rl(3),ro(3)
9       format(2x,4i5,4x,4i5,4x,4i5)
3       continue
        ang=(agmin(i)+agmax(i))/(2.*57.292)
        rxx=(cos(ang))*(cos(ang))/md(i)
        kxx(i)=1000.*rxx
c       contributions to permeability tensor
        rxy=(-1.)*(cos(ang))*(sin(ang))/md(i)
        kxy(i)=1000.*rxy
        ryy+(sin(ang))*(sin(ang))/md(i)
        kyy(i)=1000.*ryy
        write(7,81)
81      format(//,2x,'CONTRIBUTIONS TO PERMEABILITY TENSOR')
        write(7,82)kxx(i),kxy(i),kyy(i)
82      format(//,2x,'kxx=',i3,2x,'kxy='i3,2x,'kyy=',i3)
66      continue
        ipx=0
        ipc=0
        ipy=0
```

```
      difm=sum/(m*n)
      sdev=0.0
      sf2=0.0
      do 16 i=1,n
      do 12 j=1,m
      dev=difm-dif(i,j)
      dev=abs(dev)
      f2=dev*dev
      sdev=sdev+dev
16    sf2+sf2+f2
      devm=sdev/(m*n)
      var=sf2/(m*n)
      std=sqrt(var)
c     print out all results
      write(7,17)
17    format(2x,'COMPARISON  OF CALCULATED AND MEASURED
                  POTENTIALS')
      write(7,10)
10    format(1h1,//,2x,'CALCULATED NODAL POTENTIALS')
      do 19 i=1,n
19    write(7,111)(h(i,j),j=1,m)
111   format(//,2x,20f6.2)
      write(7,212)
212   format(//,2x,'MEASURED NODAL POTENTIALS')
      do 213 i=1,n
213   write(7,111)(p(i,j),j=1,m)
      write(7,314)
314   format(1h1,2x,'NODAL POTENTIAL DIFFERENCES')
      do 315 i=1,n
315   write(7,316)(dif(i,j),j=1,m)
316   format(//,2x,21f6.2)
      write(7,214)
214   format(//,2x,'STATISTICAL PARAMETER VALUES')
      write(7,215)difm,devm,var,std
215   format(//,2x,'MEAN DIFFERENCE',f9.4,//,2x,
          'MEAN DEVIATION',f9.4,//,2x,'VARIANCE,f9.4,//,
             2x,'STD DEV.'f9.4)
      end
```

APPENDIX 4

THE USE AND FORM OF THE EQUATIONS INVOLVING THE TENSOR PERMEABILITY COEFFICIENTS

The equations which describe the potential distribution in an anisotropic mass using the permeability tensor are given. Equations for most of the particular cases which occur in practice are given. The Finite Difference form of all equations is given.

Some further consideration concerning the finite difference method

The basic formulation of the finite difference method has been presented in Chapter 2. The following points regarding the method should be observed.

1. The finite difference grid can be two dimensional or three dimensional with different spacings in all directions. The grid spacing depends on the nature of the field situation.

2. The only limitation on the number of nodal points used is the availability and capacity of the computer installation on hand for the solution of the resulting finite difference expressions.

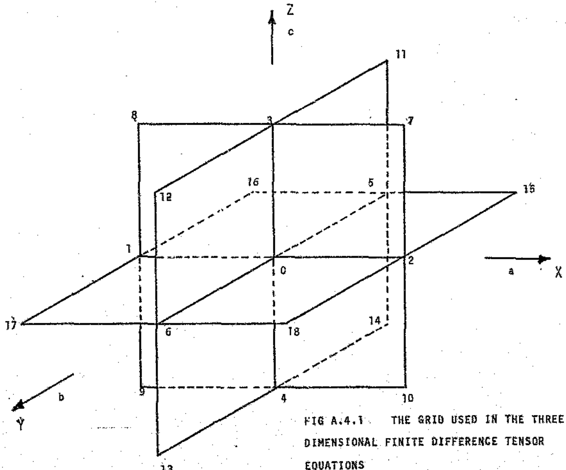

FIG A.4.1 THE GRID USED IN THE THREE DIMENSIONAL FINITE DIFFERENCE TENSOR EQUATIONS

$$\phi_0 = \frac{\left\{ d_1 \frac{k_{xx}}{a^2} \phi_1 + d_2 \frac{k_{xx}}{a^2} \phi_2 + d_3 \frac{k_{zz}}{c^2} \phi_3 + d_4 \frac{k_{zz}}{c^2} \phi_4 + d_5 \frac{k_{yy}}{b^2} \phi_5 + d_6 \frac{k_{yy}}{b^2} \phi_6 \right\} + \frac{k_{xz}}{ac} (d_7 \phi_7 + d_8 \phi_8 + d_9 \phi_9 + d_{10} \phi_{10}) + \frac{k_{zy}}{bc} (d_{11}\phi_{11} + d_{12}\phi_{12} + d_{13}\phi_{13} + d_{14}\phi_{14}) + \frac{k_{xy}}{ab} (d_{15}\phi_{15} + d_{16}\phi_{16} + d_{17}\phi_{17} + d_{18}\phi_{18}) + Y}{\left(d_1 \frac{k_{xx}}{a^2} + d_2 \frac{k_{xx}}{a^2} \; d \; d_3 \frac{k_{zz}}{c^2} + d_4 \frac{k_{zz}}{c^2} + d_5 \frac{k_{yy}}{b^2} + d_6 \frac{k_{yy}}{b^2} + X \right)}$$

FIG A.4.2 THE GENERAL EXPRESSION FOR THREE DIMENSIONAL FINITE DIFFERENCE TENSOR FLOW FIELDS

TABLE A4.1.a THE COEFFICIENTS TO BE USED IN EQUATION

FROM FIG A.4.2

CASE	d_1	d_2	d_3	d_4	d_5	d_6	d_7	d_8	d_9
1	1	1	1	1	1	1	1/2	-1/2	1/2
2	1/2	1/2	1	0	1/2	1/2	1/2	-1/2	0
3	0	1/2	1/2	0	1/4	1/4	1/2	0	0
4	1/2	1	1	1/2	3/4	3/4	0	-1/2	0
5	0	1/4	1/4	0	0	1/4	1/4	0	0
6	3/4	1	1	3/4	1	3/4	0	-7/16	3/8

	d_{10}	d_{11}	d_{12}	d_{13}	d_{14}	d_{15}	d_{16}	d_{17}	d_{18}
1	-1/2	1/2	1/2	-1/2	1/2	-1/2	1/2	-1/2	1/2
2	0	-1/2	1/2	0	0	-1/4	1/4	-1/4	-1/4
3	0	0	0	0	0	0	0	0	0
4	-1/2	-7/16	7/16	7/16	7/16	-7/6	7/16	-7/16	7/16
5	0	0	1/4	0	0	0	0	0	1/4
6	-7/16	-1/2	7/16	3/8	7/16	-1/2	7/16	-3/8	7/16

CASE	X	Y
1	0	0
2	0	0
3	$k_{xz}/2$	0
4	$-3/2*k_{xz}$	$1/8\ (k_{xy} + k_{yz})(\phi_6 - \phi_5)$
5	$1/4(k_{xy} + k_{xz} + k_{zy})$	0
6	0	$1/16\{k_{xy}(\phi_3 - \phi_4 + \phi_5 + \phi_6) + k_{yz}(-\phi_3 + \phi_4 - \phi_5 + \phi_6)\}$

TABLE A.4.1.b THE COEFFICIENTS TO BE USED IN EQUATION FROM FIG A4.2

3. The finite difference grid is normally taken as being an orthogonal network , but the axes of the network do not have to coincide with the principal axes of the region being analysed. In fact in all the succeeding work the assumption is made that the grid axes and the axes of principal permeability are not coincident. Simplifications to the equations result if

a) The axes system in which the partial differential equations are written are coincident with the principal axes of permeability.

b) The finite difference grid axes are coincident with the principal axes of permeability.

In both cases the permeability tensor is diagonalised.

4. Two methods have been used to derive the finite difference expressions presented. They are

a) By writing directly the finite difference form of the differential equations involved.

b) By considering conservation of fluid within an element formed by the nodal points.

The latter method is the preferred method for special cases and boundary nodes. In this case it has been taken that the velocity in a certain direction V_x say is given directly by the equation $\underset{\sim}{V}_x = -\underset{\sim}{K}\ \mathrm{grad}\phi$ and that the orthogonal potential gradients are those operative on the faces of the element through which flow is taking place. In all cases flow is assumed to be taking place in the positive direction of the coordinate axes system

The Three Dimensional Tensor Equations

The equation describing the potential distribution in a three dimensional flow field is

$$\sum_{i=x}^{z} \sum_{j=x}^{z} k_{ij} \frac{\partial^2 \phi}{\partial i\ \partial j} = 0 \qquad \text{(A.4.1)}$$

if both the flowing fluid and the medium are incompressible.

The finite difference form of equation (A.4.1) has been written for interior nodes and for nodes at various types of boundaries. Fig A.4.1 shows the grid system and numbering required to relate the potential at a point ϕ_o to the values of the surrounding potentials ϕ_1 to ϕ_{18}

Fig A.4.2 gives the general form of the equation into which coefficients for the various cases , taken from table A.4.1 are to be inserted.

For the two dimensional form of the equation (A.4.1) and the equation given in fig A.4.2 , put all the coefficients involving the nonexistant direction to zero.

The Mathematical Description of the Water Table Movement using Tensor Coefficients

The assumptions made in order to obtain a mathematical description of the water table movement with time are:

1. Capillary effects are neglected.
2. Below the phreatic line the rock joints are filled with water.

Taking Z_f as the height above datum of the water table , the vertical movement of the water table with respect to time is $\frac{\partial Z_f}{\partial t}$. Considering three dimensional flow the rate of change of storage of the element at the water table is (see fig A.4.3)

$$\frac{\partial Z_f}{\partial t} \quad \delta x \ \delta y \ S_y$$

where S_y denotes the specific yield of the rock mass as defined by Lyell (1968)

Taking flow into the element as positive and flow out as negative and assuming flow in the positive direction of the coordinate axes system , the following equations result.

Quantity of flow in the X direction

$$Q_x = V_x(\delta_y\delta_z + \delta_x\delta_y\tan\theta_x + 1/2\delta_y\delta_y\tan\theta_y)$$

$$-(V_x + \frac{\partial V_x}{\partial x})(\delta_x\delta_y + 1/2\ \delta_y\delta_y\tan\theta_y) \qquad (A.4.2a)$$

Quantity of flow in the Y direction

$$Q_y = V_y(\delta_x\delta_z + \delta_x\delta_y\tan\theta_y + 1/2\ \delta_x\delta_x\tan\theta_x)$$

$$-(V_y + \frac{\partial V_y}{\partial y})(\delta_x\delta_z + 1/2\ \delta_x\delta_x\tan\theta_x) \qquad (A.4.2b)$$

Quantity of flow in the Z direction

$$Q_z = V_z\delta_x\delta_y + W\delta_x\delta_x \qquad (A.4.2c)$$

Hence from conservation of mass

$$Q_x + Q_y + Q_z = \frac{\partial Z_f}{\partial t}\ \delta_x\delta_x\ S_y \qquad (A.4.3)$$

Substituting and neglecting third order terms, gives

$$W + V_x\tan\theta_x + V_y\tan\theta_y + V_z = \frac{\partial Z_f}{\partial t} . S_y \qquad (A.4.4)$$

which in matrix notation can be written.

$$W \;+\; \left(V_x \quad V_y \quad V_z \right) \begin{Bmatrix} \tan\theta_x \\ \tan\theta_y \\ 1 \end{Bmatrix} \;=\; \frac{\partial Z_f}{\partial t} \cdot S_y \qquad \text{(A.4.5)}$$

Note however that $(V_x \quad V_y \quad V_z)$ is the transpose of the velocity matrix from the equation.

$$\underset{\sim}{V} = -\underset{\sim}{K}\,\mathrm{grad}\phi$$

Hence

$$\underset{\sim}{V}^t = -\mathrm{grad}\phi^t \cdot \underset{\sim}{K}^t$$

Thus equation(A.4.5) can be written

$$W - \mathrm{grad}\phi^t \cdot \underset{\sim}{K}^t \begin{Bmatrix} \tan\theta_x \\ \tan\theta_y \\ 1 \end{Bmatrix} = \frac{\partial Z_f}{\partial t} \cdot S_y \qquad \text{(A.4.6)}$$

This is then the equation which describes the drawdown with time of the phreatic line.

In order to derive the finite difference form of eqn.(A.4.6) consider fig A.4.3

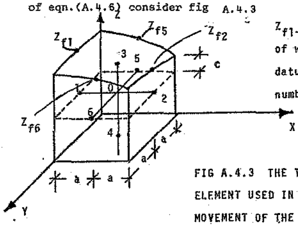

Z_{f1-5} denote height of water table above datum. 1-5 are node numbers.

FIG A.4.3 THE THREE DIMENSIONAL ELEMENT USED IN CONSIDERING THE MOVEMENT OF THE WATER TABLE.

The resulting equation is

$$\frac{W}{S_y} - \left(\frac{\phi_1 - \phi_2}{2a} \qquad \frac{\phi_5 - \phi_6}{2a} \qquad \frac{\phi_0 - \phi_3}{c} \right) \frac{K}{S_y} \begin{Bmatrix} \frac{Z_{f1} - Z_{f2}}{2a} \\ \frac{Z_{f5} - Z_{f6}}{2a} \\ 1 \end{Bmatrix} = \frac{\partial Z_f}{\partial t} \qquad \text{(A.4.7)}$$

<u>The Finite Difference form of the Equation for Interior Nodes Immediately below the Water Table</u>

The two following equations are used in the program given in APPENDIX 6 to study the drawdown rate and the final position of the phreatic line in a two dimensional anisotropic slope. They are not derived , but are merely given.

Special Case which usually occures.

$$\phi_o = \frac{k_{xx}.c.(a+c)(\phi_1+\phi_2) + 2.k_{yy}.a(c\phi_4+a\phi_3) + \dfrac{(a+c)k_{xy}.a.c.}{(a+c_1)(a+c_2)}\{ (a+c_2)(\phi_7+\phi_0)-(a+c_1)(\phi_8-\phi_5)\}}{2\{ k_{xx}(a.c+c^2) + (a^2 + a.c)k_{yy}\}}$$

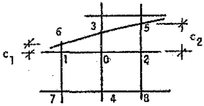

FIG A.4.4 WATER TABLE POSITION AND NODE NUMBERS FOR SPECIAL CASE

General Case

$$\phi_o \left(\frac{k_{xx}}{a.d} + \frac{k_{yy}}{a.c}\right) = \frac{k_{xx}}{(a+d)}\left(\frac{\phi_1}{d} + \frac{\phi_2}{a}\right) + \frac{k_{yy}}{(a+c)}\left(\frac{\phi_3}{c} + \frac{\phi_4}{a}\right)$$

$$+ \frac{k_{xy}}{(4a)}\left(\frac{\phi_5}{a} - \frac{2\phi_6}{y} + \frac{2\phi_7}{y} - \frac{\phi_8}{a}\right)$$

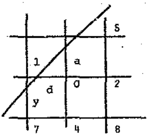

FIG A.4.5 WATER TABLE POSITION FOR GENERAL CASE

APPENDIX 5

THE RESULTS OF TESTS DESCRIBED IN CHAPTER 7

The results of tests described in Chapter 7 are presented in two forms.

a) A plot of the equipot tials.

b) The numerical value of the potentials at the nodes of a hunured element square grid.

Hence it is possible to compare the accuracy of the results in two ways. This can be done firstly by making a purely visual comparison of the equipotentials which result from the various methods of determining the potential distribution , and secondly by computing the numerical differences in the values of the potentials at the nodal points. These differences * were then analysed statistically to yield the mean nodal potential differences and the variance and the standard deviation of the values of the differences in the nodal potentials.

In those particular cases where it was not possible to measure the nodal potential i.e. where no joint coincided with the node , the results have been plotted on a grid with the figures in the block referring to

* In all results reported only the absolute difference in nodal potentials is used in computing the parameters describing the spread of the values of the differences in nodal potentials.

the node at the upper right of the block. In all cases the upper figure is the value of the nodal potential as measured on the joint analogue and the lower figure is the nodal potential as calculated by computer. The third figure in the block is the difference between the above two potentials.

RESULTS OF TEST A.1

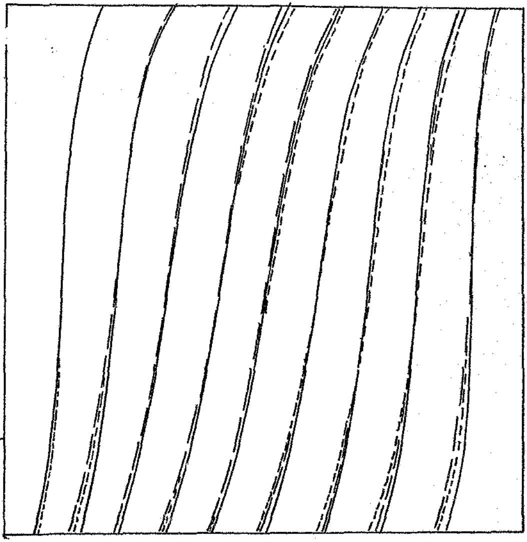

FIG. A.5.1. SUPERPOSITION OF EQUIPOTENTIALS FOR TEST A.1

LEGEND. a. Computer program ANEFF — — —
b. Teledeltos equivalent joint analogue ————
c. Transformed scale equivalent isotropic element - - - - - - -

100.00	94.90	87.97	79.91	71.03	61.48	51.30	40.46	28.79	15.79	0.0
100.00	93.46	85.85	77.38	68.21	58.43	48.07	37.10	25.43	12.95	0.0
100.00	92.47	84.22	75.31	65.84	55.85	45.40	34.49	23.16	11.53	0.0
100.00	91.72	82.90	73.57	63.81	53.67	43.20	32.47	21.57	10.66	0.0
100.00	91.09	81.76	72.05	62.02	51.76	41.33	30.83	20.35	10.02	0.0
100.00	90.53	80.72	70.52	60.62	50.00	39.64	29.37	19.28	9.46	0.0
100.00	89.98	79.65	69.67	58.66	48.24	37.97	27.95	18.24	9.90	0.0
100.00	89.33	78.43	67.53	56.80	46.33	36.19	26.42	17.10	8.28	0.0
100.00	88.47	76.84	65.51	54.60	44.14	34.16	24.68	15.78	7.53	0.0
100.00	87.01	74.57	62.90	51.93	41.56	31.78	22.62	14.15	6.54	0.0
100.00	84.20	71.21	59.54	48.70	38.52	28.96	20.09	12.03	5.10	0.0

TABLE A5.1 NODAL POTENTIALS AS CALCULATED BY COMPUTER PROGRAM ANEFF

100.00	95.30	88.90	81.00	72.60	63.60	53.20	42.70	30.40	17.50	0.0
100.00	93.80	86.70	79.00	70.30	60.60	50.30	39.50	27.20	14.30	0.0
100.00	92.70	84.90	76.80	67.60	58.00	47.50	36.50	24.60	12.30	0.0
100.00	92.30	83.60	74.50	65.30	55.60	44.90	34.10	22.80	11.40	0.0
100.00	91.50	82.30	73.30	63.60	53.30	42.80	32.20	21.40	11.50	0.0
100.00	90.80	81.10	71.60	61.80	51.20	40.50	30.30	20.20	10.00	0.0
100.00	90.10	79.90	69.80	59.60	49.30	38.60	28.70	18.80	9.30	0.0
100.00	89.60	78.50	67.80	57.80	47.10	36.50	27.00	17.40	8.60	0.0
100.00	89.00	76.80	65.80	55.30	44.50	34.90	25.00	15.60	7.30	0.0
100.00	86.50	74.80	62.50	51.90	42.10	32.00	22.50	13.40	6.10	0.0
100.00	84.00	71.70	59.10	48.60	38.60	29.10	20.00	11.20	4.60	0.0

TABLE A5.2 NODAL POTENTIALS AS MEASURED ON EQUIVALENT ISOTROPIC ANALOGUE

0.00	.40	.93	1.09	1.57	2.12	1.90	2.24	1.61	1.71	0.00
0.00	.34	.85	1.62	2.09	2.17	2.23	2.40	1.77	1.35	0.00
0.00	.23	.68	1.49	1.76	2.15	2.10	2.01	1.44	.77	0.00
0.00	.58	.70	.93	1.49	1.93	1.70	1.63	1.23	.74	0.00
0.00	.41	.54	1.25	1.58	1.54	1.47	1.37	1.05	1.48	0.00
0.00	.27	.38	.98	1.46	1.20	.86	.93	.92	.54	0.00
0.00	.12	.25	.13	.94	1.06	.63	.75	.56	.60	0.00
0.00	.27	.07	.27	1.00	.77	.31	.58	.30	.22	0.00
0.00	.53	.04	.29	.70	.36	.74	.32	.18	.23	0.00
0.00	.51	.23	.40	.03	.54	.22	.12	.75	.44	0.00
0.00	.20	.49	.44	.10	.08	.14	.09	.83	.60	0.00

Statistical Parameter Values:	Mean Difference	0.732
	Mean Deviation	0.572
	Variance	0.464
	Std. Deviation	0.681

TABLE A5.3 DIFFERENCES IN NODAL POTENTIALS AND STATISTICAL PARAMETERS DESCRIBING SUCH

TABLE A5.4 COMPARISON OF NODAL POTENTIALS
FOR JOINT ANALOGUE

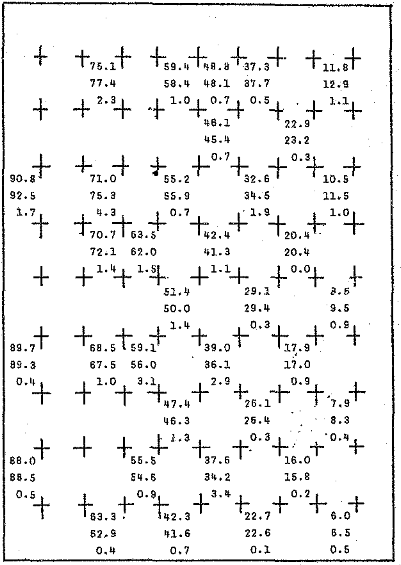

Statistical Parameter Values:

Mean Difference	1,13	Mean Deviation	0,72
Variance	0.97	Std. Deviation	0,98

RESULTS OF TEST A.2

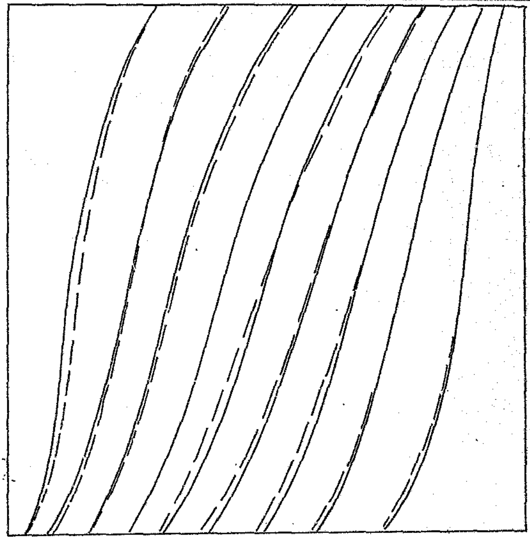

FIG. A.5.2 SUPERPOSITION OF EQUIPOTENTIALS FOR TEST A.2

LEGEND. a. Computer program ANEFF
b. Teledeltos equivalent joint analogue.

100.00	98.10	94.08	88.35	81.05	72.34	62.26	50.73	37.39	21.33	0.0
100.00	96.56	91.37	84.62	76.45	66.92	56.07	43.83	30.09	14.93	0.0
100.00	95.24	88.94	81.23	72.21	61.98	50.62	38.26	25.15	11.97	0.0
100.00	94.05	86.75	78.11	68.35	57.58	46.03	33.96	21.84	10.30	0.0
100.00	92.97	84.67	75.21	64.79	53.66	42.12	30.55	19.39	9.10	0.0
100.00	91.94	82.68	72.39	61.38	50.00	38.62	27.61	17.32	8.06	0.0
100.00	90.90	80.60	69.44	57.88	46.34	35.21	24.79	15.33	7.03	0.0
100.00	89.70	78.16	66.04	53.97	42.42	31.65	21.88	13.27	5.95	0.0
100.00	88.02	74.85	61.74	49.38	38.02	27.78	18.77	11.06	4.76	0.0
100.00	85.07	69.91	56.17	43.93	33.08	23.56	15.38	8.63	3.44	0.0
100.00	78.67	62.60	49.27	37.73	27.65	18.95	11.67	5.92	1.90	0.0

TABLE A5.5 NODAL POTENTIALS AS CALCULATED BY COMPUTER PROGRAM ANEFF

100.00	98.22	93.80	87.85	80.63	72.45	62.30	50.72	37.90	20.38	0.0
100.00	96.50	91.00	84.22	76.10	67.17	53.40	41.82	30.22	14.93	0.0
100.00	95.15	88.65	81.18	71.85	61.90	50.80	38.20	25.05	11.65	0.0
100.00	93.97	86.47	80.07	68.15	57.55	46.02	33.72	21.70	9.98	0.0
100.00	93.10	84.37	74.80	64.32	52.22	42.05	30.47	19.40	8.98	0.0
100.00	92.02	82.47	72.37	61.20	49.95	38.80	27.63	17.52	7.98	0.0
100.00	91.02	80.60	69.52	57.95	47.77	35.68	25.20	15.63	6.90	0.0
100.00	90.02	78.30	66.27	53.97	42.45	31.85	19.92	13.53	5.03	0.0
100.00	88.35	74.95	61.80	49.20	38.10	28.15	18.82	11.35	4.85	0.0
100.00	85.07	69.77	58.17	46.60	32.82	23.90	15.78	9.00	3.50	0.0
100.00	79.63	62.10	49.27	37.70	27.55	19.37	12.15	6.20	1.78	0.0

TABLE A5.6 NODAL POTENTIALS AS MEASURED ON EQUIVALENT ISOTROPIC ANALOGUE

0.00	.12	.28	.48	.42	.11	.04	.01	.51	.95	.00
0.00	.06	.37	.40	.35	.25	2.67	2.01	.13	.00	.00
0.00	.09	.29	.05	.36	.08	.18	.06	.10	.32	.00
0.00	.08	.26	1.96	.20	.03	.01	.24	.14	.32	.00
0.00	.13	.30	.41	.47	1.44	.07	.08	.01	.12	.00
0.00	.08	.21	.02	.18	.05	.18	.02	.20	.08	.00
0.00	.12	.00	.08	.07	1.43	.47	.41	.30	.13	.00
0.00	.32	.14	.23	.00	.03	.20	1.96	.26	.08	.00
0.00	.33	.10	.06	.18	.08	.37	.05	.29	.09	.00
0.00	.00	.14	2.00	2.67	.26	.35	.40	.37	.06	.00
0.00	.96	.50	.00	.03	.10	.42	.48	.28	.12	.00

Statistical Parameter Values:		
	Mean Difference	0,288
	Mean Deviation	0,292
	Variance	0,256
	Std. Deviation	0,506

TABLE A5.7 DIFFERENCES IN NODAL POTENTIALS AND STATISTICAL PARAMETERS DESCRIBING SUCH

RESUTS OF TEST A.3

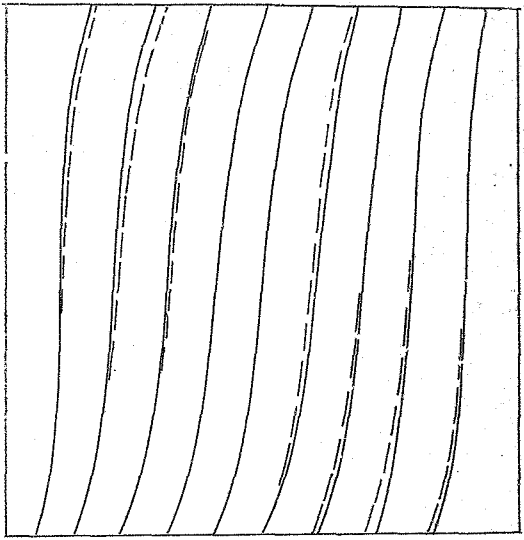

FIG A.5.3 SUPERPOSITION OF EQUIPOTENTIALS FOR TEST A.3

LEGEND a. Computer program ANEFF ———————

b. Teledeltos equivalent joint analogue — — — —

100.00	94.28	86.81	78.33	69.17	59.46	49.27	38.59	27.26	14.86	0.0
100.00	93.07	85.09	76.34	66.99	57.14	46.85	36.08	24.74	12.67	0.0
100.00	92.21	83.73	74.64	65.07	55.09	44.73	34.00	22.90	11.46	0.0
100.00	91.55	82.59	73.16	63.36	53.25	42.88	32.28	21.51	10.67	0.0
100.00	90.99	81.57	71.81	61.80	51.58	41.24	30.81	20.38	10.06	0.0
100.00	90.47	80.61	70.52	60.29	50.00	39.71	29.48	19.39	9.53	0.0
100.00	89.94	79.61	69.18	58.76	48.41	38.20	28.18	18.43	9.01	0.0
100.00	89.33	78.49	67.71	57.11	46.74	36.63	26.83	17.41	8.45	0.0
100.00	88.54	77.10	66.00	55.27	44.91	34.97	25.35	16.27	7.79	0.0
100.00	87.33	75.26	63.92	53.15	42.86	33.01	23.66	14.91	6.93	0.0
100.00	85.14	72.74	61.41	50.72	40.53	30.83	21.67	13.19	5.72	0.0

TABLE A5.8 NODAL POTENTIALS AS CALCULATED BY COMPUTER PROGRAM ANEFF

100.00	94.55	87.05	78.60	69.63	59.80	49.63	38.72	27.57	15.25	0.0
100.00	93.07	85.35	76.77	67.43	57.27	47.02	36.20	24.92	12.90	0.0
100.00	92.25	84.05	74.98	65.60	55.47	44.20	34.13	22.95	11.63	0.0
100.00	91.55	82.82	73.70	63.65	53.60	42.92	32.18	21.55	10.60	0.0
100.00	90.88	81.75	72.27	61.95	51.57	41.13	30.57	20.52	10.03	0.0
100.00	90.25	80.90	70.80	60.55	50.28	39.45	29.20	19.10	9.75	0.0
100.00	89.97	79.47	69.42	58.88	48.42	38.05	27.72	18.25	9.13	0.0
100.00	89.40	78.45	67.82	57.07	46.40	36.35	26.30	17.18	8.45	0.0
100.00	88.37	77.05	65.87	55.80	44.52	34.40	25.02	15.95	7.75	0.0
100.00	87.10	75.07	63.80	52.97	42.72	32.57	23.22	14.65	6.93	0.0
100.00	84.75	72.42	61.27	50.38	40.20	30.38	21.40	12.95	5.45	0.0

TABLE A5.9 NODAL POTENTIALS AS MEASURED ON EQUIVALENT ISOTROPIC ANALOGUE

0.00	.27	.24	.27	.46	.34	.36	.13	.31	.39	.00
0.00	.00	.26	.43	.44	.13	.17	.12	.18	.23	.00
0.00	.04	.32	.34	.53	.38	.53	.13	.05	.17	.00
0.00	.00	.23	.54	.29	.35	.04	.10	.04	.07	.00
0.00	.11	.18	.46	.15	.01	.11	.24	.14	.03	.00
0.00	.22	.29	.28	.26	.28	.26	.28	.29	.22	.00
0.00	.03	.14	.24	.12	.01	.15	.46	.18	.12	.00
0.00	.07	.04	.01	.04	.34	.28	.53	.23	.00	.00
0.00	.17	.05	.13	.53	.39	.52	.33	.32	.04	.00
0.00	.23	.19	.12	.18	.14	.44	.44	.26	.00	.00
0.00	.39	.32	.14	.34	.33	. 5	.27	.24	.27	.00

Statistical Parameter Values: Mean Difference 0.190

Mean Deviation 0,137

Variance 0,026

Std. Deviation 0,160

TABLE A5.10 DIFFERENCES IN NODAL POTENTIALS AND STATISTICAL PARAMETERS DESCRIBING SUCH

TABLE A6.11 COMPARISON OF NODAL POTENTIALS FOR JOINT ANALOGUE

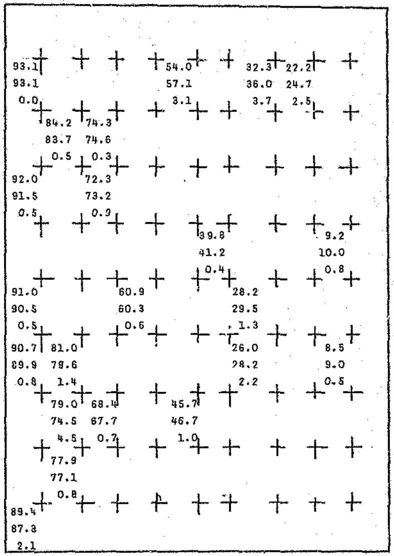

Statistical Parameter Values:

Mean Difference	1,36	Mean Deviation	0,87
Variance	1,27	Std. Deviation	1,13

RESULTS OF TEST B.1

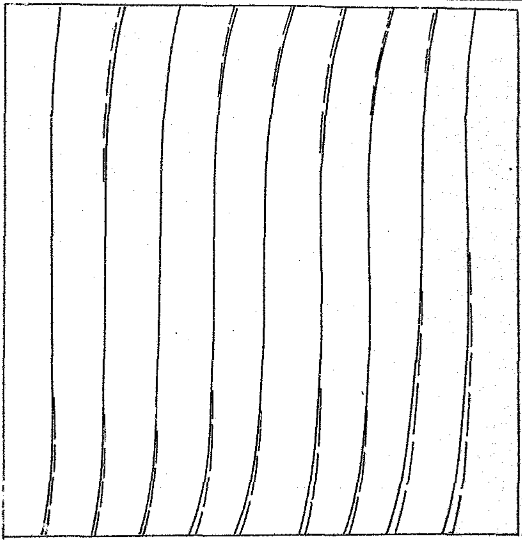

FIG. A.5.4 SUPERPOSITION OF EQUIPOTENTIALS FOR TEST B.1

LEGEND. a. Computer solution ————

b. Joint analogue — — —

TABLE A5.12 COMPARISON OF NODAL POTENTIALS FOR RANDOM JOINT TEST BI

	87.1			59.6				
	87.9			61.5				
	0.8			1.9				
93.0	86.0	76.3	66.8	58.7	48.1	37.2	23.5	12.8
93.5	85.8	77.4	68.2	58.4	48.1	37.1	25.4	12.9
0.5	0.2	1.7	1.4	1.7	0.0	0.1	1.9	0.1
92.9		73.9	64.5	55.6	47.7	37.5	22.5	
92.5		75.3	65.8	55.9	45.4	34.5	23.2	
0.4		1.4	1.3	0.3	2.3	3.2	0.7	
93.5	84.3		62.5	55.3	46.5	37.5	18.2	
91.7	82.9		63.8	53.7	43.2	32.5	21.6	
1.8	1.4		1.3	1.6	3.3	5.0	8.4	
90.9		72.8	62.1		42.1		22.1	10.0
91.1		72.1	62.0		41.3		20.4	10.0
0.2		0.7	1.0		0.8		1.7	0.0
	81.9	71.9		52.9		30.8	21.2	
	80.7	70.6		50.0		29.4	19.3	
	1.2	1.3		2.9		1.4	1.9	
	80.7		60.0			30.0		10.0
	78.7		58.7			28.0		8.9
	2.0		1.3			2.0		1.1
91.5		67.5		48.2	40.0		17.8	7.5
89.3		67.5		46.3	36.1		17.1	8.2
2.2		0.0		1.9	3.9		0.7	0.7
92.0	79.9	64.6	55.0	48.8		27.7	13.9	6.6
88.4	76.8	65.5	54.6	44.2		24.7	15.8	7.5
3.6	3.1	0.9	0.4	4.6		3.0	1.9	0.9
87.7		65.8	54.4		34.0		15.6	6.9
87.0		62.3	51.9		31.7		14.2	6.5
0.7		2.9	2.5		2.3		1.4	0.4
	74.3		53.7	42.1				
	71.2		48.7	38.5				
	3.1		5.0	3.6				

Statistical Parameters Values: Mean Difference 1,67
Mean Deviation 1,01 Variance 1,59 Std. Dev 1,26

TABLE A5.13 COMPARISON OF MEASURED AND CALCULATED NODAL POTENTIALS FOR ANALOGUE AS IN FIG 7.7a

```
66.9
71.1
4.7
85.9 38.1 10.2
89.9 37.1 12.9
4.0 1.0 2.7
93.0 83.2 76.0 66.4 50.9
92.5 84.2 75.3 65.8 55.9
0.5 1.0 0.7 0.6 5.0
91.3 84.6 43.3 19.6
91.7 82.9 53.6 21.6
0.4 1.7 10.3 2.0
71.9 53.6 24.9 9.9
72.1 51.7 30.9 10.0
0.2 1.9 6.0 0.1
64.6 35.1 18.2 8.1
60.4 39.7 19.3 9.5
4.2 4.6 1.1 1.4
87.1 75.6 63.8 37.9 15.6 7.9
79.7 69.7 58.7 37.9 18.2 9.9
7.4 5.9 5.1 0.0 2.2 2.0
71.5 23.7 8.2
67.5 26.4 8.3
4.0 2.7 0.1
91.7 77.2 66.3 47.8 6.2
88.5 76.8 65.5 44.1 7.5
3.2 1.4 0.8 3.7 1.3
77.1 62.6 43.6 32.1 22.2 14.2 10.0
74.6 62.9 41.6 31.8 22.6 14.2 6.5
2.5 0.3 2.0 0.3 0.4 0.0 3.5
```

Statistical Parameter Values:

Mean Difference	3,13	Mean deviation	2,3
Variance	11,5	Std. Deviation	3,40

TABLE A.5.14 STATISTICAL PARAMETER VALUES DESCRIBING THE DIFFERENCES OF NODAL POTENTIALS FOR TWO RANDOM JOINT SETS AS IN FIG 7.7b

MEAN DIFFERENCE	2,3
MEAN DEVIATION	1,5
VARIANCE	5,4
STANDARD DEVIATION	2,3

TABLE A5.15 COMPARISON OF MEASURED AND CALCULATED *NODAL POTENTIALS FOR ANALOGUE SHOWN IN FIG 7.8a*

```
     81.3
     87.9
      6.6
88.7 86.0 63.9      50.5           14.6
93.5 85.9 77.4      58.4           25.4
 4.8  0.1  7.5       7.9            9.8
90.0 81.4 71.5 60.0 56.3 42.6 29.8       5.0
92.5 84.2 75.3 65.8 55.9 45.0 34.5      11.5
 2.5  2.8  3.8  5.8  0.4  2.4  4.7       6.5
92.3 82.8      58.4 52.8 43.2      18.1
91.7 82.9      63.8 53.7 43.2      21.6
 0.6  0.1       5.4  0.9  0.0       3.5
86.0      71.1 62.1      44.9      19.9
91.1      72.1 62.0      41.3      10.2
 5.1       1.0  0.1       3.6       9.7
     81.0 70.3                29.9 18.9
     80.7 70.6                29.4 19.3
      0.3  0.3                 0.5  0.4
     84.3
     79.7
      4.6
90.4      69.4      51.5           14.6
89.3      67.5      46.3           17.1
 1.1       1.9       5.2            2.5
          68.4           41.8 31.4
          65.5           34.2 24.7
           2.9            7.6  6.7
84.0      69.4 60.0      40.3      18.0 18.2
87.0      62.9 51.9      31.8      14.2  6.5
 3.0       6.5  8.1       8.5       3.8 11.7
```

Statistical Parameter Values:

Mean Difference 4,1 Mean Deviation 2,7

Std. Deviation 3,1

TABLE A5.76 COMPARISON OF MEASURED AND CALCULATED NODAL POTENTIALS FOR ANALOGUE SHOWN IN FIG 7.8b

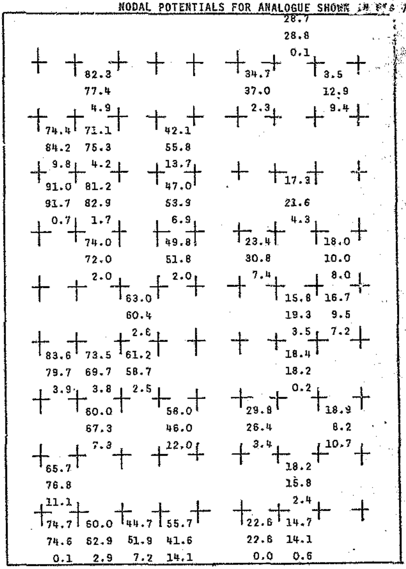

Statistical Parameter Values;

Mean Difference 4,8 Mean Deviation 3,5

Variance 16,6 Std. Deviation 4,1

TABLE A.5.17

STATISTICAL DISTRIBUTION OF DIFFERENCES IN NODAL POTENTIALS FOR THREE RANDOM JOINT SETS AS TESTED IN TEST SERIES C.

	C1	C2	C3
LENGTH	20	40	80
MEAN DIFFERENCE	1,7	3,2	3,2
MEAN DEVIATION	0,9	1,8	1,9
VARIANCE	1,4	4,5	6,1
STANDARD DEVIATION	1,1	2,1	2,4

APPENDIX 6

A PRACTICAL APPLICATION OF THE USE OF TENSOR PERMEABILITY COEFFICIENTS

Lyell's (1970) original program has been extended to enable cases of anisotropic media to be handled. The extended forms of the equations used are given in Appendix 4. The extended program is included in this Appendix.

The use and flowchart of this program are nearly identical to that given by Lyell (1970) and will thus not be given here. All that has to be supplied to the program are the absolute values of the coefficients of the permeability tensor.

Four cases have been tested and graphs showing the drawdown of the phreatic line with time for these cases are included in this Appendix.

The four cases tested are:

1. Isotropic $K = \begin{vmatrix} 1 & 0 \\ 0 & 1 \end{vmatrix}$

2. Anisotropic $K = \begin{vmatrix} 3 & 1 \\ 1 & 3 \end{vmatrix}$ $\bar{K} = \begin{vmatrix} 2 & 0 \\ 0 & 1 \end{vmatrix}$

   at 45° to the XY axis system.

   (see fig A.6.1)

3. Anisotropic $K = \begin{vmatrix} 75 & 26 \\ 26 & 105 \end{vmatrix}$ $\bar{K} = \begin{vmatrix} 2 & 0 \\ 0 & 1 \end{vmatrix}$

   at 60° to the XY axis system.

4. Anisotropic $K = \begin{vmatrix} 5 & 3 \\ 3 & 5 \end{vmatrix}$ $K = \begin{vmatrix} 4 & 0 \\ 0 & 1 \end{vmatrix}$

at 45° to the XY axis system

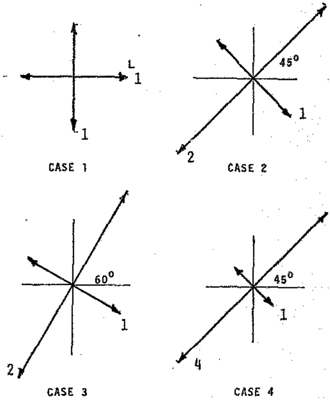

FIG. A.6.1 DIRECTIONS AND RELATIVE MAGNITUDES OF THE PRINCIPAL AXES FOR THE THREE CASES TESTED

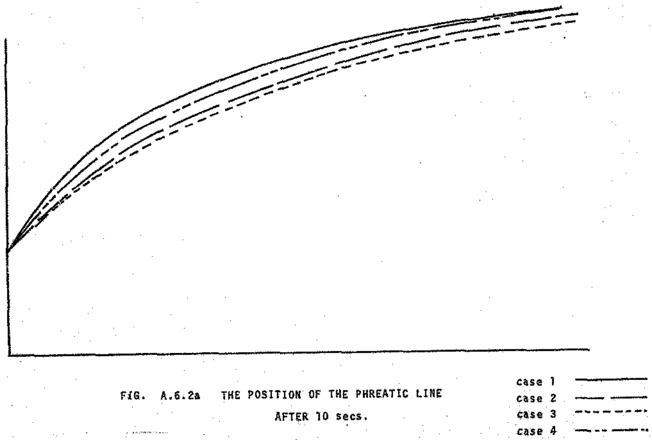

FIG. A.6.2a THE POSITION OF THE PHREATIC LINE AFTER 10 secs.

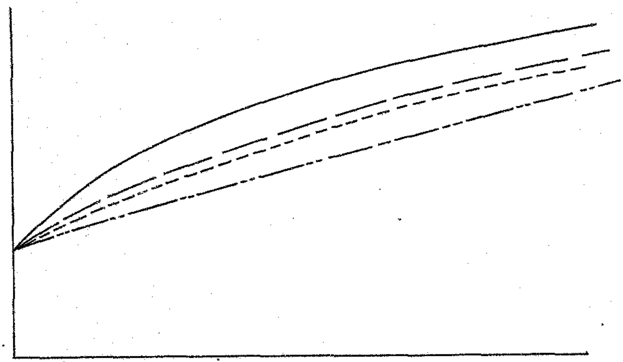

FIG. A.6.2b THE POSITION OF THE PHREATIC LINE AFTER 20 secs.

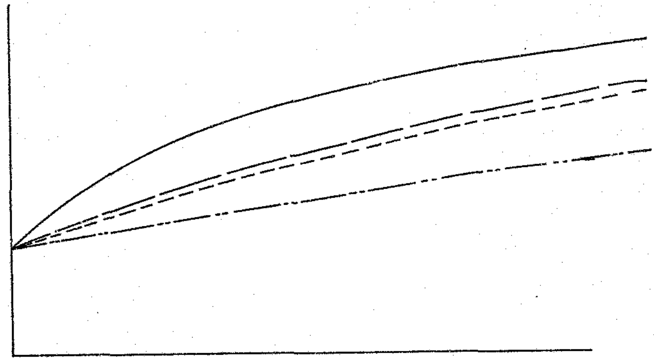

FIG. A.6.2c THE POSITION OF THE PHREATIC LINE
AFTER 30 secs.

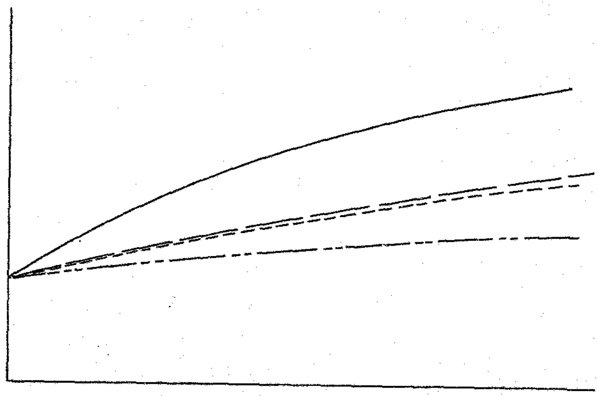

FIG. A.6.2d THE POSITION OF THE PHREATIC LINE
AFTER 40 secs.

```
******************************************************************************
PRINT/DISPLAY FOR USER NC  19                          FILE NAME DIWELL     CL
******************************************************************************
C      PROGRAM FOR SCLN OF WT=F(TIME)
       REAL KXX,KXY,KYY
       DIMENSION H(18,48),S(46),IS(46),IHWT(46),DHDZ(46),DHDX(46)
       DIMENSION TANGL(46),B(46),U(16,46),Z(46)
1      FORMAT(1H1,//,5X,'EXCESS HEAD MM',78X,'UNIT DRAWDOWN')
2      FORMAT(F7.0,15F6.0,4X,F7.3)
3      FORMAT(5X,'**************',78X,'************',//)
4      FORMAT(1H1,//,5X,'PORE PRESSURE GM PER SQ CM',70X,'DRAWDOWN')
5      FORMAT(//,4X,'INFILTRATION RATE MM PER SEC=',F10.4)
6      FORMAT(5X,'**************************',70X,'********',//)
7      FORMAT(/,4X,'TIME SINCE START SECS=',F10.2)
       NITR=250
       NITF=15
       M=16
       N=46
C      UNITS ARE MILLIMETERS AND SECONDS
       W=1.68
       ITW=12
       HW=585.
       TW=170.
       MOD=M-3
       NOD=N-3
       MD=M-1
       ND=N-1
       KXX=10.
       KYY=100.
       KXY=0.
       RII=KXX+KYY
       RXX=KXX/(2.*RII)
       RXY=KXY/(4.*RII)
       RYY=KYY/(2.*RII)
       SXX=RXX
       SXY=KXY/(2.*RII)
       SYY=KYY/RII
       SKK=KXX+KYY+KXY/2.
       DELTT=10./60.
       A=39.
       PERM=45.
       SY=0.337
       T=-10.
       ITWP=ITW+1
C      SET ENTIRE MATRIX TO ZERO FOR INITIAL VALUES
       DO 821 J=1,N
       DO 821 I=1,M
821    H(I,J)=HW/1.5
C      FIND INITIAL VALUES BY ROUGH GRID
       DO 11 J=1,N
11     H(1,J)=HW
       DO 12 I=2,ITW
12     H(I,N)=A*(M-I)
       DO 13 I=ITW,M
13     H(I,N)=TW
       DO 10 L=1,NITR
       DO 14 I=4,MOD,3
```

```
14    H(I,1)=SXX*(H(I-3,1)+H(I+3,1))+SYY*H(I,4)
      H(M,1)=(KXX*H(M,4)+KYY*H(M-3,1))/(KXX+KYY)
      DO 16 J=4,NDD,3
16    H(M,J)=SXX*(H(M,J-3)+H(M,J+3))+SYY*H(M-3,J)-SXY*(H(M-3,J-3)
     1-H(M-3,J+3))
      DO 17 I=4,MDD,3
      DO 17 J=4,NDD,3
      H(I,J)=RXX*(H(I,J-3)+H(I,J+3))+RYY*(H(I-3,J)+H(I+3,J))
17    H(I,J)=H(I,J)+RXY*(H(I-3,J+3)-H(I-3,J-3)-H(I+3,J+3)+H(I+3,J-3))
1C    CONTINUE
C     ROUGH GRID FOUND
C     SET SURROUNDING VALUES TO ROUGH GRID VALUES
      DO 21 I=1,M,3
      DO 21 J=1,N,3
      DO 21 II=1,3
      DO 21 JJ=1,3
      III=I+II-1
      JJJ=J+JJ-1
21    H(III,JJJ)=H(I,J)
      DO 22 I=1,M
      DO 22 J=1,N
22    H(I,J)=H(I+1,J+1)
      DO 122 I=1,ITW
122   H(I,N)=A*(M-I)
C     FINE GRID SET UP FOR ITER ATION
C     START RELAXATION PROCEDURE FOR FINE GRID
C     CALCULATION OF PART TWO OF THE WATER TABLE PROBLEM
C     GIVE INITIAL VALUWS TO S ETC
      DO 2CC J=1,N
      B(J)=1.
      S(J)=0.
      IS(J)=S(J)+1
2CC   IHWT(J)=M-1
      DO 6CC LLL=1,7
      DO 7CC KKK=1,40
C     CALCULATE VALUES OF TAN THETA, DHDX,DHDZ
      DO 2C1 J=2,N
      ISWT=IS(J)
      C=B(J)*A
      IF(C-A/6.)12C1,2201,2201
2201  DHDZ(J)=(H(ISWT,J)-H(ISWT+1,J))/C
      GO TO 3201
1201  DHDZ(J)=(H(ISWT,J)-H(ISWT+2,J))/(A+C)
3201  CONTINUE
      IF(IS(J)-IS(J-1))42C1,4201,5201
5201  HR=(H(ISWT,J-1)-H(ISWT+1,J-1))*B(J)+H(ISWT+1,J-1)
      GO TO 6201
4201  IF(B(J-1))7201,7201,8201
72C1  HR=H(ISWT,J-1)
      GO TO 6201
8201  HR=(H(ISWT,J-1)-H(ISWT+1,J-1))*B(J)/B(J-1)+H(ISWT+1,J-1)
6201  CONTINUE
      DHDX(J)=(HR-H(ISWT,J))/A
2C1   CONTINUE
      DO 381 J=2,NC
381   TANGL(J)=(S(J+1)-S(J-1))/2.
      DHDX(1)=0.
      TANGL(1)=C.
      TANGL(N)=3.*S(N)/2.-2.*S(N-1)+S(N-2)/2.
```

```
      ISWT=IS(1)
      IF(B(1)*6.-1.)1381,1381,1382
1381  DHDZ(1)=(H(ISWT,1)-H(ISWT+2,1))/((B(1)+1.)*A)
      GO TO 1383
1382  DHDZ(1)=(H(ISWT,1)-H(ISWT+1,1))/(B(1)*A)
1383  CONTINUE
      DHDZ(N)=1.
      DO 204 J=1,N
204   S(J)=((DHDZ(J)*KYY+KXY*DHDX(J)-KXX*DHDX(J)*TANGL(J)-KXY*DHDZ(J
     1*TANGL(J))*1./SY-W/SY)*DELTT/A+S(J)
      IF(LLL-1)1204,1204,1206
1204  CONTINUE
      DO 1205 J=1,N
1205  S(J)=0.
1206  CONTINUE
      DO 202 J=1,N
      US=S(J)+1.
      IS(J)=US
      SS=IS(J)
      B(J)=SS-S(J)
      IF(IS(J))1202,1202,1203
1202  IS(J)=1
      B(J)=1.
      S(J)=0.
1203  CONTINUE
      IF(S(J)*A-HW+TW)2202,3202,3202
3202  S(J)=(HW-TW)/A
      IS(J)=ITW-1
      B(J)=TW/A-(M-ITW)
2202  CONTINUE
202   IHWT(J)=M-IS(J)
C     FIND NEW FLOW NET FOR NEW POSN OF WATER TABLE
      DO 300 J=1,N
      ISD=IS(J)
      SHWT=IHWT(J)
300   H(ISD,J)=(B(J)+SHWT-1)*A
      DO 301 J=1,N
      ILS=IS(J)+1
      DO 301 I=1,ILS
      ISD=IS(J)
      IF(I-ISD)302,301,301
302   H(I,J)=0.
301   CONTINUE
      ISD=IS(N)+1
      DO 1301 I=ISD,M
1301  H(I,N)=A*(M-I)
      DO 2301 I=ITW,M
2301  H(I,N)=TW
      DO 500 LL=1,NITF
      C=B(1)*A
      LIMN=IS(1)+1
      H(LIMN,1)=((A*C+C*C)*H(LIMN,2)+A*A*H(LIMN-1,1)+A*C*H(LIMN+1,1))
     1((A+C)*(A+C))
      LIM=LIMN+1
      DO 305 I=LIM,MC
305   H(I,1)=SXX*(H(I-1,1)+H(I+1,1))+SYY*H(I,2)
      H(M,1)=(KXX*H(M,2)+KYY*H(M-1,1))/(KXX+KYY)
      DO 306 J=2,ND
306   H(M,J)=SXX*(H(M,J-1)+H(M,J+1))+SYY*H(M-1,J)
```

```
      DO 5551 J=2,ND
5551  Z(J)=B(J)*A
      DO 307 J=2,ND
      C1=Z(J+1)
      C=Z(J)
      C2=Z(J-1)
      C=B(J)*A
      LIMN=IS(J)+1
      IDCD=IS(J+1)-IS(J)
      IF(IDCD)3072,3072,3071
3072  CONTINUE
      DEN=2.*(KXX*C*(A+C)+KYY*(A*(A+C)))
      DEN2=A+C2
      DEN1=A+C1
      VAR=KXX*C*(A+C)*(H(LIMN,J-1)+H(LIMN,J+1))
      VAR=VAR+2.*KYY*A*(A*H(LIMN-1,J)+C*H(LIMN+1,J))
      VAR=VAR+KXY*A*C*((H(LIMN+1,J+1)-H(LIMN-1,J+1))/DEN1-(H(LIMN+1,
     1-H(LIMN-1,J+1) /DEN2)*(A+C)
      H(LIMN,J)=VAR/DEN
      LIM=LIMN+1
      GO TO 3074
3071  D=C/(S(J+1)-S(J))
      DO 919 ICNT=1,IDCD
      CNT=ICNT-1
      D=D+CNT*A/(S(J+1)-S(J))
      ILIM=LIMN+ICNT-1
      RA=(A+C)*C*C
      SA=(A+D)*A*D
      TA=(A+C)*A*C
      UA=(A+D)*C*D
      DEN=KXX*(TA+RA)+KYY*(SA+UA)
      H(ILIM,J)=(KXX*(RA*H(ILIM,J-1)+TA*(M-ILIM)*A)+KYY*(SA*H(ILIM-1
     1+UA*H(ILIM+1,J)))/DEN
      DEN2=DEN*2.
      IF(ILIM-2)9995,9996,9995
9996  DRATIT=Z(J-1)+A
      GO TO 9997
9995  III=H(ILIM-2,J-1)
      IF(III)9998,9996,9998
9998  DRATIT=2.*A
9997  CONTINUE
      UA=A+D
      IF(Z(J+1)-0.125*A)9991,3073,3073
9991  Z(J+1)=Z(J+1)+A
      H(ILIM,J)=H(ILIM,J)+KXY*RA*UA*((H(ILIM+2,J+1)-H(ILIM,J+1))/Z(J
     1+1)-(H(ILIM+1,J-1)-H(ILIM-1,J-1))/DRATIT)/DEN2
      Z(J+1)=Z(J+1)-A
      GO TO 919
3073  H(ILIM,J)=H(ILIM,J)+KXY*RA*UA*((H(ILIM+1,J+1)-H(ILIM,J+1))/Z(J
     1+1)-(H(ILIM+1,J-1)-H(ILIM-1,J-1))/DRATIT)/DEN2
919   CONTINUE
      LIM=LIMN+IDCD
3074  CONTINUE
      DO 307 I=LIM,MD
      H(I,J)=RXX*(H(I,J+1)+H(I,J-1))+RXY*(H(I-1,J+1)-H(I-1,J-1)
     1-H(I+1,J+1)+H(I+1,J-1))
3075  H(I,J)=H(I,J)+RYY*(H(I-1,J)+H(I+1,J))
307   CONTINUE
500   CONTINUE
```

```
700   CONTINUE
      DO 402 J=1,N
      ISDD=IS(J)
      ISD=IS(J)+1
      DO 401 I=1,ISDD
401   U(I,J)=0.
      DO 402 I=ISD,M
402   U(I,J)=(H(I,J)-A*(M-I))/10.
      WRITE(6,1)
      WRITE(6,3)
      WRITE(6,2)((H(I,J),I=1,M),S(J),J=1,N)
      WRITE(6,5)W
      T=T+10.
      WRITE(6,7)T
      WRITE(6,4)
      WRITE(6,6)
      WRITE(6,2)((U(I,J),I=1,M),S(J),J=1,N)
600   CONTINUE
      STOP
      END

PRINT * NO OF LINES PRINTED-    253
```